NTNU

Norwegian University of
Science and Technology

Modeling of CO2 Storage in the Smeaheia Field

Ida Irene Brobakken

Petroleum Geoscience and Engineering
Submission date: June 2018
Supervisor: Jon Kleppe, IGP
Co-supervisor: Bamshad Nazarian, Statoil

Norwegian University of Science and Technology
Department of Geoscience and Petroleum

Preface

This report is the final work of my master's thesis at the Department of Geoscience and Petroleum at the Norwegian University of Science and Technology, NTNU, spring 2018. The thesis is written in cooperation with Equinor ASA.

I would like to thank Equinor ASA for letting me use their reservoir model and giving me the opportunity to use real-time and valuable data. Further, I would like to thank my supervisor in Equinor ASA, Bamshad Nazarian, for helping me and being supportive throughout this project, and Ali Mojaddam Zadeh for helping me with my simulations.

A great thank you to my supervisor at NTNU, Jon Kleppe, Professor at the Department of Geoscience and Petroleum. I am really grateful for his guidance and positive attitude regarding the thesis, and for initializing this cooperation with Equinor ASA and Bamshad Nazarian.

Trondheim, 11.06.2018

Ida Irene Brobakken

Abstract

Carbon capture and storage, CCS, is a method that can reduce today's carbon emissions by approximately 20 %. Since the world still highly depends on the use of fossil fuel energy, this method is necessary for reaching the world's 2 °C goal. This master thesis describes the CCS technology in total, including capture, transport and storage of carbon dioxide.

Smeaheia is a new Norwegian full-scale CCS project planned to be in operation in 2022. The storage site consists of two important structures, Alpha and Beta, which both can store about 100 Mt of CO_2. However, the Alpha structure is found to be the best alternative as the Beta area may cause vertical CO_2 migration up to the surface. Further, a reservoir simulation model of the Smeaheia area has been developed by Equinor. The model is used for different studies in this thesis, including simulations of injection well locations, perforation depths and the use of outflow control devices. Comparisons of different well designs are completed to find the optimal alternative maximizing the CO_2 storage.

The optimal well location found within the Alpha structure has a storage capacity of 135 Mt CO_2 in total when CO_2 is being injected for 25 years. This well is located in the northern part of Alpha, far away from the leaking Beta area. The best alternative outside the Alpha structure is found to be in the southern part of the reservoir model. Two injection wells with each an annual rate of 100 Mt of CO_2 will result in a total storage volume of 5000 Mt after 25 years. Further, it is seen that perforations made in the lower part of the Fensfjord and Krossfjord formations will maximize the storage capacity.

The effect of outflow control devices is studied in high-permeable and low-permeable layers. Results show that such a control device has better effect in high-permeable zones. At last, the injected CO_2 is tracked during the simulation. The carbon dioxide will migrate within the Alpha structure and between the Alpha and Beta areas as time goes by and as the Alpha structure is being filled up to its spill point.

Sammendrag

Karbonfangst og -lagring, CCS, er en metode som kan redusere dagens karbonutslipp med ca 20 %. Siden verden er avhengig av fossilt brensel er denne metoden nødvendig for å nå det globale 2 °C-målet. Denne masteroppgaven forklarer karbonfangst og -lagringsteknologien som inkluderer fangst, transport og lagring av CO_2.

Smeaheia er et nytt, norsk fullskala CCS-prosjekt som planlegges å være i operasjon i år 2022. Feltet består av to sentrale strukturer, Alpha og Beta, som begge har mulighet til å lagre ca 100 millioner tonn CO_2. Det er vist at Alpha-strukturen vil være det beste alternativet, da lagring i Beta kan føre til vertikal CO_2-bevegelse opp til overflaten. Videre har en reservoarmodell av Smeaheia-feltet blitt utviklet av Equinor. Modellen har blitt brukt til å utføre flere studier i denne masteroppgaven, inkludert simuleringer av ulike plasseringer for injeksjonsbrønnen, injeksjonsdybder og bruk av outflow control devices. De ulike brønndesignene er sammenlignet for å finne det optimale alternativet for CO_2-lagring.

Den beste brønnplasseringen funnet i Alpha-strukturen i denne oppgaven har en total lagringskapasitet på 135 millioner tonn når CO_2 er injeksert i 25 år. Injeksjonsbrønnen er plassert i nordre del av Alpha, langt unna Beta-strukturen hvor sannsynligheten for lekkasje er høy. Den beste plasseringen utenfor Alpha er funnet sør i reservoarmodellen. To injeksjonsbrønner med en årlig rate på 100 Mt CO_2 hver vil resultere i en lagringskapasitet på 5000 millioner tonn etter 25 år med injeksjon. Videre er det vist at injeksjon i nedre del av Fensfjord- og Krossfjord-formasjonene vil maksimere lagringskapasiteten i Smeaheia.

Bruk av outflow control devices er undersøkt i formasjonslag med høy og lav permeabilitet. Det er vist at kontrollenhetene har bedre effekt i lagene med høy permeabilitet. Til slutt er CO_2-strømningen gjennom Smeaheia sporet. Resultatene viser at den injekserte karbondioksiden vil bevege seg mellom øvre og nedre del av Alpha-strukturen, i tillegg til å bevege seg fra Alpha til Beta over tid. Dette skyldes at Alpha-strukturen fylles opp, og den ekstra injekserte CO_2-en vil bevege seg over til Beta.

Table of contents

List of Figures

List of Tables

Chapter 1

Introduction

Carbon dioxide, CO_2, is a well-known greenhouse gas often associated with global warming. Today the level of atmospheric CO_2 is 410.31 ppm or 0.041 %, and the trend shows that this level is rising (CO2-Earth, 2018). Due to the increasing proportion, carbon dioxide makes up an important trapping gas in the atmosphere resulting in several greenhouse gas changes. The Earth's average surface temperature has risen by about 1 °C since 1906, causing changes in the plant photosynthesis, ice to melt and water to evaporate (Nasa Earth observatory, 2018) and (Ringrose, 2017a). To mitigate additional temperature rise, and thus prevent further changes in Earth systems, a CO_2 reduction is necessary.

Multiple technologies can be used to reduce the atmospheric CO_2 level. The method described in detailed in this thesis is the carbon capture and storage operation, CCS. CCS is an optimal solution for reducing the amount of CO_2 in the atmosphere while still meeting the world's high energy demand. The CCS technology makes it possible to combine further use of fossil fuel energy and 20 % CO_2 reduction, causing this to be a necessary method for reaching the world's 2 °C goal (Ringrose, 2017a).

This thesis is focusing on optimizing a Norwegian carbon capture and storage operation, and several important topics are therefore studied. The next chapter will describe the physical properties of CO_2 such as the phase diagram, density and viscosity. Further, chapter 3 explains the reasons for implementing the CCS technology, discussing the CO_2 development over time and today's challenges related to CCS.

A CCS project consists of several operations, and chapter 4 to 6 describe this technology in whole. The CO_2 has to be captured and separated from a gas stream before it is transported, injected and stored in a formation storage site. Several techniques can be used to capture CO_2, and this thesis is describing the post-combustion, pre-combustion and oxygen-fired combustion processes. Further, transportation by ships, pipelines, trucks and railways are explained. In addition, this thesis is highly focusing on CO_2 storage. Multiple factors are considered to

ensure a safe, efficient and economical storage operation; storage sites, trapping mechanisms and storage integrity.

Further, chapter 7 and 8 describe the principle of integrity, both geological integrity and integrity related to the injection well design. It should be stated that chapter 2 to 8 are modified from my semester project, CO_2 storage - Review of theory and literature (Brobakken, 2017).

However, as mentioned this thesis will mainly focus on simulations related to a new, large-scale CCS project located in the North Sea, Norway. The Smeaheia storage area is planned to be in operation in 2022 and has an estimated storage capacity of 100 Million tonnes of carbon dioxide. To maximize the CO_2 storage in this field, an optimized well design is needed. Chapter 9 explains some of the choices made in the completed simulations for storage optimization.

Chapter 10 gives a detailed description of the Smeaheia storage field. The storage site consists of two structures, Alpha and Beta, which will be described in detail in this report. Further, an explanation of the project design, the field geology and the Smeaheia simulation model is given. Section 10.1, describing the CCS process at Smeaheia, is mainly based on my semester project (Brobakken, 2017).

Multiple simulation studies are completed to optimize the storage capacity in the Smeaheia field. Components such as well location, injection rate, perforation depth and outflow control devices will highly impact the storage volume and are thus necessary to discuss in this thesis. Chapter 11 gives an overview of all simulations completed in this thesis, while chapter 12 discuss the results. Chapter 13 gives the main conclusions from this thesis in addition to some suggestions for further work.

Chapter 2

Physical properties of CO2

This chapter is modified from my semester project, CO_2 storage - Review of theory and literature (Brobakken, 2017).

CO_2 is the most important greenhouse gas in the atmosphere, constituting 0.04 % of all the atmospheric gases (Ringrose, 2017a). To understand how this gas can be captured, transported and stored safely, it is important to study its physical behaviour at different conditions.

At standard conditions, 1 atm and 15 °C, the CO_2 is 1.5 times as dense as air and has a molecular weight of 44.01 g/mol (Whitson and Brulé, 2000). The CO_2 is stable, nontoxic and colourless. It exists in a gaseous state and is relatively non-reactive (White et al., 2003), (Whitson and Brulé, 2000) and (Ringrose, 2017b). However, at higher pressures and temperatures, CO_2 may exist as a liquid-like supercritical fluid or as a gas.

The physical properties of CO_2 will vary with different pressure and temperature conditions, causing a potential change in the phase envelop. Such a change will affect how the CO_2 behaves at different environments. A CCS project includes several operations with different pressure and temperature scenarios, making it important to study the physical properties of CO_2. An understanding of the physical behaviour will improve safe and long-term CO_2 storage.

2.1 Phase diagram

Fig. 2.1 illustrates the CO_2 phase diagram. The diagram highlights two important points, the triple point and the critical point. The triple point defines the condition where all three phases, solid, liquid and vapour, coexist in a thermodynamic equilibrium. This is at a temperature of -56.6 °C and a pressure of 5 atm, which is equal to approximately 5.2 barsa. The critical point is located where the temperature is 31 °C and the pressure is 73 atm, 73.8 barsa, and defines the condition where there are no boundaries between the different phases. (d. Koeijer et al., 2017).

As can be observed in Fig. 2.1, the pressure and temperature condition defines the CO_2 phase. To the left of the triple point and at very low temperatures, CO_2 will be in a solid state acting as snow or dry ice. At standard condition and at temperatures above -80 °C where the pressure is relatively low, the CO_2 will be in a vapour phase. CO_2 in liquid state will occur above the triple point.

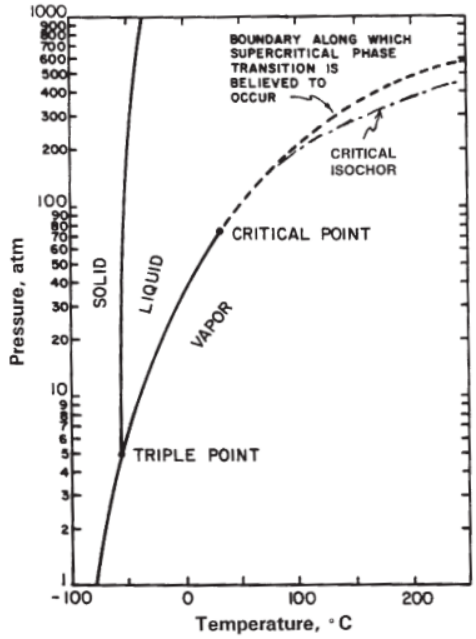

Fig. 2.1: CO_2 phase diagram (Whitson and Brulé, 2000).

A supercritical phase is characterized by the unclear interface between liquid and gas (Petrowiki, 2017). The fact that the physical properties of a supercritical CO_2 are representative for both vapour and liquid phases, makes it hard to determine whether the CO_2 is in a gas or liquid form. For instance, CO_2 will have a gaseous viscosity and a liquid-like density when it is in a supercritical phase.

The pressure and temperature condition will vary with different CCS operations. The CO_2 is in a vapour phase when it is captured and separated. Different transport options have varying pressure and temperature requirements, but the optimal way to transport CO_2 is in its liquid phase. As can be seen from Fig. 2.1, the liquid state requires a relative low temperature and low-medium pressure. As will be explained later in the thesis, this condition can be achieved by CO_2 compression.

The optimal way to store CO_2 is when the CO_2 is in a supercritical phase. This condition represents the safest and most efficient option for long-term storage of carbon dioxide. To meet this requirement, environments with pressures and temperatures found above the critical point are necessary. Storage sites fulfilling these conditions can be found at depths of 800-1000 m (Gibbins and Chalmers, 2008).

2.2 Density

Figs. 2.2 and **2.3** illustrate how the CO_2 density varies with different pressures and temperatures. It can be observed that an increase in pressure will cause the density to rise, while an increase in temperature will result in a density reduction.

Fig. 2.2 shows that the density is sensitive at lower pressure changes, meaning that the density varies in a greater degree at lower pressures compared to higher pressure conditions. Fig. 2.3 corroborates the same observation. The density is more sensitive at lower pressures, assuming the same temperature rise.

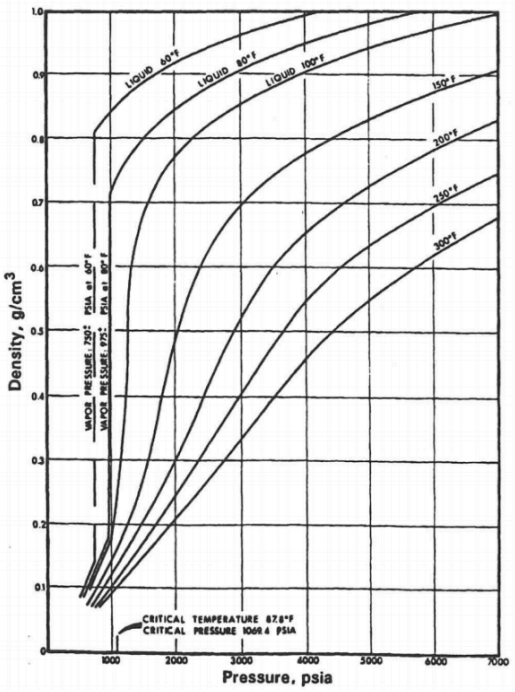

Fig. 2.2: CO_2 density as a function of pressure (Whitson and Brulé, 2000).

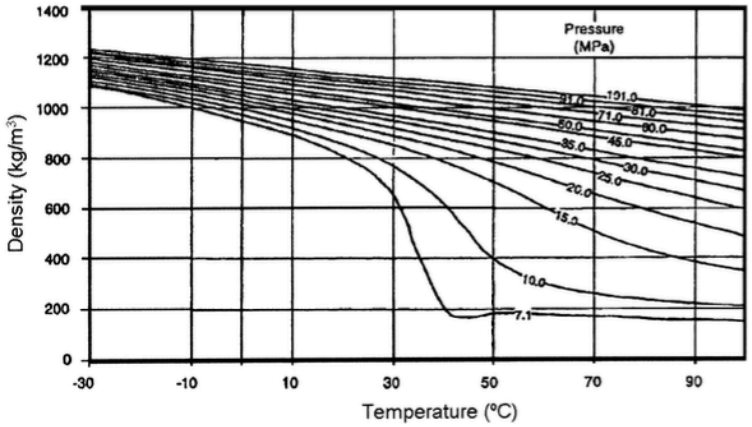

Fig. 2.3: CO_2 density as a function of temperature (White et al., 2003).

Fig. 2.4 illustrates the variation in CO_2 density as a function of depth. The density will be low at shallow depths causing the CO_2 to act as a gas. As the depth increases, the density will rise and the CO_2 will behave as a supercritical fluid. This phase transition will occur at the critical depth, which mentioned previously, is at approximately 800 m.

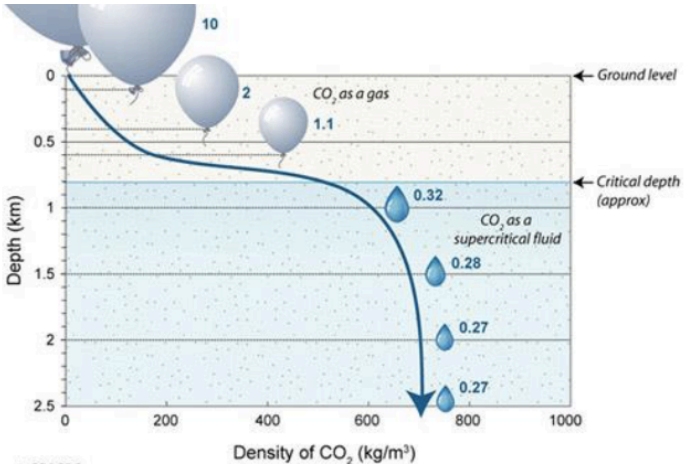

Fig. 2.4: CO_2 density as a function of depth (Ringrose, 2017b).

2.3 Viscosity

The relationship between CO_2 viscosity, pressure and temperature is given in **Fig. 2.5**. The viscosity will increase when pressure rises, meaning that the CO_2 stream will be thicker and flow at a lower rate when the pressure gets higher. As temperature rises, the CO_2 becomes less viscous and flows more rapidly. It can be seen from Fig. 2.5 that the viscosity is sensitive to changes at low temperatures and pressures.

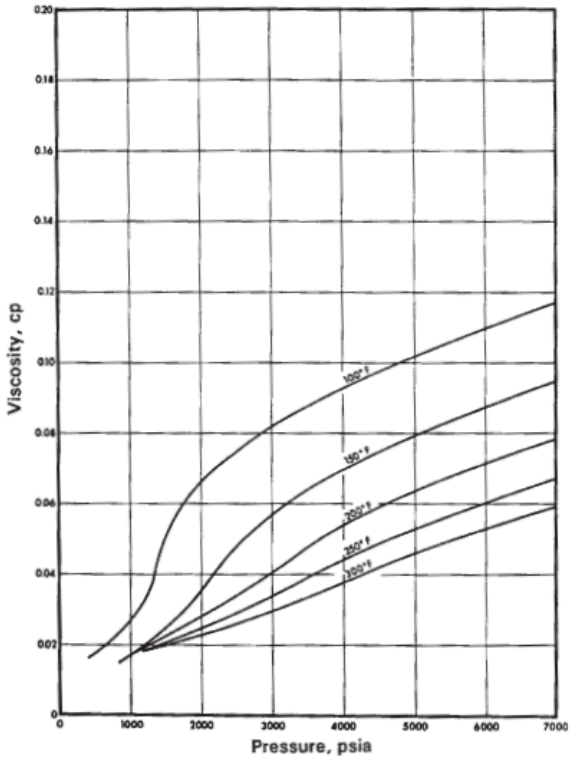

Fig. 2.5: CO_2 viscosity as a function of pressure and temperature (Whitson and Brulé, 2000).

As mentioned earlier in the thesis, the viscosity of a supercritical CO_2 will be low and vapour-like. This can be observed in the figure above by locating the area where the pressure is higher than 73.8 barsa, which equals about 1070 psia, and the temperature is 31 °C. This point is located in the lower-left part of the figure, representing a CO_2 stream with low viscosity.

2.4 Formation volume factor

The formation volume factor, FVF, gives the relationship between the CO_2 volume at a given pressure and temperature and the CO_2 volume at standard conditions (Whitson and Brulé, 2000). In other words, the FVF compares the CO_2 volume in a reservoir at a specific pressure and temperature with the surface volume.

Fig. 2.6 shows the formation volume factor for carbon dioxide as a function of temperature and pressure. It can be observed that the formation volume factor is low for high-pressure conditions. The CO_2 will be compressed in the reservoir, but as it reaches the surface and the pressure decreases, the CO_2 will expand and the FVF will increase. Further, it may be observed that the formation volume factor reduces as the temperature decreases.

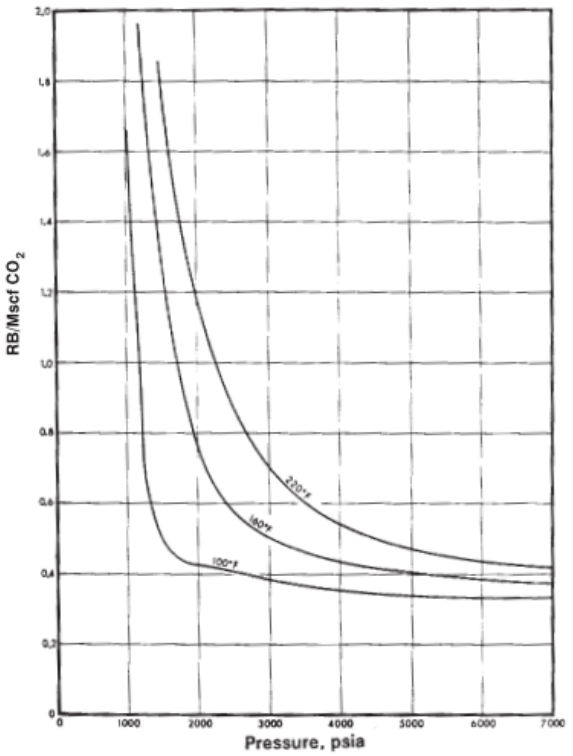

Fig. 2.6: CO_2 formation volume factor as a function of pressure and temperature (Whitson and Brulé, 2000).

2.5 Solubility in water

When CO_2 is injected in the subsurface it will most likely react with water. Either with brine already existing in the formation or with water being injected into the field. The salinity level in formation water is normally high, which affects the CO_2 solubility (White et al., 2003).

Fig. 2.7 illustrates how CO_2 dissolves in different types of water at various pressures. The graph shows the CO_2 solubility at 100 °F, as the solubility is not sensitive to temperatures higher than 100 °F (Whitson and Brulé, 2000). As can be noticed from the figure below, the solubility will increase with rising pressure. Further, the solubility will be higher in fresh water compared to salt water, meaning the CO_2 solubility will be lower as the water gets saltier.

The CO_2 solubility in water is an important factor considering storage of carbon dioxide. The reaction between CO_2 and brine will be an essential trapping mechanism ensuring long-term storage (White et al., 2003). The different trapping mechanisms will be carefully described in chapter 6.

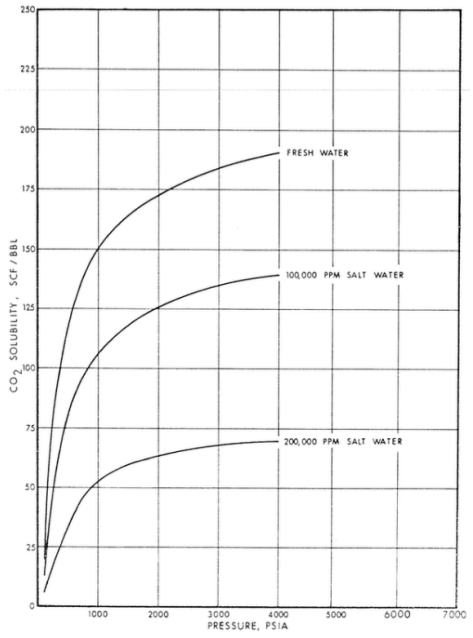

Fig. 2.7: CO_2 solubility in water as a function of pressure (Whitson and Brulé, 2000).

2.6 Acidity

Another important factor regarding CO_2 storage is acidity. When CO_2 reacts with formation water, carbon acid is generated (White et al., 2003). This may cause minerals to dissolve, which could result in higher porosity and permeability due to precipitation.

The degree of acidity determines the pH level of the solution. The pH depends on pressure and temperature, where a pressure rise causes the pH to reduce and a temperature increase causes the pH to rise (White et al., 2003).

Although this makes up an important factor, acidity will not be further discussed in this thesis.

Chapter 3

CO2 capture and storage

This chapter is modified from my semester project, CO_2 storage - Review of theory and literature (Brobakken, 2017).

Carbon capture and storage, CCS, is the process of removing carbon dioxide from industrial plants, transport and inject it into the subsurface to isolate it from the atmosphere. Although the CO_2 should be stored for a long time, it is important to mention that CO_2 storage is not a permanent disposal (Ringrose, 2017a). A permanent storage is difficult to establish and, in principle, the CO_2 only needs to be isolated for a few thousand years to have an effect on the amount of carbon in the atmosphere. Further, CO_2 is an essential part of the carbon cycle, not a waste product. The main purpose of CCS is thus to store and isolate the CO_2 in geological structures for a geological period of time. (Cooper, 2009).

3.1 CO2 emissions over time

CO_2 has been stored in different types of carbon reservoirs for a long time. Naturally occurring CO_2 has been detected in rocks, oceans, terrestrial plants and in the atmosphere. Fluxes between these carbon holders have been important for the carbon cycle, enabling sustained life on Earth. The carbon cycle, illustrated in **Fig. 3.1**, involves carbon exchange between the atmosphere, geosphere, hydrosphere and the biosphere (Ringrose, 2017a). Due to human activity and increased emissions of CO_2, the carbon ecosystem changes and the CO_2 exchange between the atmosphere and terrestrial plants is no longer in balance.

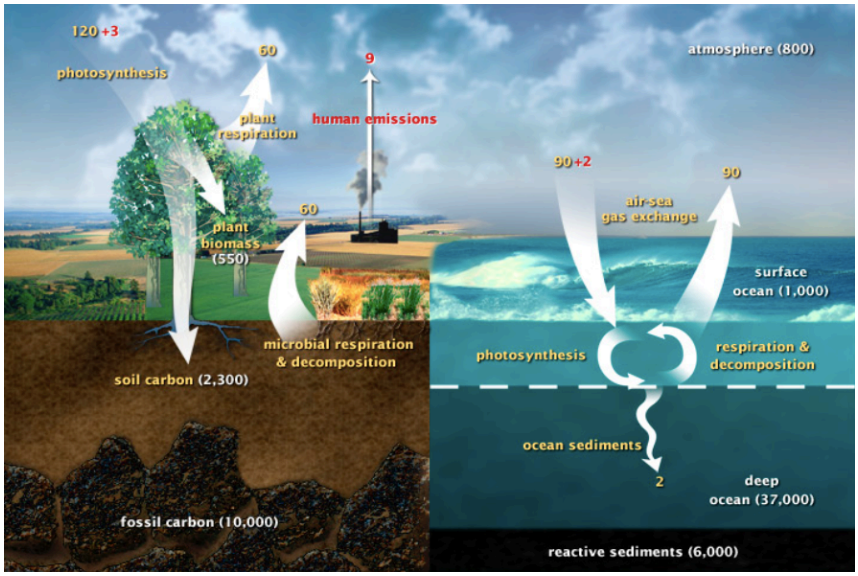

Fig. 3.1: The carbon cycle (Ringrose, 2017a).

The concentration of atmospheric CO_2 was 34 % higher in 2003 compared to the levels in 1750, and the measurements have continued to increase (Ringrose, 2017a). **Fig. 3.2** shows the rise in carbon emissions over time. As can be observed, the amount of CO_2 has increased rapidly since 1950, mostly caused by emissions from gas, liquid and solid fuels. To be able to reduce the amount of CO_2 in the atmosphere, carbon emissions from these sources have to be minimized.

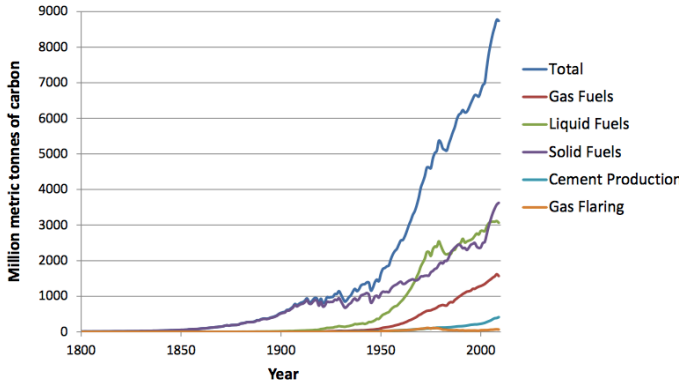

Fig. 3.2: Carbon emissions over the years (Ringrose, 2017a).

Although it is important to reduce the CO_2 emissions, the world highly depends on energy from fossil fuels. Today, 85 % of the primary energy originates from fossil fuels and it is likely to remain this way for a long time (Herzog, 2009). Thus, it is necessary to find a method that both reduces carbon emissions and allows for further use of fossil fuels. Carbon capture and storage in the subsurface is the only method combining these requirements.

3.2 Why CO2 capture and storage?

The main reason to store carbon dioxide in the subsurface is to reduce the greenhouse gas emissions into the atmosphere. Solar energy is absorbed in the atmosphere by greenhouse gases and sunlight is reflected back to the Earth's surface. The ground is being heated up, causing the Earth to act as a radiator. The heating will impact the plant photosynthesis, result in evaporation of water and large amounts of melted ice and snow (Ringrose, 2017a).

CO_2 capture and storage is a discussed topic and there are several arguments for and against the CCS method. The risk of CO_2 leakage during and after injection, and the fact that the required technology may not be ready to have a considerable impact on the climate changes, are arguments against implementing carbon capture and storage. In addition, multiple solutions such as use of renewables, improved efficiency in power generation and end the use of fossil-fuel energy offer potential alternatives (Ringrose, 2017a).

On the other hand, the world highly depends on fossil fuel energy, and this need is not likely to decrease rapidly. CO_2 storage is a good option combining CO_2 reduction in the atmosphere and continuous meeting of the world's energy demand. Further, CCS is the only method that can capture and store significant amount of CO_2 from industry plants, and the only method that can extract CO_2 from the atmosphere by capture carbon from biomass. The CCS method has shown to be the cheapest option for large-scale carbon reduction and a necessary operation for reaching the world's 2 °C goal. (Ringrose, 2017f).

Although CCS is currently a key to obtain significant CO_2 reduction, the focus on renewables will have an increasing importance in the future. The CCS process will act as a bridging technology during the transformation to a future with new energy solutions. (Ringrose, 2017a).

3.3 How much CO2 must be stored and why is CCS not moving?

Huge amounts of CO_2 have to be stored to make a difference in the atmosphere's carbon dioxide volume. Today, about 40 Mt of CO_2 in total are captured and stored annually. By 2040, the amount of stored CO_2 has to be approximately 4000 Mt per year to reduce the carbon level in the atmosphere, requiring a high number of large-scale CCS projects (Ringrose, 2017f).

Fig. 3.3 illustrates a graph representing the reduction of CO_2 that should be achieved to realize the prevention of 2 °C heating. Line 1 shows the reduction already reached. A depletion that may be underway is represented by line 2, and line 3 shows the necessary reduction which can be achieved partly by using carbon capture and storage.

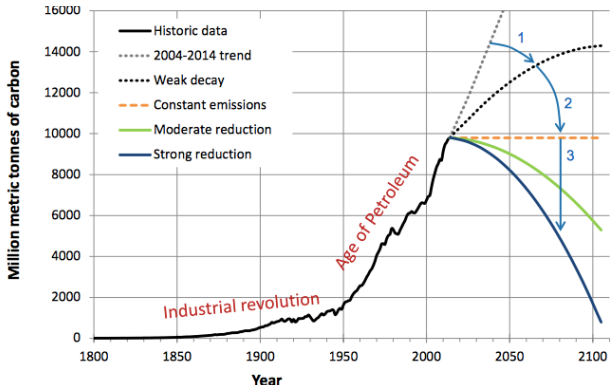

Fig. 3.3: Energy transition (Ringrose, 2017a).

Although there is an increased recognition of carbon capture and storage, an increase in financial support has not been following. Political fluctuation and missing financial support are the main reasons why CCS has not been moving. Several large-scale projects have not progressed due to financial shortage, although there have been technological investments. (Ringrose, 2017f).

Chapter 4

CCS technology: CO2 capture

This chapter is modified from my semester project, CO_2 storage - Review of theory and literature (Brobakken, 2017).

A carbon capture and storage project begins with the capture of carbon dioxide from point sources of gas emissions. CO_2 may be captured from the chemical industry or from power-generation. The purpose of carbon capture is to separate and concentrate CO_2 from gas streams, making the carbon transport and storage easier and safer.

There are mainly three different technologies used for CO_2 capture; post-combustion, pre-combustion and oxygen-fired combustion processes (Feron and Hendriks, 2005). All of them includes a combination of conversion, either of energy or fuel, and CO_2 separation. **Fig. 4.1** illustrates an overview of the different capture options.

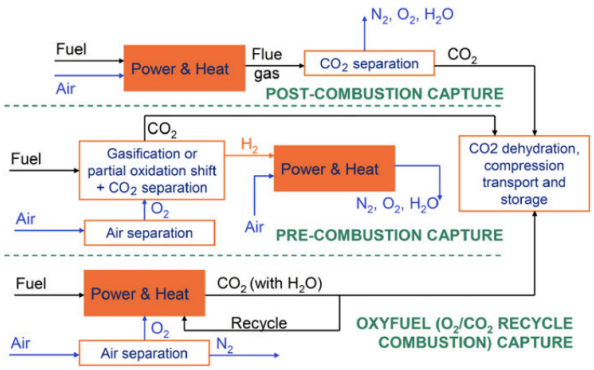

Fig. 4.1: CO_2 capture processes (Gibbins and Chalmers, 2008).

4.1 Post-combustion capture

In a post-combustion decarbonisation process, the CO_2 is captured at a low pressure and from a flue gas with low carbon dioxide content (3-20 %) (Feron and Hendriks, 2005). The capture operation mainly consists of two steps; an energy conversion and a CO_2 separation.

Fig. 4.2 illustrates the two stages in a post-combustion capture. Fuel from industrial plants is combined with air and burnt, resulting in an energy conversion and generation of power. CO_2 is then separated from the produced flue gas by using a physical-chemical process, generating a concentrated CO_2 stream. (Feron and Hendriks, 2005).

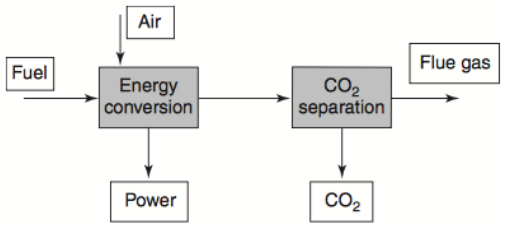

Fig. 4.2: Post-combustion process (Feron and Hendriks, 2005).

The CO_2 can be removed from the mixed gas by using several physical-chemical processes. The most common options include solvents, sorbents, cryogenic and membranes. The solvent-based process uses absorption liquids to separate CO_2 from the flue gas. Using an amine-based solvent, such as monoethanolamine (MEA), has been the dominated separation process so far. The sorbent-based methods use solid particles to separate the CO_2, membranes use solid-state chemical barriers, and the cryogenic processes use different gas condensate temperatures for separation. (Ringrose, 2017a) and (Feron and Hendriks, 2005).

The concentrated CO_2 is then dehydrated and compressed, ready to be transported to a storage site (Gibbins and Chalmers, 2008).

4.2 Pre-combustion capture

Fig. 4.3 illustrates a pre-combustion decarbonisation process. Such a capture operation generally consists of three steps; a fuel conversion, separation of carbon dioxide and energy conversion.

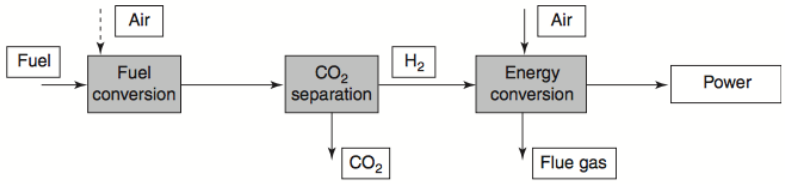

Fig. 4.3: Pre-combustion process (Feron and Hendriks, 2005).

The first step in a pre-combustion capture process is the fuel conversion. The fuel is blended with air and converted into a mix of CO_2 and hydrogen, H_2. This mixture has a high pressure, making it possible to separate the CO_2. The dominated separation option involves an absorption process, where the solvent may be physical or chemical. The fuel will be hydrogen-rich after the separation and may be burnt in a gas turbine before the energy conversion generates power. The captured CO_2 is then prepared for transportation (Feron and Hendriks, 2005).

4.3 Oxygen-fired combustion

The oxygen-fired combustion process, shown in **Fig. 4.4**, is another important CO_2 capture option. Such a process is often combined with separation of air and a de-nitrogenation process (Ringrose, 2017a). The presented nitrogen in air is removed, creating an oxygen stream. This stream is used in the energy conversion process, making it possible to separate the CO_2 and thus create a carbon dioxide stream (Feron and Hendriks, 2005). The concentrated CO_2 can then be transported to a storage site.

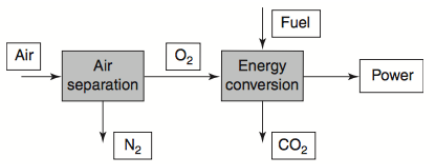

Fig. 4.4: Oxygen-fired combustion process (Feron and Hendriks, 2005).

Chapter 5

CCS technology: CO2 transport

This chapter is modified from my semester project, CO_2 storage - Review of theory and literature (Brobakken, 2017).

Transport of CO_2 is the necessary step between CO_2 capture and the storage operation in a CCS project. It is a complex process which may involve compression, liquefaction and pumping of the captured CO_2 stream, transport to an intermediate storage and transport to a storage site (d. Koeijer et al., 2017). A general transport system is illustrated in **Fig. 5.1**.

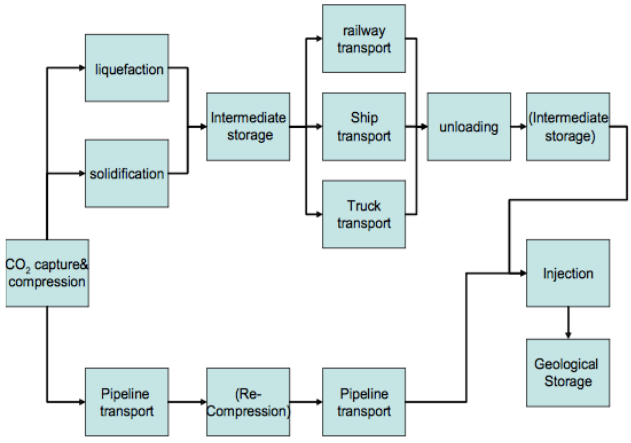

Fig. 5.1: Transport systems for CO_2 (Wildbolz, 2007).

Transport of a CO_2 stream is a complicated operation facing several challenges. The transport system must be able to handle CO_2 across different phase boundaries. A CO_2 stream may be in a gas-phase, liquid-phase or a supercritical phase, each requiring different transport conditions. A CO_2 stream may also contain impurities such as hydrocarbons, nitrogen and oxygen, complicating the transport. Further, CO_2 is corrosive when mixed with water or oxygen, setting important requirements to corrosion resistant material. (Ringrose, 2017a).

There are several options for transporting CO_2-rich gas or liquid streams. Most commonly are ships, pipelines, railways and trucks. The choice of transport is highly determined by safety, costs and efficiency, which again are determined by the CO_2 pressure and temperature condition, geography, type of storage site and the distance between the capture source and the storage complex. (Wildbolz, 2007).

The following sections will give a description of the different types of transport, challenges related to them and a brief discussion on their economic perspective.

5.1 Pipelines

Pipelines are widely used for transport in the petroleum industry. Pipelines have been applied in conjunction with enhanced oil recovery and transportation of oil and natural gas for many years (Wildbolz, 2007). The gained experience and knowledge have been transferred to CO_2 transport, making pipelines a good and valuable option for carbon dioxide movement both onshore and offshore.

One advantage with pipeline transportation is the availability to transport CO_2 in a desired phase. Pipeline transport can be used for gas-phase, liquid-phase and two-phase streams, although the transport is most efficient when the CO_2 stream is dense. A high-density fluid occupies less volume compared to a gas, causing a dense stream to be desirable. The high-density condition is achieved when the CO_2 is transported as a liquid or as a supercritical fluid, established at temperatures of approximately 4 °C and pressures assuring single-phase. (Skovholt, 1993) and (d. Koeijer et al., 2017).

5.1.1 Challenges related to pipeline transport

Several important aspects should be studied carefully when considering pipeline transport. The diameter size, quality of material and pressure requirements are determined by the physical condition of the CO_2 stream. The fact that a CO_2 stream may be corrosive sets requirements to corrosion resistant material of high quality, while the desire to avoid two-phase flow determines the pressure and temperature condition within the pipeline. Further, the pipeline path is determined by the topography (Wildbolz, 2007).

Other important considerations are given in the following list (d. Koeijer et al., 2017):

- The probability of a dry-out zone near the well.
  Water is removed during CO_2 capture to reduce the risk of corrosion and hydrate generation in pipelines. The dehydration process is controlled by knock-out drums, which may cause the CO_2 to be too dry, leading to precipitation and a dry-out zone near the well.
- Impurities.
  A CO_2 stream may contain impurities such as hydrocarbons, nitrogen and oxygen, which affect the physical properties of the stream. Methane has lower density compared to CO_2, causing the phase diagram to change and the CO_2 stream to become less dense if mixed with methane. Water and oxygen will cause the CO_2 to become corrosive, while nitrogen will lower the stream's boiling point, leading to an increased possibility of two-phase flow.

- Decrease in injectivity.
  A reduction in injectivity may cause a rise in pipeline pressure and higher compression requirement.
- Accident or maintenance at pipeline or well.
  Accident or maintenance may cause a reduction of pressure and temperature in the pipeline. Low temperatures may result in ice and fractures, while a reduced pressure could cause depressurization.
- Corrosion.
  Corrosion may occur if there are water, oxygen or NO_x left in the captured CO_2 stream. Pipelines may in worst case be damaged.
- Dispersion of CO_2 into the atmosphere due to leakage.
- Blow-outs may happen if the well control is lost.

5.1.2 Economic perspective

Pipeline costs vary with time and place. **Fig. 5.2** illustrates the costs as a function of mass flow rate. It can be observed that offshore pipelines are most expensive and that an increase in flow rate will generally lead to lower costs.

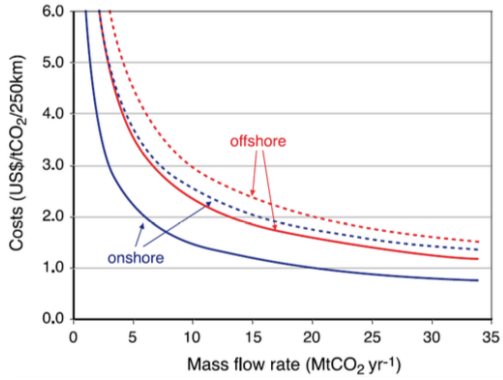

Fig. 5.2: Pipeline cost as a function of mass flow rate (d. Koeijer et al., 2017).

5.2 Ships

Ships have been used to transport liquefied petroleum gas, LPG, for a long time, and the gained experience have made it possible to design ships used for CO_2 transport. Ship transport make up a good alternative to pipelines. It is a flexible option which is needed when CO_2 sources are spread over large areas. Further, the growth in the CO_2 market is currently uncertain, making ships an economic option. (Aspelund et al., 2006).

Like pipelines, the most efficient way to transport CO_2 by ships is in the liquid phase. The size of a ship is determined by the pressure and temperature condition. Smaller ships are needed for pressure and temperature values near the triple point, while bigger ships are needed for medium pressures and temperatures, approximately 15 bars and -30 °C. (d. Koeijer et al., 2017).

5.2.1 Challenges related to ship transport

Fig. 5.3 shows the five processes included when CO_2 is transported by ship; liquefaction and gas conditioning, intermediate storage, loading, ship transport and offshore unloading (Aspelund et al., 2006). Gained experience from LPG transport have been transferred to most of these CO_2 processes, although there may still be some challenges regarding offshore unloading.

A brief description of the different processes, as well as several offshore unloading options, will be discussed in the following sections.

Fig. 5.3: Processes of ship transport (Aspelund et al., 2006).

As described previously in this thesis, the first step in a CCS process is to capture and separate the CO_2 from a produced gas stream. The concentrated CO_2 should have a high density and a low water content during the transport, which can be ensured by the liquefaction and gas conditioning process. During this operation, the CO_2 pressure and temperature are increased, and the stream is dehydrated. (Aspelund et al., 2006).

After the liquefaction process, the CO_2 can be stored in tanks until a ship is ready for transport. It is important that the carbon dioxide is stored at a pressure and

temperature level such that it contains a dense phase (Aspelund et al., 2006). The CO_2 is transferred from the storage tanks to the ship during the loading process.

There are three types of ships that can be used for CO_2 transport; fully pressurized ships, low temperature/fully refrigerated ships and semi-pressurized ships (Aspelund et al., 2006). Different ships are used for different pressure and temperature conditions, but the semi-pressurized ship is the most common one due to the fact that it keeps the CO_2 in a liquid phase. Such a ship is shown in **Fig. 5.4**.

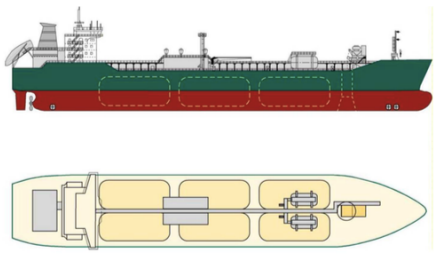

Fig. 5.4: Semi-pressurized ship design (d. Koeijer et al., 2017).

The last transport process is the offshore unloading operation. There are several ways to transfer CO_2 from a ship to a storage site. The first method is to use the submerged turret loading system, STL. The CO_2 is transferred to a platform via a riser and a pipeline before it is injected into the reservoir (Aspelund et al., 2006). The STL system is shown in **Fig. 5.5**.

Other methods include directly injection from the ship, injection via a FSI vessel and injection from a land-based terminal (d. Koeijer et al., 2017). **Fig. 5.6** illustrates these options.

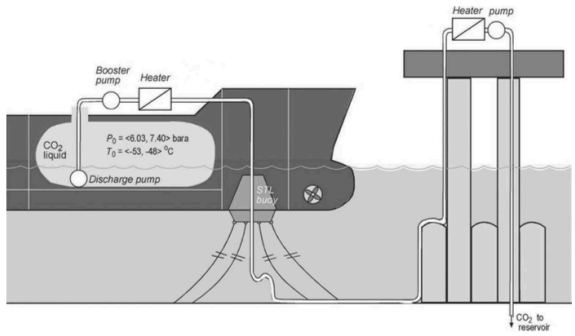

Fig. 5.5: Submerged turret loading (STL) system (Aspelund et al., 2006).

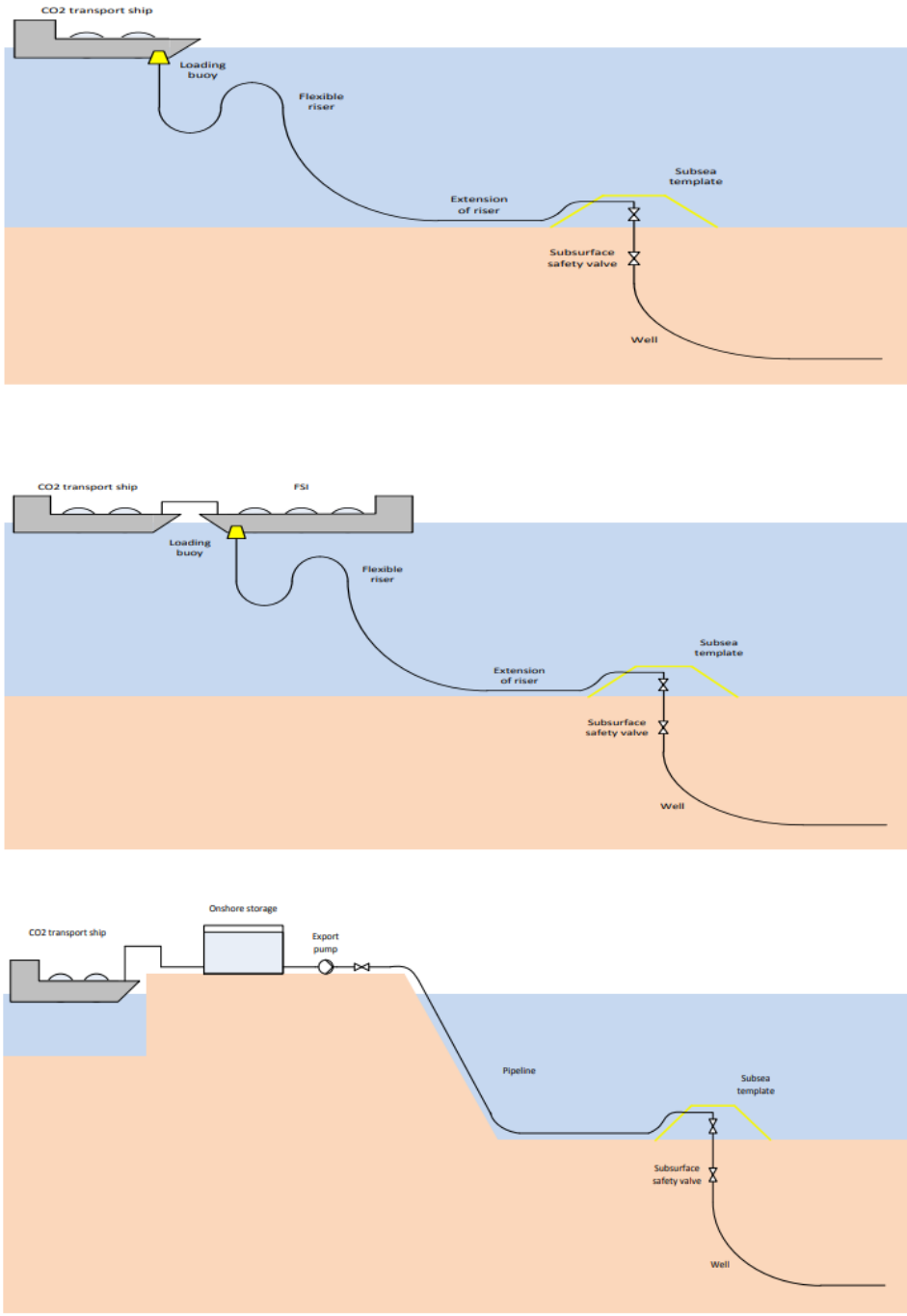

Fig. 5.6: Different offshore unloading systems (d. Koeijer et al., 2017).

5.2.2 Economic perspective

Ship costs vary with economic fluctuations. **Fig. 5.7** shows the costs as a function of distance. It can be observed that ship is the cheapest option for long-distance transport compared to onshore and offshore pipelines.

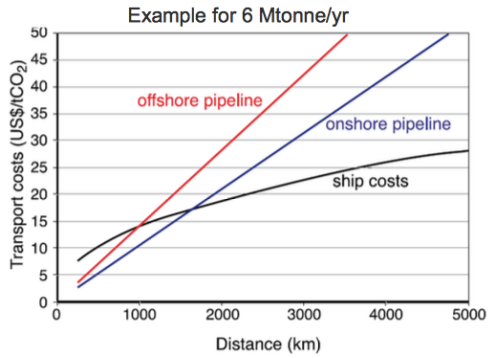

Fig. 5.7: Ship cost as a function of distance (d. Koeijer et al., 2017).

5.3 Road/railway

The last transport option, transport by truck or railway, is shortly described in this thesis. These alternatives have a much lower capacity compared to pipelines and ships, and are only good options on small scale and when flexibility is very important (Wildbolz, 2007). In general, transport by trucks or railways are uneconomical and not attractive compared to ship and pipeline transportation.

Chapter 6

CCS technology: CO2 storage

This chapter is modified from my semester project, CO_2 storage - Review of theory and literature (Brobakken, 2017).

If CO_2 storage is going to reduce the amount of greenhouse gases in the atmosphere, a billion metric tonnes must be captured and stored annually (Rutqvist, 2012). The storage has to be safe and long-term, setting requirements to several factors. A safe geological formation with the right pressure and temperature, where different trapping mechanisms work over time is necessary. Another important factor is the distance to the CO_2 source, which is closely related to the type of transport. Proximity to the CO_2 source will in general increase the storage opportunities (Cooper, 2009).

To collect the needed information to ensure safe CO_2 storage may take years and requires huge quantities of data. Luckily, there are some studied natural CO_2 accumulations in the world, making it easier to understand and compare the long-term CO_2 behaviour in a formation. The collected information makes it possible to recognize structures and formations suitable for storage. Several locations holding promise of safe storage over a geological period of time include depleted oil and gas reservoirs, deep saline aquifer formations, coalbed formations and storage in association with enhanced oil recovery (Cooper, 2009). These storage sites will be carefully discussed in section 6.2.

Three geological characteristics must be considered when analyzing a storage site; the capacity, containment and injectivity of the formation (Cooper, 2009). These factors will be discussed in the next section. Further, several trapping mechanisms prevent CO_2 migration out of the storage site, causing the storage to be safe. Different mechanisms will work over time, fixing long-term storage. The trapping mechanisms are an essential part of the storage operation and will be described in section 6.3. (Cooper, 2009).

Fig. 6.1 shows a typical time-line for a carbon capture and storage process. As can be seen, such a project consists of several operations which each may take years and decades to finish. This chapter focus on the post-closure operation, where the overall goal is to store CO_2 safely over a geological period of time.

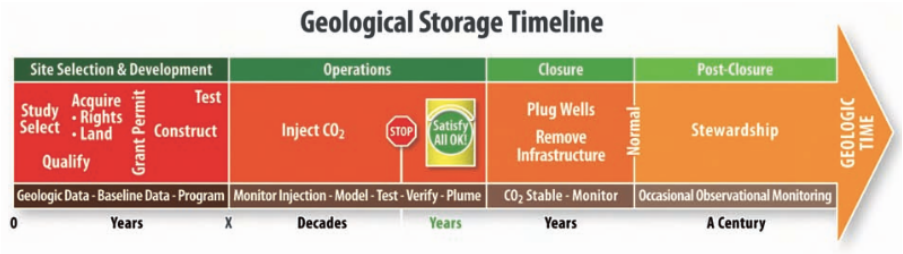

Fig. 6.1: Time-line for CO_2 storage operations (Cooper, 2009).

6.1 Geological characteristics

Several factors must be considered before storing CO_2 in the subsurface. Capacity, containment and injectivity are the three most important components determining whether a formation behaves as a good storage structure or not.

Another important factor is the storage depth with the respective temperature and pressure condition. As mentioned previously in this thesis, a proper storage site requires a depth of about 800-1000 m to ensure supercritical CO_2 and an efficient caprock. Storing the carbon dioxide as a supercritical fluid will be the most efficient and safest option, resulting in enhanced storage capacity and containment ability. (Cooper, 2009) and (Ringrose, 2017b).

6.1.1 Capacity

Capacity describes the available pore volume for CO_2 storage, in other words, the amount of CO_2 that can be stored in the respective formation. The capacity of a potential storage site depends on several factors; formation thickness, porosity, CO_2 density, area of storage structure and storage efficiency (Cooper, 2009).

The formation thickness determines how much of the porous media that can be used for storage. A thick formation will make it possible to store a larger CO_2 volume compared to a thin formation. A common requirement for storage sites is a thickness of approximately 20 m, depending on the formation continuity and quality (Cooper, 2009). Porosity describes the pore volume distribution in the formation, which highly affects the CO_2 volume. The higher porosity, the larger CO_2 volume may be stored in the formation. Generally, sandstones and carbonates contain the desired porosity for CO_2 storage (Rutqvist, 2012).

The CO_2 density is an important factor impacting the storage volume as well. As mentioned previously in the thesis, the density increases with depth, making the CO_2 density liquid-like at the preferred storage depth. When the carbon dioxide is in a supercritical phase, a greater volume can be stored in the pore space compared to CO_2 in a vapour phase. Further, the storage efficiency represents the effects of buoyancy, heterogeneity and sweep efficiency in a formation. It only considers the pore volume actually saturated with CO_2 and is commonly in the range of 0.5-5 %. (Cooper, 2009) and (Ringrose, 2017b).

In addition to the factors above, components such as pressure limitations, barriers and size of the storage complex make up important capacity constraints (Ringrose, 2017b). Pressure limitations such as maximum wellhead pressure and fracture pressure will affect the injected and stored CO_2 volume, while the formation size and its barriers may physically limit the storage capacity.

6.1.2 Containment

It is important to prevent leakage of CO_2 from storage sites. There is no point of storing carbon dioxide if it migrates out of the formation and into shallow groundwater or to the surface (Rutqvist, 2012). Ensuring that CO_2 is stored in a storage complex, also known as containment, depends on several factors; the seal geometry, rock distribution, pressure regimes and trapping mechanisms (Cooper, 2009).

Formations acting as safe storage sites are often found at a depth of approximately 800-1000 m where the seals are impermeable or low-permeable. Caprocks typically have a permeability of 1 nD to 1 mD, making it hard for a CO_2 stream to migrate (Ringrose, 2017e). A seal's rock distribution makes up another important factor affecting the storage containment. A caprock may be heterogeneous, creating both secondary storage opportunities and several migration barriers, or homogeneous, creating one large barrier. Evaporites, shales, anhydrites and salt beds are examples of effective seals (Rutqvist, 2012).

Faults and fractures in the seal will highly impact the storage containment. Presence of faults will not directly imply a leakage problem, but it is important to notice any fractures or faults that could cause CO_2 migration under present-time conditions (Cooper, 2009). An understanding of pressure and stress regimes in the subsurface is necessary to avoid reactivation or generation of faults and fractures. Such geological changes may occur if the pore pressure gets higher than the fracture pressure, which highly depends on the subsurface stress system.

Another containment mechanism is related to trapping mechanisms and fluid flow. Residual gas saturation describes the amount of immobile gas that is left behind in the pores due to gas migration. Density difference between the formation fluids causes the CO_2 to move. Some of the carbon dioxide may be left behind and trapped in pores, being immobile due to low permeability. This mechanism reduces the amount of CO_2 moving around in the subsurface due to accumulation in the pores, and will be further described later in this thesis. (Cooper, 2009).

6.1.3 Injectivity

The last important factor is injectivity, defined as the storage characteristics ensuring sufficient amount of CO_2 is being injected from the wellbore (Cooper, 2009). The amount of injected CO_2 depends on the permeability in the formation. A site with high permeability allows the fluid to flow rapidly through the pores because it is well connected. Ideally, CO_2 storage sites require a highly permeable zone near the wellbore, allowing the injected CO_2 to access the pores quickly (Cooper, 2009).

Although high permeability values are desired, formations with very high permeability may not be an advantage (Cooper, 2009). High-permeable pathways may lead to migration of the injected CO_2, reducing the storage efficiency and making the formation unsuitable for storage. Further, a geochemical reaction can affect the permeability as the injected CO_2 may react with the surrounding rocks in the subsurface. This may either cause an increase or decrease of the permeability.

6.2 Geological formations available for storage sites

In order for a geological structure to be used as a storage site, it must contain a porous basin and an impermeable rock working as a migration barrier. Such formations are often found near existing oil and gas fields, both onshore and offshore, and are often close to CO_2 sources (Cooper, 2009). Several structures may work as storage sites for CO_2 injection and the discussed options in this thesis are presented in **Fig. 6.2**.

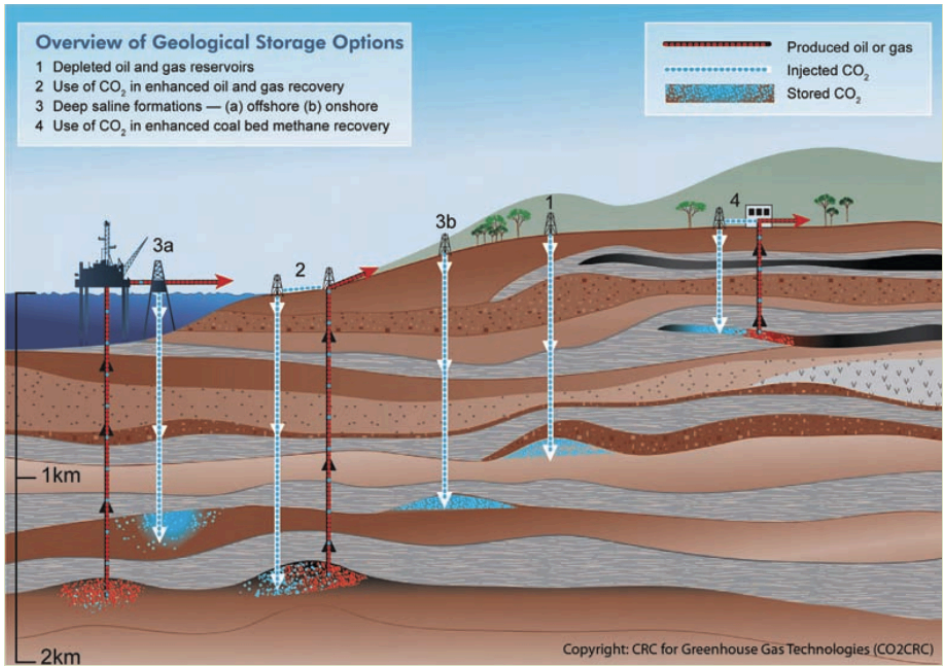

Fig. 6.2: Storage options (Cooper, 2009).

6.2.1 Depleted oil and gas reservoir

Depleted oil and gas reservoirs make up the most appealing sites for CO_2 storage (Li et al., 2005). The reservoirs consist of a porous basin, for instance a sandstone or carbonate rock, and an overlying impermeable caprock such as shale or salt. The caprock is essential for keeping the CO_2 stored in the subsurface, while the reservoir basin must have a certain porosity and permeability to be able to store CO_2 in the pores. Platform 1 in Fig. 6.2 shows CO_2 injection in a depleted oil and gas reservoir.

Advantages

There are several reasons why depleted hydrocarbon fields are the most practical solutions for CO_2 storage. First, these reservoirs have been extensively characterized and thus have a lot of data available for analysis and understanding of CO_2 behaviour in the formation (Cooper, 2009).

Further, depleted reservoirs contain suitable pressure regimes for CO_2 storage. The pore pressure will decrease when a reservoir is being depleted, for instance during production. The low reservoir pressure allows a refilling of the field up to its original pressure, which will happen when CO_2 is being injected (Loizzo et al., 2010).

Another advantage is the existing knowledge and experience regarding CO_2 injection into hydrocarbon reservoirs. Injection of carbon dioxide is a widely used technique for enhanced oil recovery, EOR, making it possible to adapt experience from such operations to guide injection for CO_2 storage. In addition, depleted reservoirs often have available infrastructure such as wells and pipelines that may be reused. This will make it easier and faster to run a CO_2 injection process. (Cooper, 2009) and (Li et al., 2005).

Challenges

Although depleted reservoirs are considered to be good options for CO_2 storage, there are some factors that may cause difficulties when injecting into these geological sites. As mentioned, an advantage with these reservoirs is the available equipment that can be reused. Even though the accessible equipment will reduce the operational costs, the expenses may increase due to necessary improvements such as higher pressure rating, corrosion resistant material and pumping equipment (Loizzo et al., 2010). Further, there is shown that 5-20 % of all wells may leak, which will make the CO_2 injection much more complex (Loizzo et al., 2010).

Other important factors are the injectivity pressure and temperature. As shown in Fig. 2.1, the CO_2 needs a high temperature to be in a dense phase. This may be problematic for most types of wellheads, because such a temperature may be out of their range. Further, to be able to inject the CO_2 safely, an acceptable downhole pressure has to be achieved. This downhole pressure depends on several components, for instance the CO_2 density. When CO_2 is injected as a dense fluid, the hydrostatic pressure will increase, resulting in a downhole pressure rise. Whether the CO_2 is injected as a vapour or as a dense fluid highly impacts the downhole pressure difference, also known as the injectivity gap. This gap is important considering the injection efficiency. If the CO_2 is injected as a vapour phase, larger volumes must be injected compared to injection of CO_2 as a dense phase (Loizzo et al., 2010).

A large difference between the pore pressure and the pressure of the injected CO_2 may cause complex scenarios. Especially two issues are considered: failure

of the reservoir or/and the caprock, and cooling of the reservoir. A high flow rate may cool the reservoir, making it brittle and easy to fracture. A colder reservoir will also cause a less dense CO_2, which will reduce the amount of stored carbon dioxide (Loizzo et al., 2010). The reservoir and the caprock may also fracture if the injection pressure is too high.

The geological containment requires some consideration as well. The pore pressure will decrease when hydrocarbons are being produced, making a pressure margin available for re-pressurization. Although a large amount of pore space is available for storage, the production may have caused some changes in the seal capacity, rock properties, thermal and chemical destabilization, which will make it harder to store the CO_2. The low pore pressure may also increase effective stresses in the reservoir causing a compaction, which can result in lower porosity and permeability (Loizzo et al., 2010).

6.2.2 Deep saline aquifer formations

Platform 3a and 3b in Fig. 6.2 show CO_2 injection into deep saline aquifer formations. Such formations are widely spread all over the world and have the largest potential for CO_2 storage in terms of duration and volume. They are often in proximity to CO_2 capture sites, making them efficient and profitable for storage.

There are different variants of deep saline aquifer formations including aquifers in the same stratigraphic structure as an oil and gas reservoir, aquifers above or below reservoirs and aquifers far away from reservoirs. The Norwegian carbon capture and storage projects Sleipner and Snøhvit, located in the North Sea and in the Barents Sea, are examples of deep saline aquifer formations lying respectively above and below hydrocarbon reservoirs (Cooper, 2009).

CO_2 storage in a deep saline aquifer is mainly affected by the characteristics of the aquifer, the caprock and the storage operations. These factors have to be carefully considered before CO_2 is injected for storage, as they highly affect the storage efficiency. The following sections will describe the components impacting a saline aquifer formation, with the main emphasis on aquifer characteristics.

Affecting factors related to the aquifer

An aquifer's size and boundaries highly affect a CO_2 storage as it will be the first factors controlling the storage capacity. A closed aquifer, shown at the bottom in **Fig. 6.3**, consists of boundaries preventing fluid migration. When CO_2 is injected into this type of aquifer, the CO_2 will be stored due to compressibility of the brine and matrix. The CO_2 stream will rapidly reach the boundaries, and the formation pressure will quickly build up due to the captured fluids. The only way CO_2 can be kept injected into a closed aquifer is if some of the water leaks

out through the caprock. In such case, the aquifer will be semi-closed, allowing brine to migrate but preventing CO_2 movement out of the storage site. A totally closed aquifer will have a limited storage capacity resulting in a lower storage efficiency. (Bachu, 2015) and (Birkholzer et al., 2015).

In an open system, shown at the top in Fig. 6.3, the aquifer may be laterally open and vertically closed by a caprock. In such an aquifer, the CO_2 accommodation will be generated due to water displacement. The formation water will mainly migrate in the lateral direction, although some of it may leak through the overlying caprock (Bachu, 2015). The brine migration will cause the pressure buildup to be slower in an open system compared to a closed system, but the pressure may propagate far within the formation, affecting the storage capacity (Birkholzer et al., 2015). The storage efficiency is in general better in an open aquifer.

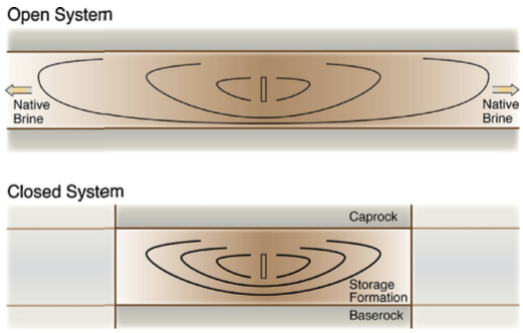

Fig. 6.3: Open and closed system (Birkholzer et al., 2015).

The driving forces and the CO_2 properties are other factors impacting the storage capacity. The CO_2 flow is determined by the buoyancy and hydrodynamic forces, as well as the difference in mobility between the injected CO_2 and the existing brine (Bachu, 2015). These differences cause the CO_2 to rise and spread on top of the aquifer, and thus affect the storage efficiency. The efficiency will increase when the mobility ratio and the buoyancy forces are low.

Irreducible water and CO_2 saturation will obviously impact the storage efficiency, as well as the capillary entry pressure in caprocks (Bachu, 2015). As the amount of water decreases in the aquifer, the storage capacity increases due to more available pore space for CO_2 storage. In addition, characteristics such as aquifer thickness, permeability, porosity and heterogeneity affect the storage efficiency. An aquifer with high porosity and permeability values will have a high efficiency. Furthermore, a thin aquifer will have better sweep efficiency, thus better storage efficiency, compared to a thick reservoir (Bachu, 2015).

Factors such as downhole pressure, temperature and salinity also affects the efficiency. When pressure rises and temperature drops, the density and viscosity of

both CO_2 and brine will increase. This will affect the buoyancy and the mobility ratio, and thus the storage efficiency. For instance, higher pressure will cause a reduction in buoyancy and mobility, resulting in a higher storage efficiency. Further, the salinity will affect the brine density and viscosity. When the salinity increases the water density and viscosity will rise, causing higher buoyancy and mobility, hence a lowered storage efficiency (Bachu, 2015).

Affecting factors related to caprocks

There are mainly two important factors affecting the storage efficiency when considering seal characteristics; permeability and capillary entry pressure (Bachu, 2015). Caprocks have to be low-permeable or impermeable to prevent migration of the CO_2. Further, a lower capillary entry pressure will make CO_2 movement out of the storage site harder, resulting in a better storage efficiency.

Affecting factors related to well operations

Storage operation properties such as injection rate, duration and number of wells will also influence the efficiency. For instance, as the number of injection wells increase, the storage efficiency increases, but fewer wells will be an advantage considering CO_2 containment (Loizzo et al., 2010). Further, the pressure will increase when CO_2 is injected. This could cause the caprock to fracture, resulting in CO_2 leakage and inefficient storage.

6.2.3 Storage in association with Enhanced Oil Recovery, EOR

Another option for CO_2 storage is storage in association with enhanced oil recovery, EOR. Reservoirs using CO_2 injection for increased oil production have the porous basin and the impermeable caprock required to store both oil and CO_2. Platform 2 in Fig. 6.2 shows such a storage alternative. Due to the increased focus on climate change, it is shown that CO_2-EOR can be a good solution for CO_2 storage. (Ringrose, 2017f).

Oil production typically includes three main phases; primary production, secondary recovery and tertiary recovery (Heidug et al., 2015). The primary production includes the natural production of oil where oil flows in the low-pressure direction to the production well. The secondary recovery covers injection of immiscible substances causing the pressure to rise without mixing with the oil. The tertiary recovery includes processes such as maintaining of pressure, change in oil properties and flow patterns to increase the production. To be able to change properties and patterns, the injected substance must interact with the reservoir fluid. CO_2 is a good example of such an injection substance. In this section, the focus will be on the tertiary recovery stage, where CO_2 is used for EOR and storage.

Advantages

CO_2 storage in association with EOR is a cost-effective and available solution due to the existing infrastructure, experience and knowledge. The main advantage with the CO_2-EOR method is the combination of increased oil production and storage of carbon dioxide (Ringrose, 2017f). Carbon storage in combination with EOR would increase the possibility of prolonging the lifetime of the oil production.

Especially the USA argues that CO_2-EOR is an essential solution to reduce the world's carbon emissions. CO_2 becomes a valuable product due to the increase in oil production, and not a simple waste product. Further, CO_2-EOR will allow growth of developing countries as they can use their fossil fuels combined with reduced CO_2 emissions (Ringrose, 2017f). The CO_2-EOR method may also work as a bridge between the currently low-leveled action and the work required to reduce the amount of greenhouse gases.

Challenges

When CO_2 is used for EOR, some of the carbon dioxide is produced at the production well, while a significant part is left behind in the reservoir. Unfortunately, the CO_2 that is left behind is only stored temporarily due to continuous injection of substances maintaining the reservoir pressure and increasing the oil production. To be able to increase this stored amount and thus extend CO_2-EOR to CO_2 storage, four main activities must be included; site characterization and risk assessment, measurement of emissions, surveillance of the field and changed abandoned processes (Heidug et al., 2015).

Site characterization and risk assessment are important activities considering the possibility for CO_2 leakage. Thus, it is necessary to collect information about the caprock and eventual wellbores. Another pre-operational activity is to measure emissions from equipment. Monitoring of the field during and after CO_2 storage is necessary to identify any leakage and is discussed later in this report. After the CO_2 has been stored, appropriate abandonment processes are required to guarantee safe CO_2 storage for a long time. These activities will increase the amount of stored CO_2 in an EOR process, but they will also increase the costs.

Another challenge with CO_2-EOR is the huge amount of CO_2 needed to make such an operation beneficial for the environment. The combination of CO_2 storage and enhanced oil recovery will not result in negative emissions, meaning that there will be produced more CO_2 than the stored amount during an EOR operation. Optimized CO_2-EOR could result in a neutral CO_2 footprint, meaning that the amount of stored CO_2 is equal to the amount of produced carbon dioxide (Ringrose, 2017f).

6.2.4 Coalbed formations

The Earth consists of significant quantities of coal, and a coalbed formation has the potential to store large volumes of CO_2. A coal seam may therefore be a good alternative for CO_2 storage. Such a storage is often combined with CO_2 coalbed methane recovery, CO_2-ECBM, which is an emerging technology combining improved efficiency and profitability of methane recovery and CO_2 storage (Shi and Durucan, 2005). Platform 4 in Fig. 6.2 shows such a storage option. This thesis will mainly focus on CO_2 storage in coalbeds, but it is necessary to discuss some aspects of methane recovery as well.

Injection of CO_2 for enhanced recovery of both oil and gas is a well-developed technology, and CO_2-ECBM is broadly equivalent to EOR. The contrast is that coal seams work both as reservoir and source rock, making the storage operations different for coalbeds compared to oil and gas reservoirs (Shi and Durucan, 2005).

Coalbeds can be highly porous due to their porous structure and natural fractures, called cleats. The fractures are divided into butt cleats and face cleats, as shown in **Fig. 6.4**. The face cleats are often continuous throughout the formation, whereas the butt cleats are discontinuous. The pore structure within a coalbed can vary a lot and is said to be heterogeneous. It is important to determine the pore volume and the pore distribution to understand how the CO_2 is stored in coal seams (Shi and Durucan, 2005).

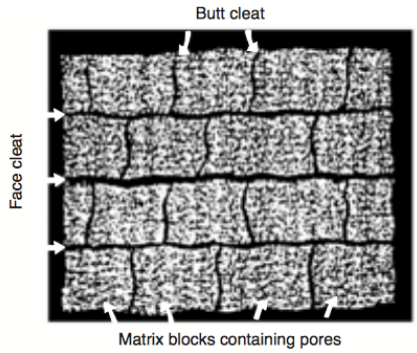

Fig. 6.4: Natural fractures in coalbeds; face cleats and butt cleats (Shi and Durucan, 2005).

Storage mechanisms in coalbed formations

There are mainly three mechanisms determining the CO_2 storage in coalbed formations; adsorption, absorption and storage within fractures and pores. Adsorption accounts for up to 95-98 % of the gas stored in coalbeds and is thus the main

storage mechanism. Gas can be adsorbed on the internal surface, primarily in the micropores, which contain significant space for storage. The fact that coal can adsorb twice as much CO_2 volume as methane, makes it possible to store large volumes of carbon dioxide in coalbeds (Shi and Durucan, 2005). Gas may also be stored within the molecular structure or within pores and fractures. The injected CO_2 will then be physically trapped in the cleats.

Several processes will start to occur when CO_2 is being injected into a coalbed formation. An undisturbed coalbed is often saturated with water. During methane production, this water will be produced, and the coalbed will eventually behave as a dry gas reservoir containing methane. When CO_2 is being injected, it will displace the methane due to its higher adsorption capacity in coal (Shi and Durucan, 2005). The desorption of methane will cause the matrix to shrink, while the absorption of CO_2 will cause the matrix to swell. This will highly affect the storage capacity in coal seams.

The understanding of the CO_2 behaviour in a coalbed formation is very incomplete, but there are several hypotheses trying to explain the processes that occur after a CO_2 injection and thus influence the storage capacity. Some of the hypotheses are shown in the following list (White et al., 2003);

- The coal will plasticize.
  Coals can exist as two states, either as a glass-like phase or as a rubber-like phase, depending on temperature and other factors. A glassy coal is brittle and the diffusion is slow, while a rubbery coal is flexible and has a fast diffusion. The temperature causing the coal to transform is called the glass-to-rubber transition temperature, T_g. T_g could decrease when CO_2 is injected into a coalbed, due to swelling caused by the injection. The CO_2 will act as a plasticizer causing the coal to turn into the rubber state by rearranging the structure, and the diffusion to become more rapid.

- Swelling.
  As mentioned, the coal will start to swell when CO_2 is injected due to the desorption of methane and absorption of carbon dioxide. A hypothesis is that the absorption effect is greater than the shrinkage effect, causing the coal to swell. The change in matrix will highly impact the permeability, which will decrease during swelling and increase during shrinkage, and thus affect the storage capacity.

- Molecule movement.
  Interactions between macromolecules will break during coal swelling, and will be replaced by interactions between CO_2 and macromolecules. Trapped molecules will be released and transported with the flowing CO_2 through the coalbed.

- Minerals dissolve in acidic formation water.
  A large amount of the minerals found in coal are soluble in acidic water solutions. When high-pressure CO_2 is injected, the CO_2 will dissolve in the

formation brine, causing minerals such as Ca and Mg to be removed from the coal. These minerals will flow with the CO_2 throughout the coalbed.

- Precipitation of compounds.
  There will be a pressure drop throughout the coalbed, causing the CO_2 to flow in the low-pressure direction. Areas with original high permeability will become low-permeable due to swelling and the coal's pressure will decrease. This will cause the extracted compounds to precipitate and plug the pores, which will increase the pressure, CO_2 density and solubility.

As mentioned, CO_2 storage in coal seams with enhanced methane recovery could potentially be a good storage site, storing large volumes of greenhouse gas. To achieve a safe and efficient storage, it is important to consider environmental aspects with this site. A coalbed reservoir contains several possible leakage paths such as faults, fractures, caprock failure, wellbore failure and CO_2 dissolved in groundwater (Shi and Durucan, 2005). Thus, it is important to inject CO_2 with an appropriate pressure which prevents caprock fracture and maintains the sealing capacity.

6.3 Trapping mechanisms

After the CO_2 has been injected into a geological structure, it should stay there for a long time. The injected CO_2 is stored in a storage site by different trapping mechanisms, involving both geochemical and physical factors. These mechanisms make sure that the CO_2 stream does not migrate, making them very important for the storage. Different types of mechanisms such as structural trapping, stratigraphic trapping and geochemical trapping are often active within the same reservoir, but at different degrees. (Cooper, 2009).

The physical trappings described in this report include basin-scale processes, geometry trapping and fluid flow processes, while the geochemical mechanisms involve several CO_2 reactions such as dissolution in formation water, CO_2 precipitation and CO_2 absorption. **Fig. 6.5** illustrates that different trapping mechanisms work at different times, which will increase the storage security. Physical trapping will affect the storage mostly the first years after injection but will have a great effect for thousands of years. Solubility and mineral trapping are mechanisms that will gradually fix long-term CO_2 storage in the subsurface. (Ringrose, 2017b).

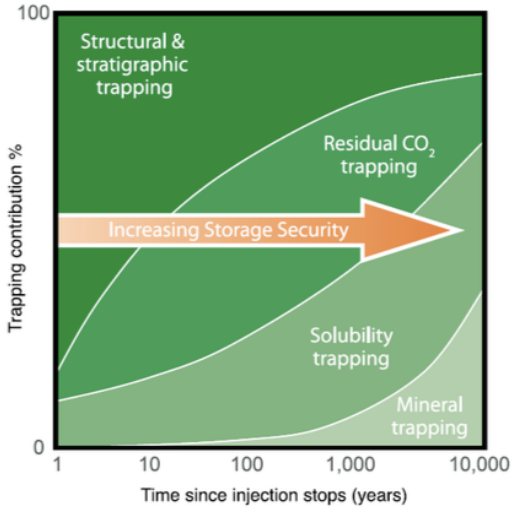

Fig. 6.5: Trapping mechanisms over time (Ringrose, 2017b).

6.3.1 Physical trapping mechanism: Basin-scale processes

Looking at the whole basin is important when considering a formation for CO_2 storage. To understand how CO_2 can be stored is essential for such an operation. Regional structures, history and pressure regimes are factors that should be considered when analyzing storage sites. These characteristics will greatly impact the fluid flow and trapping mechanisms, which again determine the efficiency of the storage site. (Cooper, 2009).

A storage site is often part of a larger system containing a porous basin and an impermeable caprock. Such storage systems will require studies of migration and trapping mechanisms to determine the storage efficiency. In addition, the hydrogeological systems, meaning the movement of groundwater, are important for determining the reservoir's connectivity (Cooper, 2009). A typical storage site is seen in **Fig. 6.6**, consisting of aquifers, aquitards and aquicludes.

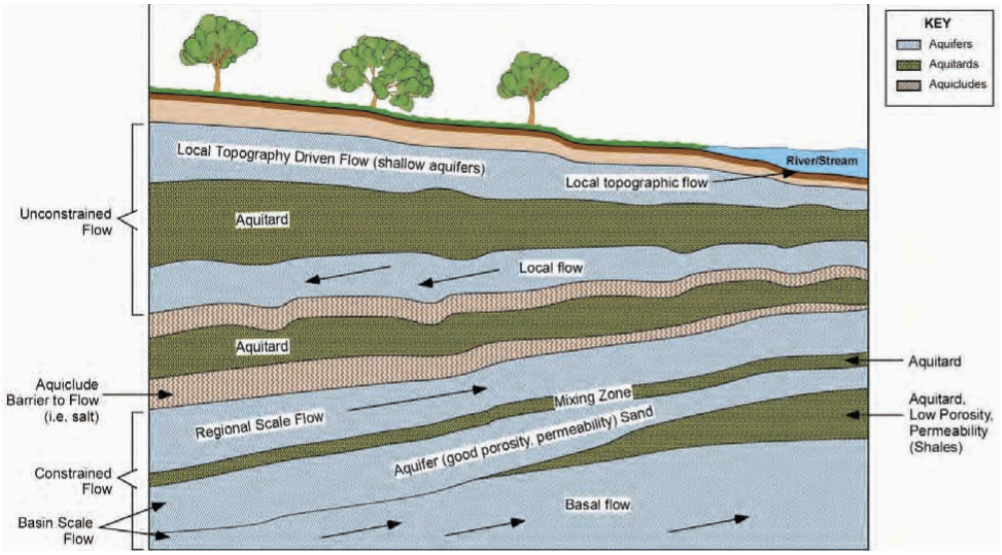

Fig. 6.6: Hydrogeological system (Cooper, 2009).

Aquifers are permeable and highly porous units that allow water to flow through the formation. Sandstones, limestones and dolomites are examples of rocks working as aquifers. Aquitards have lower permeability compared to aquifers, causing a limited flow through the formation. Although the values for porosity and permeability are low, aquitards can still allow some flow into surrounding aquifers over time. Aquicludes are units with really low permeability that do not allow any flow through the formation. Thus, these zones will act as flow barriers. Evaporites are an example of such aquicludes. (Cooper, 2009).

The recharge and discharge area of a hydrogeological system will affect how the fluids flow within the formation, impacting the flow rate and direction. Such a system can either be defined as regional, local or intermediate. A regional reservoir will recharge at huge topographic heights, while discharge at major topographic basins. A local reservoir will recharge at local heights and discharge at local basins, while an intermediate reservoir combines the characteristics of the two flow systems (Cooper, 2009). In addition to fluid flow systems, porosity and permeability are essential factors that must be considered when choosing storage sites (Cooper, 2009).

6.3.2 Physical trapping mechanism: Geometry of traps

Structural and stratigraphic traps are both examples of physical trapping mechanisms. Due to a combination of permeable and impermeable rocks and structures, these traps often prevent migration of CO_2, making the storage of CO_2 safe and efficient (Cooper, 2009).

Structural traps include different types of faults and anticlines. Faults will enclose a region, preventing fluids from migrating out of this area. Anticlines consist of folds surrounded by impermeable rocks, making CO_2 storage possible. (Cooper, 2009).

Stratigraphic traps include lateral facies changes, unconformities and pinch-outs. Facies change include areas where permeable and impermeable layers are alternating, causing no migration of formation fluids. Pinch-outs and unconformities erode permeable and porous material, causing a direct contact to a low-permeable layer. This impermeable layer will act as a flow barrier trapping the fluids. (Cooper, 2009).

6.3.3 Physical trapping mechanism: Fluid flow processes

Geological structures working as storage sites are concealed by an overlying caprock. This caprock has often low permeability and porosity, which causes the pores to be narrow. Small pore throats can generate a capillary seal preventing the CO_2 to move, thus the CO_2 will be trapped in the reservoir. **Fig. 6.7** shows such a scenario. The caprock consists of small pores making it impossible for the CO_2 to migrate from the reservoir rock and into the seal. In addition, the caprock often contains formation water creating an interfacial tension between the brine and the CO_2. Both the capillary forces and the interfacial tension will trap the CO_2 in the reservoir (Cooper, 2009).

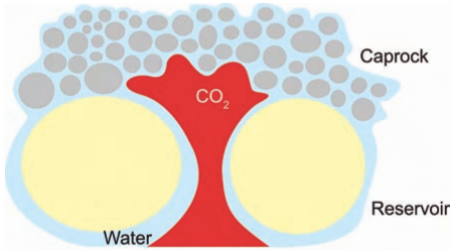

Fig. 6.7: Capillary forces (Cooper, 2009).

Another trapping mechanism occurring due to fluid flow is residual gas trapping. As the CO_2 migrates in the subsurface, the ratio between CO_2 and water will change. Gas trapping will occur when the water saturation increases and the CO_2 saturation decreases. In other words, when the amount of water in the pores is much higher than the amount of CO_2. Some of the carbon dioxide will be left behind in the pores as the rest of the fluid migrates. The left-behind CO_2 will have a very low permeability, causing this CO_2 to be in an immobile residual phase. The gas trapping may limit the size of the migrating CO_2 plume and thus work as an efficient storage mechanism (Cooper, 2009). The residual CO_2 trapping mechanism is illustrated in **Fig. 6.8**.

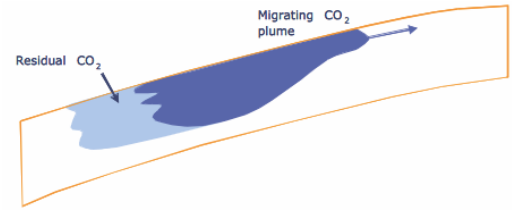

Fig. 6.8: Residual CO_2 trapping (Cooper, 2009).

6.3.4 Geochemical trapping mechanism: CO2 dissolution in brine

When CO_2 is injected into a deep saline aquifer it will migrate upwards until it reaches the caprock. The migration is caused by the buoyancy force, also known as the difference between brine and CO_2 density. The CO_2 will accumulate and create a plume in the aquifer, which will extend laterally due to the impermeable caprock. Some of the CO_2 will be dissolved in the formation brine during the migration. This mechanism is defined as solubility trapping and is one of the main trapping mechanisms in aquifers (Suekane et al., 2007).

The solubility trapping is important for CO_2 storage, but the effect can vary enormously in the aquifer. In the CO_2 plume, brine and CO_2 coexist, causing the dissolution to be in equilibrium (Suekane et al., 2007). In the aquifer, the amount of water exceeds the amount of CO_2 making the dissolution slow.

6.3.5 Geochemical trapping mechanism: Mineral trapping

When CO_2 is dissolved in the formation water, a weak carbonic acid is generated. This acid can react with the surrounding minerals and create solid carbonate minerals. Depending on the strength of the acid, this process can either happen rapidly or slowly. However, mineral trapping binds the CO_2 to the formation and thus increases the storage efficiency. (Cooper, 2009).

6.3.6 Geochemical trapping mechanism: CO2 adsorption in clay minerals

When CO_2 is being injected into a coalbed formation, the main trapping mechanism will be adsorption. As mentioned earlier in this thesis, CO_2 can be adsorbed on the internal surface, as can be observed in **Fig. 6.9**. This adsorption will cause the coal to swell, which highly affects the storage capacity in these formations (White et al., 2003).

CO_2 injection in a coal seam is often associated with enhanced methane recovery. Due to the fact that a coalbed formation can adsorb twice the volume of CO_2 compared to methane, the adsorption of CO_2 will cause swelling of the matrix, while the desorption of methane will cause shrinkage (White et al., 2003). This will impact the storage efficiency.

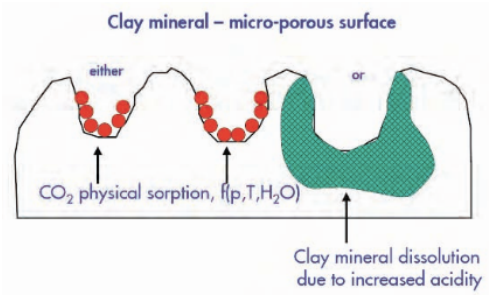

Fig. 6.9: CO_2 absorption in clay minerals (Cooper, 2009).

Chapter 7

Geological storage integrity

This chapter is modified from my semester project, CO_2 storage - Review of theory and literature (Brobakken, 2017).

When CO_2 has been injected into a storage site it should stay there for a long period of time. To be able to achieve this, it is necessary to ensure long-term integrity of the geological storage complex and the wellbore. Monitoring of the subsurface is an important method considering observation and control of the storage site. It can be used to observe CO_2 movement in the storage complex, making it possible to detect any unwanted processes. Different monitoring techniques will be described in the following section, while wellbore integrity will be discussed in the next chapter.

To be able to ensure integrity of a geological storage complex it is necessary to consider the relevant geological system. Such a system often consists of the storage formation, the caprock, surrounding and hydraulically areas and spill points. A typical offshore storage complex is illustrated in **Fig. 7.1**.

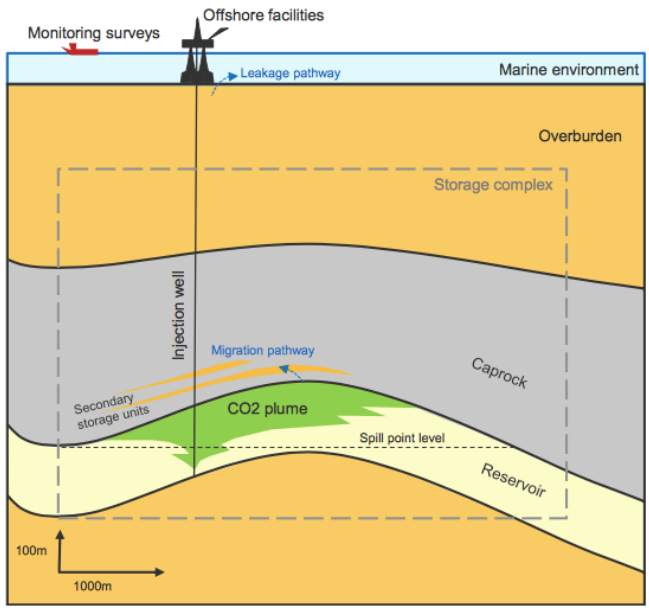

Fig. 7.1: Storage complex relevant to containment (Ringrose, 2017e).

Three factors are important to study when geological storage integrity is considered; the caprock, capillary trapping and rock mechanics. The caprock, shown as the grey layer in Fig. 7.1, has to be impermeable and without fractures to prevent migration of CO_2. A permeability between 1 nD and 1 mD is desirable, and the fracture pressure must not be exceeded (Ringrose, 2017e). Further, a caprock may be heterogeneous. Due to the heterogeneity, both secondary storage sites and multiple barriers may be created, ensuring long-term storage. Capillary mechanisms will cause the CO_2 to be trapped below the overlying caprock, while preserved rock mechanics will prevent the CO_2 from migrating.

7.1 Monitoring of the storage site

Different monitoring techniques can be used to observe CO_2 propagation in the storage complex and hence, any undesirable processes can be noticed. Monitoring can take place on the surface and in the subsurface. Surface monitoring may include soil gas, gas/water chemistry, CO_2 soluble tracers and biology, whereas downhole monitoring can include seismic surveys, gravimetry surveys, pressure and temperature monitoring, downhole geophones and saturation logging. (Ringrose, 2017d). The different monitoring techniques are described next.

7.1.1 Surface monitoring

Surface geochemical monitoring can be used to detect CO_2 leakage from the storage site. This is a complicated operation mainly due to the natural occurrence of CO_2 in the subsurface. Natural sources of carbon dioxide, such as organic carbon and groundwater degassing, generate fluctuating CO_2 streams, making it hard to detect leakage from an injection. Further, placing surface detectors near a possible leakage point is difficult. (Ringrose, 2017d).

However, several surface monitoring techniques can be used to detect possible leakage from the injected and stored CO_2; infrared gas analyzer, light detection and range finding, accumulation chamber and eddy covariance. The infrared gas analyzer, IRGA, can be used to measure CO_2 concentration in soil or in the atmosphere. The light detection and range finding, LIDAR, measures trace atmospheric gases. The accumulation chamber measures the CO_2 flux rising from the soil, while the eddy covariance method measures the atmospheric CO_2 concentration at a particular height over ground. (Ringrose, 2017d).

7.1.2 Downhole monitoring

Downhole monitoring is important for understanding CO_2 movement and reactions in the storage formation. It can be used to detect formation changes such as reactivation of faults and fractures, as well as CO_2 leakage. (Ringrose, 2017d).

Seismic surveys can be used to get an image of the subsurface. Lateral formation changes can be detected, large-scale features can be observed and a distribution of rock characteristics can be specified (Ringrose, 2017d). 3D and 4D seismic constitute valuable monitoring techniques in a carbon capture and storage project, giving useful information about the geology.

Gravimetric surveys measure the density change in a formation. Such monitoring may therefore give information about CO_2 distribution in a storage site, as the carbon dioxide will displace the formation fluid and change the fluid density in a specific area (Ringrose, 2017d).

Pressure and temperature monitoring can be used to get a better understanding of the formation connectivity, as well as observing the reservoir performance (Ringrose, 2017d). Downhole gauges measure the wellbore pressure at fixed time intervals, making it possible to pay attention to a reservoir's condition.

CO_2 detection techniques include carbon isotopic composition, bulk gas chemistry, groundwater chemistry and tracers. Carbon isotopic composition of CO_2 can be used to detect CO_2 from injection. C^{13} and C^{14} are naturally occurring carbon isotopes in the subsurface, and by detecting these isotopes it is possible to separate the injected CO_2 from the natural carbon. Bulk gas chemistry is used to determine the origin of CO_2 and hence detect whether the CO_2 is fossil-fuel derived or not. Groundwater chemistry can give information about CO_2 influence on the formation water, while tracers make it possible to recognize the injected CO_2. Nobel gases are commonly mixed with the CO_2 stream and thus used as tracers, making it possible to detect leakage of injected CO_2. (Ringrose, 2017d).

As can be understood, monitoring of the storage complex is an important part of a carbon capture and storage process. It ensures secure site operations and long-term storage by giving important information about the subsurface situation.

Chapter 8

Well design and wellbore integrity

This chapter is modified from my semester project, CO_2 storage - Review of theory and literature (Brobakken, 2017).

Storing CO_2 is a complex process that highly impacts the wellbore design. Since CO_2 is corrosive in contact with water, factors such as type of material, cement and well hardware will be different when injecting carbon dioxide compared to other injections. A CO_2 injection may also cause specific issues that must be considered when designing the well. Difficulties such as reactions between CO_2 and formation water, thermal effects, rock mechanical effects and field heterogeneity effects must all be carefully thought through in the planning of such an injection well (Ringrose, 2017c).

Although designing an injection well for CO_2 storage can be complex, the petroleum industry has a lot of experience from designing production wells and different injection wells. In addition, wells used for CO_2-EOR have been successfully drilled for over 35 years (Cooper, 2009). The existing experience and knowledge are valuable when designing a CO_2 injection well that must ensure operational reliability, long-term capacity and safe operation (Ringrose, 2017c).

Fig. 8.1 shows an illustration of a typical CO_2 injection well. The well should ensure safe and efficient carbon dioxide injection throughout the whole injection process. A standard CO_2 storage operation consists of four main stages constituting a well's life time; selection of site and development, operation, closure and post-closure (Cooper, 2009). The different stages contain different activities and issues that will be discussed in the following sections.

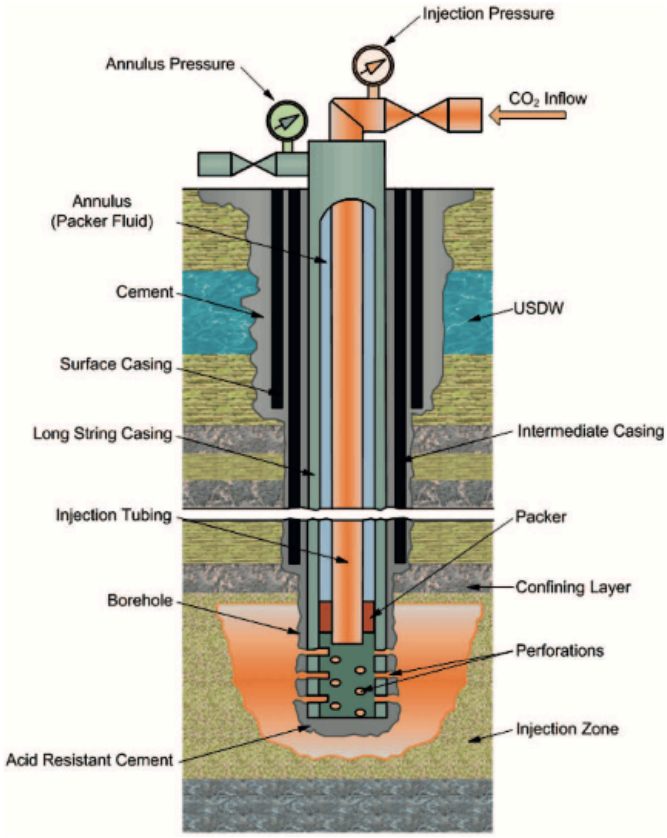

Fig. 8.1: CO_2 injection well (Gaurina-Međimurec and Pašić, 2011).

8.1 Site selection and development

8.1.1 Site selection and basis for well design

Previous sections have described important aspects considering a storage formation. Factors such as reservoir heterogeneity, rock mechanical effects, CO_2-brine reactions and thermal effects must be carefully studied when a CO_2 injection is planned (Ringrose, 2017c). These factors are essential when considering a site selection for CO_2 storage.

The well placement is the first important choice when determining the design of an injection well. Good reservoir quality, completion intervals, type of well and plume migration are important considerations regarding effective use of storage space (Ringrose, 2017c).

The next step in the process is to establish a basis of design, which is a guide for wells and their design to meet the defined requirements. This guide should for instance cover the construction and completion of a well, in addition to the operation and abandonment processes. The following list covers other important considerations that should be included in a basis of design (Cooper, 2009);

- Duration and general information about the stages.
  It is important to know the expected time of each stage. The operation period will for instance be relatively short compared to the closure and post-closure period, which will affect the decision regarding materials. It is also important to know how the pressure develops during different operations, as well as the risk of leakage.
- Injection parameters.
  Parameters such as injection rate and pressure, saturations of the reservoir fluids, injection volume, viscosity and content of the injected fluids are necessary information. The injection pressure depends on numerous subsurface factors including reservoir depth, storage capacity, plume behaviour, overburden properties and regional aquifers (Ringrose, 2017c).
- Information about wells.
  The type and number of wells, as well as performance efficiency must be described.
- Type of completion.
  This point should describe the completion type that provides injectivity and optimizes the number of penetrations.
- Barrier components.
  Multiple barriers should be established to provide isolation; barriers between each geological interval, between well annuli and between wellhead and external environment (Ringrose, 2017e). Information about the cement, tubulars and wellhead system used for the injection is thus required.

- A corrosion program.
  The accepted corrosion level of wells and other equipment should be stated for each stage.
- Safety requirements.
  Safety requirements for surface and downhole conditions should be specified.
- Service.
  Well maintenance should be considered regarding the well integrity and when choosing materials.

8.1.2 Selection of materials used for well design

As mentioned, Fig. 8.1 shows an example of well design used for CO_2 injection. It can be observed that this injection well is almost similar to wells using a conventional gas as the injectant. The main differences are the higher pressure and upgraded corrosion resistance downhole equipment needed for a CO_2 injection.

There are mainly two CO_2 properties affecting the selection of wellbore materials. First, the CO_2 is corrosive in contact with water, oxygen and hydrogen sulfide, H_2S. Second, CO_2 has a lower density compared to most reservoir fluids, causing it to migrate upwards in the injection zone (Gaurina-Međimurec and Pašić, 2011). These characteristics, especially the possibility of corrosion, will affect the choice of cement, casing, tubing and packer, which are discussed in the following paragraphs.

Injection fluids, their rate and reservoir fluids must be considered when planning well design. The composition of the injected fluid determines its phase behaviour and thus its velocity and compression limits (Cooper, 2009). It will also affect whether the injectant is sour or not, which again impacts the selection of materials. Other factors influencing the equipment material are the injection rate and the reservoir fluid. High injection rate of CO_2 could cause the materials to erode. Further, the reservoir fluid will affect the corrosivity near the well, and thus have an impact on the well design. (Cooper, 2009).

Cement

There are several important aspects of a well cementation; the cement supports the casing, prevents contact between casing and CO_2 and hinders the CO_2 to migrate vertically. In addition, the cement will prevent blow outs and seals off zones where lost circulation can be problematic. (Nygaard, 2010).

The primary cement will be the first material exposed to CO_2. During injection, the cement will encounter pure CO_2, whereas a mixture of CO_2 and brine will react with the cement after the injection (Gaurina-Međimurec and Pašić, 2011).

In other words, the cement interfaces will highly be exposed to CO_2 and are the most likely paths for CO_2 migration (Ringrose, 2017e). Thus, it is important that the zones where an interaction between cement and CO_2 is likely to happen, still ensures well integrity. This can be maintained by using CO_2 resistant cement such as ThermaLock and EverCRETE, or regular Portland cement. Most important is the cement job, which has to be done properly to ensure well integrity. (Nygaard, 2010).

When CO_2 reacts with the regular Portland cement, solid calcium carbonate is formed. The following reactions show the chemical process called cement carbonation (Nygaard, 2010);

$$CO_2 + H_2O = HCO_3^- + H^+ = CO_3^{2-} + 2H^+ \tag{8.1}$$

$$Ca(OH)_2 + CO_3^{2-} + 2H^+ = CaCO_3 + 2H_2O \tag{8.2}$$

Calcium carbonate is created when CO_2 mixes with water, as shown in equation 8.1. The second equation, equation 8.2, shows the chemical reaction between Portland cement and the carbonic acid. This carbonation process will continue as long as CO_2 is injected and the cement contains $Ca(OH)_2$. Furthermore, this process will change the cement composition. The porosity will decrease and the cement will get harder, which will weaken the cement and increase the possibility for leakage (Gaurina-Međimurec and Pašić, 2011). However, the cement carbonation is a self-healing process which could prevent migration of CO_2. It may therefore be concluded that the cement placement is more important than the cement itself.

Casing, tubing and packers

The carbonic acid created when CO_2 mixes with water, oxygen or hydrogen sulfide, may react with both casing and tubing. These are often made up of steel, which will corrode in contact with carbonic acid. The following equation, equation 8.3, shows the reaction where solid iron dissolved into ions (Nygaard, 2010). This reaction could result in a corroded surface on the casing and tubing, which will reduce the wall thickness and weaken the strength.

$$Fe(s) + 2H^+(aq) \rightarrow Fe^{2+}(aq) + H_2(g) \tag{8.3}$$

Corrosion resistant materials should be used to prevent this reaction from happening. Stainless and alloy steels could be used for both casing and tubing,

whereas chemically resistant fluids such as oxygen and biocide could be flowed in the annulus (Nygaard, 2010).

Another important aspect regarding downhole equipment is that the packers must be made of materials that are carbonic acid resistant (Nygaard, 2010). Packers will be in contact with downhole fluids as they prevent the fluids to migrate upwards in the annulus. Thus, packers must withstand being in contact with CO_2 throughout the well's lifetime.

8.2 Operations

Well integrity is an important aspect in a carbon capture and storage process. It can be achieved by controlling operational results and getting real time response, which require well monitoring and maintenance (Cooper, 2009). The following sections give a description of maintenance and monitoring regarding an injection well.

8.2.1 Maintenance

Maintenance of the wellbore design is an important factor that may prevent future issues and ensure long-term well integrity. Issues related to the following operational processes must be considered to preserve storage safety; the start-up, shut-down, intervention and stimulation operations.

A start-up operation may be different for a CCS process compared to an ordinary start-up, making it necessary to consider some factors carefully. First, the fluids left behind in the wellbore may cause implications such as corrosion, growth of bacteria and precipitant drop out. Further, hydrate formation in a well should be considered and prevented, as well as the possible displacement of fluids into the reservoir (Cooper, 2009). Issues related to shut-downs do often occur when the injection is re-started. Hydrates could form or the facilities do not have the required pressure to start back up (Cooper, 2009).

There are mainly two factors that should be considered before an intervention process. First, the high injection rate could cause fluid loss and near wellbore damage. Second, hydrates could be formed due to an intermix between the CO_2 and the well control fluid (Cooper, 2009). It is important to prevent such issues to maintain a safe carbon storage.

Stimulation of a CO_2 injection well will be needed if the injectivity decreases rapidly over time. Although a stimulation is designed to increase the near wellbore permeability, fracturing may occur, and the stimulation fluids could damage the well materials. This would cause an inefficient and non-safe operation if it is not done carefully. (Cooper, 2009).

8.2.2 Well monitoring

Well monitoring is completed to ensure that the integrity of well equipment is maintained for a long period of time. The integrity is preserved if the equipment is operated at a tolerable risk and within design limits during its entire life. When considering a CO_2 injection well, the well maintains its integrity if the risk of CO_2 migration is reduced over the entire service life (Cooper, 2009).

Well monitoring is important during the whole storage operation. Pressure monitoring and well control are important processes during the injection. It is necessary to check the cement integrity, possible corrosion, the CO_2 injection profile

and pressure isolation barriers as long as the carbon dioxide is being injected. Ensuring functional barriers are important in the post-closure period. (Ringrose, 2017e).

Well monitoring techniques

Several monitoring techniques are of great importance when considering CO_2 storage and the following are now discussed; cased hole logging, cement logging, mechanical integrity and pressure monitoring.

Several cased hole logs can be used to keep the well integrity under observation. A leak detection log, LDL, can be used to specify a leak point location. Fluid is pumped into the well and a downhole tool detects the leak point. Other logs include the tubular inspection log, which measures the condition of the tubing and potential leaks, and the production profile log, which determines injectivity and the injectivity profile. (Cooper, 2009).

Cement integrity logging should be completed to define defects and migration paths. Such defects could occur due to poorly cement placement, a mixture between the formation fluid and the cement, and generation of a micro-annulus between cement and casing, or between cement and formation. (Cooper, 2009).

Mechanical integrity tests are used to observe the integrity of the used well equipment. For instance, sealing elements should be tested to determine if they are able to close the well pressure. Further, pressure tests are important to monitor annular pressures. Such tests can help detecting potential leakage paths and establish a safe storage operation. (Cooper, 2009).

8.3 Closure and post-closure

The main operation during a well closure is the plug and abandonment process, which happens after the injection of carbon dioxide. It is important that such an operation is carefully and correctly completed, as the main purpose of this operation is to prevent vertical fluid migration through the well. The injected CO_2 is expected to be stored in a reservoir for a long time, and there will be no well activities during the post-closure stage. In other words, a plug and abandon operation has to be done properly to ensure long-term integrity and safe storage. (Cooper, 2009).

When considering long-term well integrity, issues related to geochemical reactions, corrosion and fractures along interfaces should be carefully studied (Ringrose, 2017e). Migration paths may be located between the casing and the cement, between cement and formation, between cement plug and casing, through fractures and pores in the cement and through the casing. Thus, it is necessary to keep monitoring for a long time to detect possible leakage pathways as soon as possible. (Ringrose, 2017e).

Chapter 9

Optimizing the CO2 injection

There are several factors that will impact and optimize an injection operation, and thus a storage, of CO_2. Such factors may be the inclination of the injection well, well location, depth of perforations and the use of outflow control devices, OCDs.

The following section will describe the impacts of a horizontal injection well. The advantages of using such a well will be discussed, which will explain why this type of well is used in later simulations.

Further, the use of control devices will be explained in section 9.2. The effect of outflow control devices will be studied later in this report, making it necessary to understand how control devices work, why such devices are used and what types of devices that exist in the industry. Although the simulations completed in this thesis uses OCDs, the theory will focus on both outflow and inflow control devices, ICDs. The functionality of both ICDs and OCDs are described, showing that an ICD is functioning in the opposite way of an OCD.

As for the impact of well location and perforation depth on the CO_2 storage, this will be discussed and studied later in this thesis.

9.1 Horizontal injection well

CO_2 distribution and storage in a reservoir highly depend on whether the injection well is vertical or horizontal. Although vertical injection wells have been used for a long time, ensuring a high level of knowledge and experience in the industry, horizontal and multilateral wells have become the first choice when developing reservoirs (Fernandes et al., 2009). This section will focus on the advantages of horizontal wells, explaining why this type of injection well is used in the simulations discussed later in the thesis.

An important factor considering optimal CO_2 injection is the wellbore length. Due to the fact that a horizontal well has the possibility to be considerable longer than a vertical well, a greater part of the wellbore will be exposed to the formation. The perforation area is larger, causing the injection or production rate to be higher in a horizontal well. (Petrowiki, 2018). A larger perforation area will further cause a reduction in pressure drop, which will optimize an injection or production flow by balancing the outflow or inflow of a fluid. Further, a horizontal well will cause reduced fluid velocities around the wellbore, reveal more information about the lateral geology in the reservoir and decrease the chance of water and gas coning (Petroblogweb, 2018).

Due to the characteristics mentioned above, a horizontal injection well is used in all simulations completed in this thesis. The injection well, *ALPHA_F*, is illustrated in **Fig. 9.1**, showing that the well has a horizontal part that extends over five gridblocks, which is 1250 m. The horizontal well will be located at different depths and gridcells depending on the study, but is most commonly found in gridblock 70, 69, 68, 67 and 66, where gridcell 70 represents the well heel and 66 the well toe. However, it will be stated later in this thesis if the location changes.

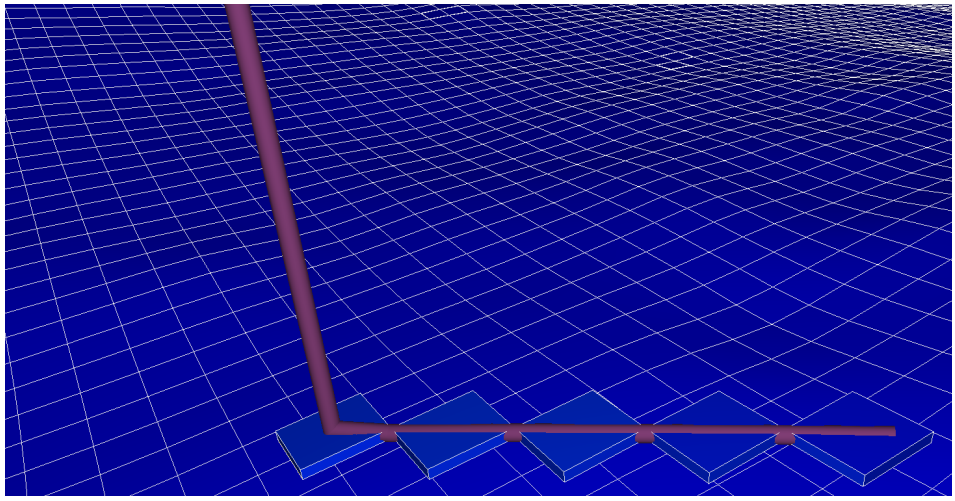

Fig. 9.1: Horizontal injection well in the Alpha structure.

9.2 Control device

A control device is a component installed as a part of a well completion to optimize production from or injection into a reservoir (Fernandes et al., 2009). Such a device installation is mainly determined by reservoir properties and performance predictions. As known, reservoir conditions such as fluid density, viscosity and velocity may change over time, making it important that a control device is reliable throughout a well's lifetime. In other words, such a device must be able to adapt to reservoir changes to prevent negative effects on injection and production.

9.2.1 The functionality of an inflow control device

The main purpose of using a control device in a well is to optimize the inflow or outflow profile along the wellbore (Schlumberger, 2014). An inflow control device, ICD, balances the inflow profile by generating an additional pressure drop between the wellbore and the formation. When considering a production operation, this is done by changing the initial Darcy radial flow existing in the reservoir, to a pressure-drop flow in the inflow control device (Ellis et al., 2009). **Fig. 9.2** shows such a pressure drop profile in a production well.

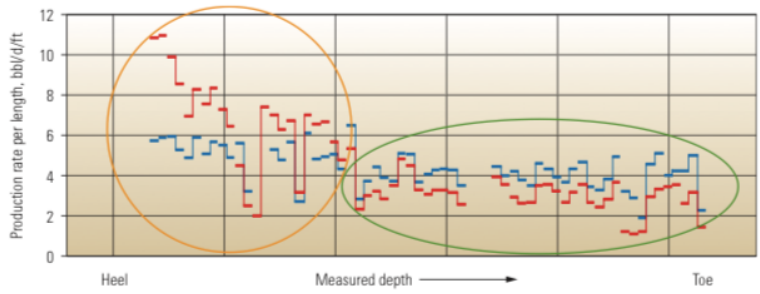

Fig. 9.2: Pressure drop profile in a production well (Ellis et al., 2009).

Fig. 9.2 illustrates two cases; the red line represents production without ICDs, whereas the blue line represents a production where ICDs are installed. As can be observed, the production without inflow control devices is not balanced, while the use of ICD will stabilize the fluid flow. The ICDs reduce the inflow rate at the wellbore heel and increase the flow at the wellbore toe, creating a flow balance throughout the well. A so-called heel-toe effect may occur if control devices are not installed in a well. To be able to prevent this effect, and most likely prevent an unbalanced flow, it is important to understand the concept behind this term.

The heel-toe effect

The heel-toe effect can be described as a pressure loss profile along the wellbore. As fluids flow from the total depth, TD, and further out in the horizontal well path, a pressure reduction will occur. The decrease in tubing pressure will cause the pressure to be higher at the well's toe compared to the well heel. This again will highly impact the inflow of reservoir fluids along the well path. (Ellis et al., 2009).

As can be seen in the top figure in **Fig. 9.3**, this heel-toe effect may cause an early gas and/or water coning near the well heel, which probably will cause the production to end. However, the coning may also be generated due to reservoir heterogeneity and varying distances from reservoir fluids and the horizontal well, (Ellis et al., 2009).

To reduce the risk of early gas and water breakthroughs, control devices can be installed in the wellbore. The bottom of Fig. 9.3 illustrates the balancing effect of inflow control devices. The ICDs will create a constant pressure along the well path, causing a balanced inflow of reservoir fluids and delayed gas and/or water coning. (Ellis et al., 2009).

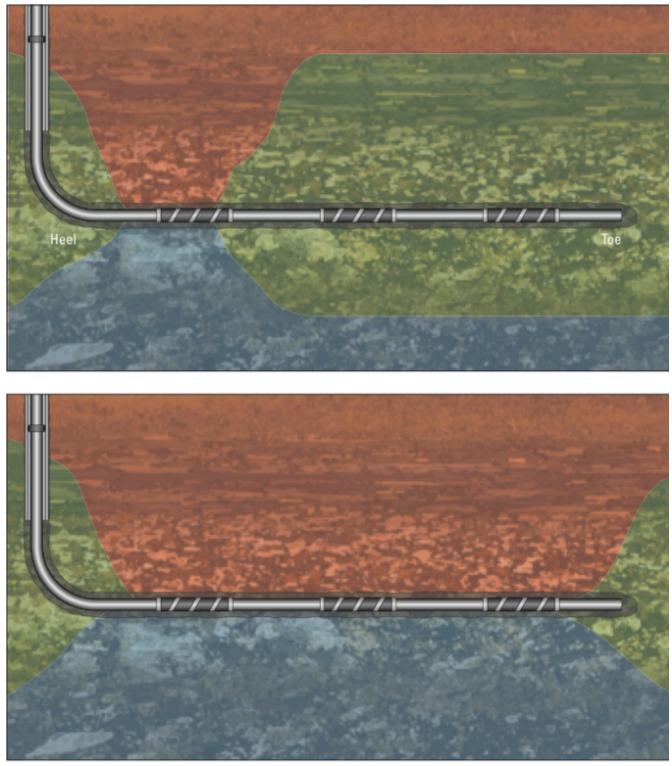

Fig. 9.3: The heel-toe effect (Ellis et al., 2009).

9.2.2 Outflow control device during injection

When outflow control devices are installed in an injection well, the OCDs will generate a fluid outflow balance throughout the entire wellbore. This balance helps solving the reservoir related challenges connected to varying reservoir characteristics over time, such as permeability, formation damage, injectivity and heel-toe effects (Ellis et al., 2009). Because different reservoir zones may consist of different reservoir properties, the use and location of OCDs are important for control and optimization of the injection process along the wellbore.

The OCD has the ability to control fluid mobility through the wellbore and out in the formation. For instance, the device prevents a significant increase in the injected fluid's velocity in reservoir zones with high permeability, whereas in low-permeable areas the OCD increases the injection rate. This control will cause the injection rate to be relatively stable throughout the wellbore. It will improve the pressure support, and thus the sweep efficiency in the reservoir. Further it may delay gas and/or water breakthrough and prevent fractures. (Ellis et al., 2009).

9.2.3 Types of control devices

There are mainly two types of control devices in the industry; the channel-type and the nozzle-type (Ellis et al., 2009). Several channel and nozzle designs exist, but the principles of how the different types work are the same and will be described in this section. It should be stated that the following figures and descriptions apply to ICDs, but the same types are found for outflow control devices, only for OCDs the fluid will flow the opposite way.

Fig. 9.4 illustrates a channel inflow control device. This ICD creates a pressure drop by using surface friction (Fernandes et al., 2009). The formation fluid flows along the annulus, through several channels and into the production tubing. The channels force the fluid to change its direction several times, causing a distribution of the pressure drop along a long path.

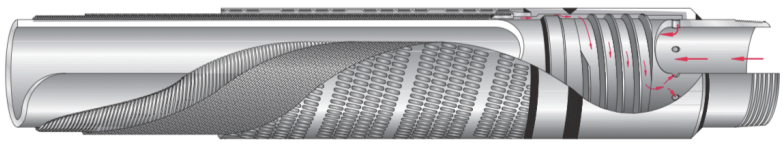

Fig. 9.4: Channel ICD (Birchenko et al., 2010).

The main advantage of using the channel-type ICD is the low flow velocities (Fernandes et al., 2009). Due to the channels the fluid velocity is lowered, which reduces the possibility of erosion and plugging. However, the device is highly dependent on fluid viscosity as friction is used to create the pressure drop. This may be a disadvantage since different fluids have various viscosities, making it hard to maintain a uniform influx.

The other type of inflow control device is the nozzle-type, shown in **Fig. 9.5**. Such an ICD is a function of fluid flow rate and generates pressure drop by using fluid restriction (Fernandes et al., 2009) and (Ellis et al., 2009). The fluid is forced through the nozzles, which usually have a small diameter, before it flows through the pipe.

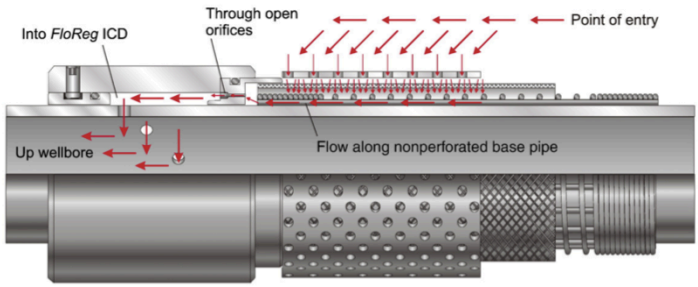

Fig. 9.5: Nozzle ICD (Birchenko et al., 2010).

The nozzle ICD depends on fluid density and velocity, causing the pressure drop to reduce instantaneously when fluids cross the ICD (Fernandes et al., 2009). Another advantage regarding this control device is the simple design, which makes it possible to change the configuration easily.

It should be mentioned that the effect of nozzle outflow control devices is being simulated and discussed later in this thesis. How to include such devices in the simulation is described in the next chapter.

As mentioned, there are several different designs of nozzle and channel control devices in the industry, in addition to combinations of these designs. A hybrid control device, which is a relatively new design, is shown in **Fig. 9.6**. This device creates a pressure drop by using restriction in a distributed format (Ellis et al., 2009). Fluids are forced to flow through several chambers, which generates the pressure drop. However, this design will not be further discussed in this report.

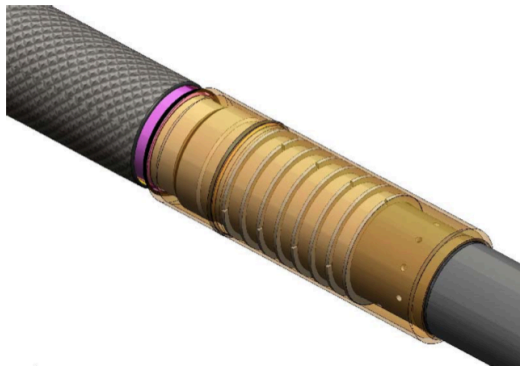

Fig. 9.6: Hybrid ICD (Coronado et al., 2009).

Chapter 10

Description of the Smeaheia storage area and the simulation model

The following section, section 10.1, is modified from my semester project, CO_2 storage - Review of theory and literature (Brobakken, 2017).

This chapter gives a description of the carbon capture and storage project at Smeaheia. The first section, section 10.1, gives an explanation of the whole CCS project at Smeaheia. The Smeaheia area is briefly described to get an overview of the location, while the project design and planned monitoring techniques are explained in detail in this section.

Further, a complete description of the Smeaheia storage site and its geology is given in section 10.2 and 10.3. Section 10.2 gives an explanation of the Sognefjord delta aquifer as well as the important Alpha and Beta structures. Section 10.3 covers the geological data used in this thesis, including permeability and porosity, closure capacity estimation and permeability thickness.

At last, an explanation of the reservoir simulation model is given at the end of this chapter. Section 10.4 shortly describes important aspects considering the model, as well as the use of outflow control devices and the keyword FIPNUM.

10.1 CO2 capture and storage process at Smeaheia

Smeaheia is a new Norwegian full-scale CCS project planned to be operational in 2022. The storage site is located in the North Sea approximately 50 km from shore, as shown in **Fig. 10.1**, and about 20 km east of the producing Troll field (Equinor, 2016).

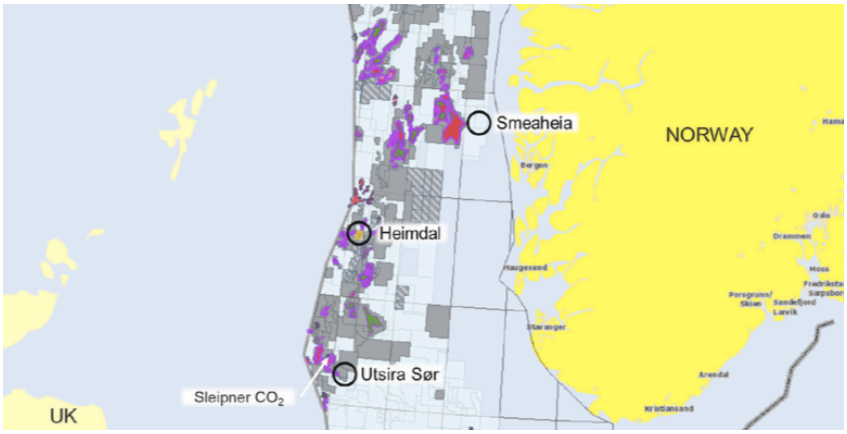

Fig. 10.1: Location of Smeaheia storage site (Furre et al., 2017).

The Smeaheia field includes two main structures, Alpha and Beta, which can be seen in **Fig. 10.2**. The Alpha structure is located in the western part of the Smeaheia site, while the Beta structure can be found in the eastern part. As will be illustrated later in this chapter, both structures are estimated to have a storage capacity of approximately 100 Mt (Equinor, 2016).

Further, it can be observed from Fig. 10.2 that Alpha is the deepest structure. The green colour symbolizes a depth of about 1200 m, while the yellow colour in the Beta area represents a depth of 800 to 1000 m. The deep location of the Alpha structure will benefit the CO_2 storage operation in the Smeaheia field. As will be studied later in this thesis, the Smeaheia field pressure will vary with time as the Troll reservoir is producing. The production will affect the pressure development in the area and thus impact the CO_2 storage. However, a deep storage site will increase the likelihood of keeping the CO_2 in a supercritical phase as the pressure and temperature will be above the critical point. (Furre et al., 2017).

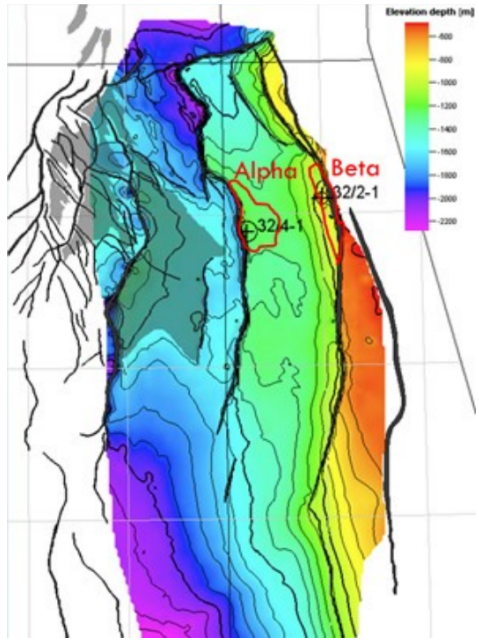

Fig. 10.2: The Alpha and Beta structures (Olje-og energidepartementet, 2017).

10.1.1 Project design

The planned CCS project at Smeaheia includes capture, transport and storage of carbon dioxide. CO_2 from three different land plants is planned to be separated, cooled and compressed before the carbon dioxide is temporary stored. The captured CO_2 will then be transported by ship to a land-based terminal, where it will be stored before injected into the Alpha structure. An overview of the total process and the project design is illustrated in **Fig. 10.3** (only in Norwegian) and **Fig. 10.4**.

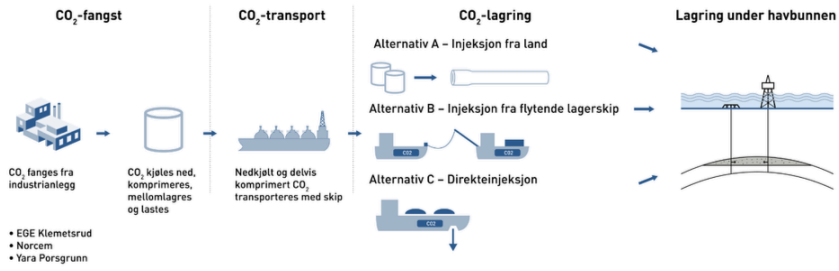

Fig. 10.3: Overview of the project design for Smeaheia (Olje-og energidepartementet, 2017).

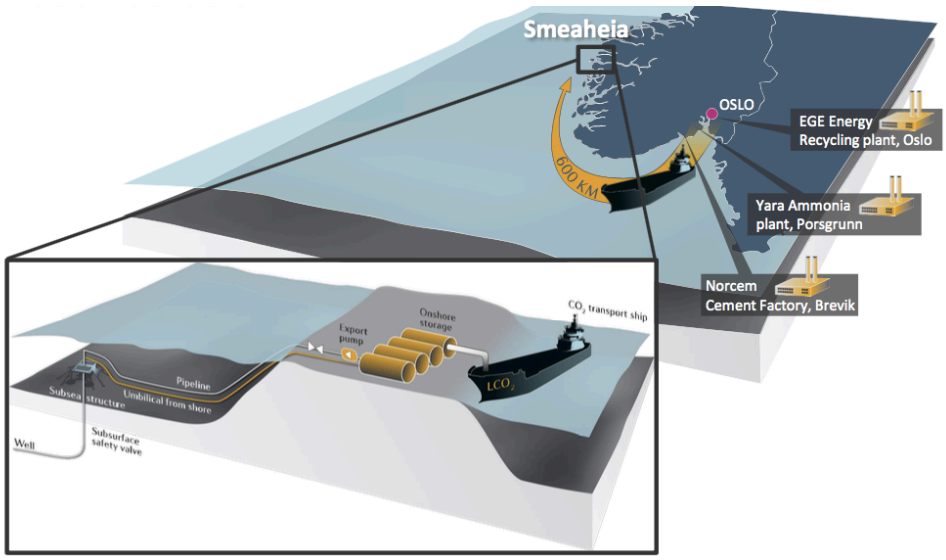

Fig. 10.4: The selected project design for Smeaheia showing the industrial land plants (Ringrose et al., 2017).

As mentioned, CO_2 will be captured from three different land plants in Norway. The industrial plants can be seen in Fig. 10.4 and includes an incineration plant at Klemetsrud, Oslo, Yara ammonia plant at Porsgrunn and Heidelberg Norcem at Brevik. A study has been completed to look at different opportunities to capture CO_2 from the plants, and the currently results are given below. Further, it has been shown that a total amount of 1.5 to 4 Mt of CO_2 can be captured annually from these three industrial plants. (Ringrose, 2016).

Norcem is a cement factory where approximately 400 000 tonnes of CO_2 can be captured annually. This represents approximately 50 % of Norcem's total CO_2 emission per year and will be achieved by a post-combustion operation using amine as the solvent. (Ringrose, 2016). Yara is an ammonia plant where almost 90 % of the annually emissions can be captured. This constitutes about 805 000 tonnes of CO_2, which will be separated and captured by using amine. (Ringrose, 2016). 315 000 tonnes of CO_2 can be captured from the incineration plant in Oslo, representing approximately 90 % of the total emissions. The CO_2 will be separated by a post-combustion process using different solvents. Both amine and cooled ammonia have been successful solutions. (Ringrose, 2016).

The captured CO_2 is transported to an intermediate storage location before it is further transported by ship to a land-based terminal at Smeaheia. Different types of ship designs have been studied for CO_2 transport; ships transporting CO_2 at low, medium or high pressure, and all of the solutions are found to be technically feasible (Ringrose, 2016).

The land-based terminal in Smeaheia is illustrated in **Fig. 10.5**. The CO_2 stream is transported to the terminal before it is injected into the Alpha structure for storage. As can be seen in Fig. 10.5, one horizontal injection well will be sufficient for an annually injection of 1.5 to 4 Mt of CO_2 (Equinor, 2016).

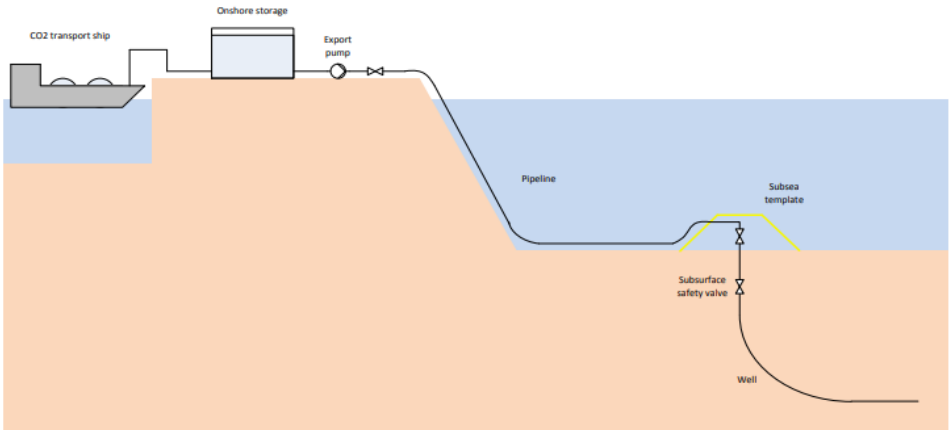

Fig. 10.5: Land-based terminal at Smeaheia (Ringrose et al., 2017).

10.1.2 Monitoring of the CO2 storage

Several monitoring techniques can be used to ensure safe and long-term CO_2 storage in the Smeaheia structure. The following techniques are shortly described in the following paragraphs; seismic surveys, gravimetric and electromagnetic surveys, sonar and echo sounding, pressure and temperature measurements (Furre et al., 2017).

4D seismic ensures a detailed monitoring of the subsurface, giving a better understanding of the CO_2 distribution and pressure development in the reservoir. Furthermore, the seismic can be used as the main method for detection of possible CO_2 migration out of the storage site (Equinor, 2016).

Gravimetric and controlled-source electromagnetic surveys measure density and saturation changes occurring when the injected CO_2 replaces the initial reservoir fluid. Although the resolution is of poorer quality compared to imaging from seismic, these monitoring techniques make it possible to follow and study the CO_2 distribution in the reservoir (Furre et al., 2017).

Pressure and temperature measurements, both at the wellhead and downhole, should be completed to keep the reservoir pressure development under observation. Production from the Troll reservoir will cause the Smeaheia field pressure to vary over time, which again will highly affect the behaviour of the injected CO_2 (Olje-og energidepartementet, 2017). Further, sonar and echo sounding can be used to define abnormalities at the sea bed (Furre et al., 2017).

10.2 The geology at Smeaheia

As mentioned earlier in this thesis, the Smeaheia area is located in the North Sea. More specific, this storage field is found in the Viking group on the Horda platform located in the Stord basin (Equinor, 2016). Sandstones belonging to the Viking group are referred to as the Sognefjord delta aquifer, which includes the Sognefjord, Fensfjord and Krossfjord formations (Oljedirektoratet, 2018). Further, the Smeaheia area is divided into two storage structures, the Alpha and Beta structures. A detailed description of the Sognefjord delta aquifer and the two structures forming the Smeaheia storage site is given in this section.

10.2.1 The Sognefjord delta aquifer

As already stated, the Sognefjord delta aquifer consists of three sandstone formations; Sognefjord, Fensfjord and Krossfjord. These are coastal-shallow marine sandstones separated by thin shale layers making up the Heather formation. The Heather formation works as an internal barrier within the delta aquifer (Halland et al., 2011). Further, the overlying Draupne formation acts as a vertical barrier in the storage site as it contains a high amount of shale as well (Furre et al., 2017). **Fig. 10.6** gives a lithostratigraphic illustration of the North Sea where the Viking Group is highlighted by the red circle. As can be noticed from this figure, the light green colour represents shallow-marine deposits, while the dark green colour symbolizes deep-marine deposits.

The geological setting of the Viking group is strongly associated to the North Sea basin evolution during the Permian time. Tectonic movement, rift phases and faulting highly affected the depositional settings of the Sognefjord, Fensfjord and Krossfjord formations (Equinor, 2016).

Deposition of the sand-rich deltas characterizing the underlying Krossfjord formation took place during the beginning of the rifting period (Equinor, 2016). This layer is thin compared to the overlying formations and has relatively low porosity and permeability values. The Fensfjord formation is the thickest layer in the Sognefjord delta aquifer with approximately 300 m (Amjad, 2014). It was created in a period of quietness, which generated a layer with high permeability and a porosity of 25 to 30 %.

The overlying Sognefjord formation was deposited when the rifting period reached its climax (Equinor, 2016). The reservoir quality is excellent as the permeability varies between 1 and 30 D and the porosity between 26 and 35 % (Evensen et al., 1993) and (Amjad, 2014). In other words, the formation makes up a good reservoir with its characteristics and a maximum height of approximately 220 m. This is emphasized by the fact that the Sognefjord layer constitutes the main reservoir in the producing Troll field.

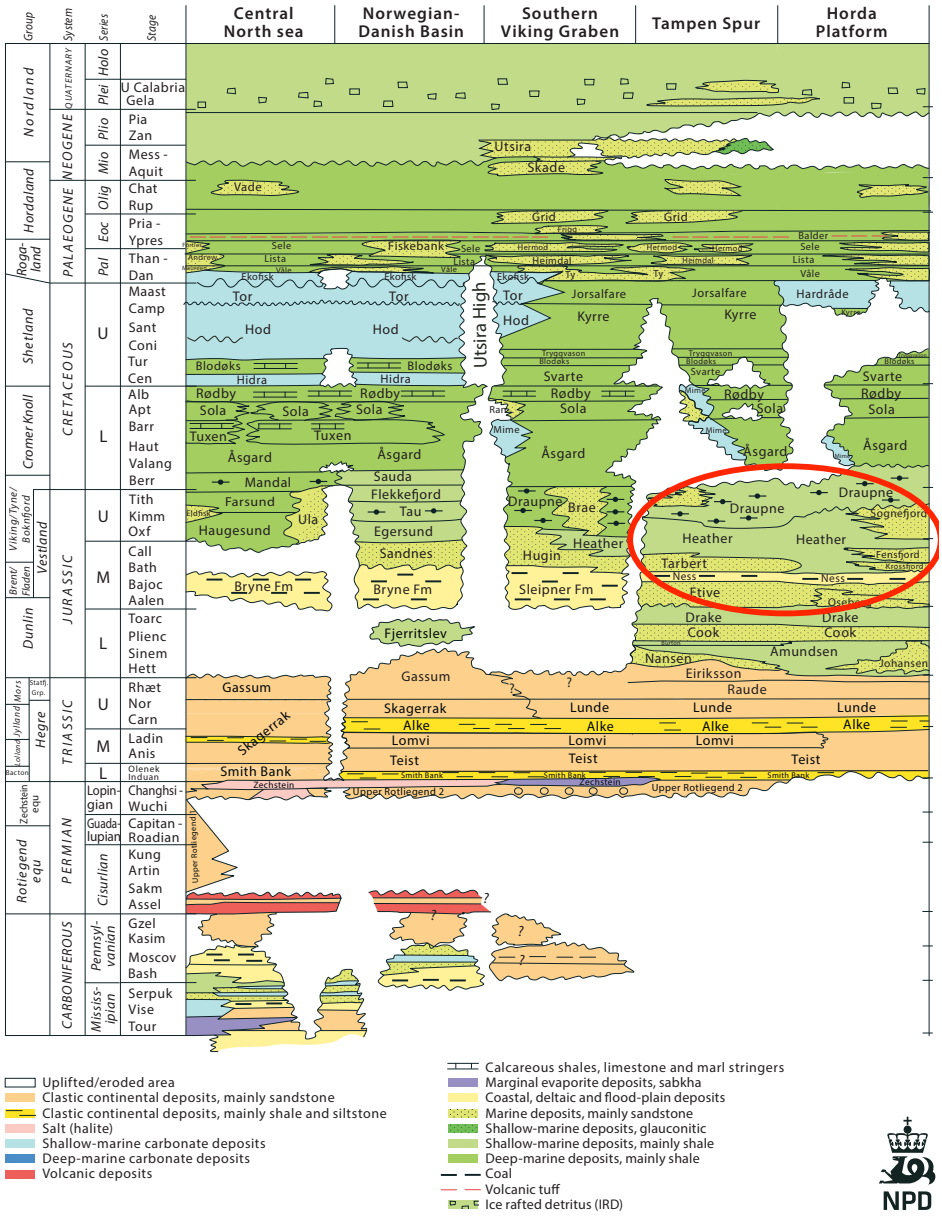

Fig. 10.6: Lithostratigraphic chart of the North Sea and the Viking Group (Directorate, 2018).

10.2.2 The Alpha and Beta structures

Fig. 10.7 shows the two most important areas in the Smeaheia field, the Alpha and Beta structures. As can be seen from the illustration below, the storage site is bounded by two faults. The Vette fault, VF, is separating the Alpha structure from the western producing Troll field, while the Beta structure is closed in by the Øygarden fault, ØGF, (Equinor, 2016).

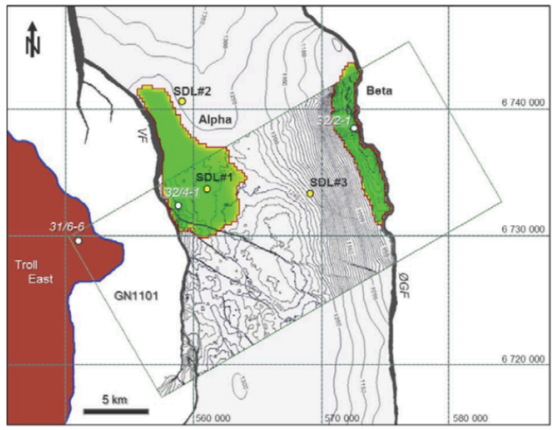

Fig. 10.7: The Vette and Øygarden faults (Equinor, 2016).

Fig. 10.8 shows the top view of the reservoir simulation model as a function of depth. The shallower area, symbolized with the blue colour, represents the platform where the Alpha and Beta structures are located. The producing Troll field is located at a deeper depth, presented by the green and light blue colours.

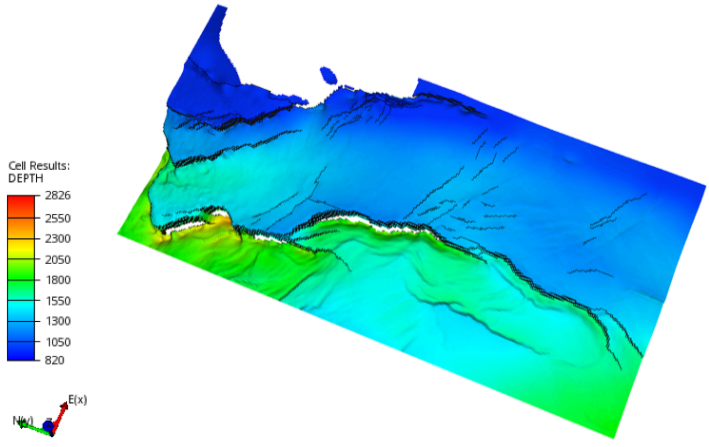

Fig. 10.8: Reservoir geometry of the Smeaheia storage, showing the depth to different grid blocks.

Fig. 10.7 may give the impression that Alpha has the largest area, and thus a higher storage capacity, compared to the Beta structure. However, as stated earlier in this thesis and as will be shown later in this chapter, both structures have an estimated capacity of about 100 Mt of CO_2. Further, the structures are located on a fault block being at a shallower depth compared to the Troll reservoir, making CO_2 migration from the structures to the Troll field impossible (Equinor, 2016). In other words, considering the size and depth, both Alpha and Beta could work as effective storage sites.

However, as can be noticed in Fig. 10.8, the Smeaheia storage site consists of several faults and fractures. Some faults are small and will not affect the CO_2 storage, while others will have a big impact due to their size and vertical extension. The eastern Øygarden fault closing in the Beta structure extends vertically upwards, causing a CO_2 leakage to the surface to be most possible. The high risk of leakage connected to CO_2 storage in the Beta area causes Alpha to be the preferred storage structure.

The possibility of leakage from the Beta structure makes it important to prevent CO_2 movement in this direction. **Fig. 10.9** illustrates an existing connection between the two structures. As can be seen, Alpha and Beta are connected by a spill point, causing movement of CO_2 between the areas to be possible. If the Alpha structure is filled up with CO_2 to its spill point, which is located at approximately 1240 m, the carbon dioxide will move about 8 km upwards and into the Beta structure (Equinor, 2016). To prevent this movement from happening, a suitable injection well design with optimal injection rate, perforation depth and well location, has to be selected. Such a design is studied in the next chapter.

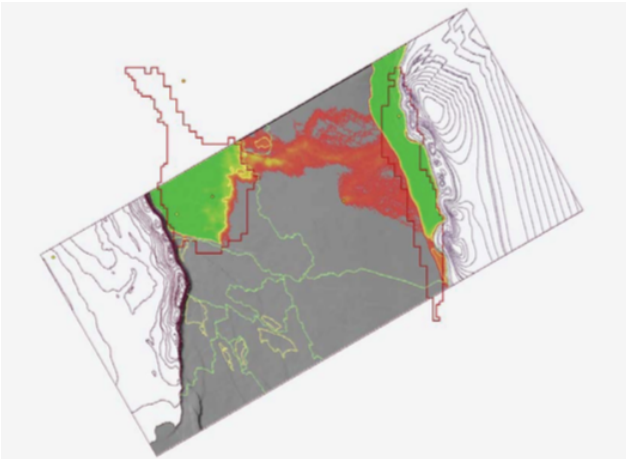

Fig. 10.9: Connection between Alpha and Beta structures (Equinor, 2016).

10.3 Geological data

To ensure a safe and efficient CO_2 storage it is necessary to have geological information about the area of interest. Since the Alpha and Beta structures are of special importance in the CCS operation at Smeaheia, this section covers the geological data regarding these areas and not the Sognefjord delta aquifer in whole.

10.3.1 Closure capacity estimation

To be able to design an optimal injection well with respect to injection rate, well location and further well design, a calculation of the maximum storage field capacity has to be completed. Equation 10.1 shows how to calculate the site capacity, while Tables 10.1 and 10.2 give the data necessary to solve this equation.

$$Mass_{sc} = BRV_{trap} * Net_{res} * Phi_{res} * Sat_{gas} * Rho_{gas} \tag{10.1}$$

In the equation above, $Mass_{sc}$ is representing the structural closure capacity, BRV_{trap} the bulk rock volume, Net_{res} the reservoir net-to-gross range, Phi_{res} the reservoir porosity range, Sat_{gas} the saturation range and Rho_{gas} the CO_2 density. (Equinor, 2016).

Table 10.1 presents the geological data considering the Alpha structure, while table 10.2 describes the Beta structure (Equinor, 2016). The tables represent expected field conditions such as mean pore saturation and available net reservoir for the Alpha and Beta areas (Equinor, 2016). The presented scenarios give a capacity estimate under the assumption that the structures are filled to their spill points.

Table 10.1: Capacity estimate for the Alpha structure (Equinor, 2016).

	Low	**Mid**	**High**
Bulk rock volume [m^3]	634 000 000	634 000 000	634 000 000
Net [%]	75	85	95
Permeability [mD]	440	1300	4000
Porosity [%]	31	35	39
Saturation [%]	70	80	90
Structural capacity [Mt]	**82.7**	**98.6**	**117**

Table 10.2: Capacity estimate for the Beta structure (Equinor, 2016).

	Low	Mid	High
Bulk rock volume [m^3]	669 000 000	669 000 000	669 000 000
Net [%]	75	85	95
Permeability [mD]	440	1300	4000
Porosity [%]	31	35	39
Saturation [%]	70	80	90
Structural capacity [Mt]	**87.8**	**105**	**124**

As can be seen from the tables above, three different density values are evaluated; low, mid and high. The three scenarios are studied due to uncertainty related to variations in reservoir pressure and temperature. The mid scenarios give a total storage capacity of approximately 100 Mt of CO_2 for both structures. These estimations assume good reservoir quality and high net reservoir (Equinor, 2016). It should be mentioned that although the Beta structure has a slightly higher capacity estimate, which is due to its larger bulk rock volume, it will not be preferable as storage area due to the high risk of leakage to the surface.

Further, the producing Troll field should be considered when estimating the Smeaheia storage capacity. The capacity will be reduced due to pressure connection with the neighbouring Troll reservoir (Equinor, 2016). The production will cause an associated pressure depletion, which will have a great impact on the CO_2 density and thus the storage capacity. The capacity estimates with respect to pressure depletion are illustrated in Table 10.3 and Table 10.4. It should be noticed that the depletion effect will be larger in the Beta structure compared to Alpha. This is due to the deeper depth in the Alpha area, causing the storage capacity to be sufficient for almost all of the studied depletion scenarios.

Table 10.3: Capacity estimate for the Alpha structure with respect to pressure depletion (Equinor, 2016).

Depletion scenario	Drawdown (bars)	Reservoir (bars)	Density (kg/m^3)	Capacity (Mt)
Ambient (dense)	- 00	120	658	**100**
Low (dense)	- 30	90	338	**51**
Medium (dense)	- 40	80	241	**37**
High (gas)	- 50	70	183	**28**

Table 10.4: Capacity estimate for the Beta structure with respect to pressure depletion (Equinor, 2016).

Depletion scenario	Drawdown (bars)	Reservoir (bars)	Density (kg/m^3)	Capacity (Mt)
Ambient (dense)	- 00	90	662	**100**
Low (gas)	- 30	60	159	**24**
Medium (gas)	- 40	50	118	**18**
High (gas)	- 50	40	87	**13**

10.3.2 Estimation of permeability thickness

The permeability thickness, referred to as the product of formation permeability and thickness, kh, provides important information about the storage structure and the flow potential (Schlumberger, 2018). Table 10.5 shows estimations of the permeability thickness for the Alpha and Beta structures at different density conditions (Equinor, 2016).

Table 10.5: Permeability thickness estimate (Equinor, 2016).

	Low	**Mid**	**High**
Permeability (D)	0.44	1.3	4.0
Reservoir thickness (m)	40	60	80
Net reservoir (%)	75	85	95
kh (Dm)	**13**	**66**	**304**

The estimated kh values make it possible to calculate the injectivity index for the CO_2 injector in the Smeaheia field. Equation 10.2 shows the inflow performance relationship for a gas well used to calculate the injectivity index (Equinor, 2016). The equation makes it possible to do calculations regarding CO_2 injection at high pressures.

$$q_g = \frac{(1.406kh(p/\mu_g Z)(p_R - p_{wf})}{T[ln\frac{r_e}{r_w} - 0.75 + s + Dq_g]} \tag{10.2}$$

In the equation above, q_g represents the gas flow rate, k is permeability, h is net thickness, p is pressure, μ_g is CO_2 viscosity, Z is compressibility, p_R is reservoir pressure, p_{wf} is bottomhole flowing pressure, T is temperature, r_e is external boundary radius, r_w is wellbore radius, s is steady-state skin factor and Dq_g is rate dependent skin.

Table 10.6 shows the injectivity index for the Smeaheia injection well at expected pressure differences. It should be stated that there are not expected any injectivity problems in the Smeaheia field as the reservoir quality is assumed to be good (Equinor, 2016).

Table 10.6: Estimation of injectivity index in the Smeaheia field (Equinor, 2016).

	Low	**Mid**	**High**
kh (Dm)	13	66	304
Injectivity Index (t/hr/bars)	**50.3**	**255.2**	**1175.5**

10.3.3 Permeability and porosity

The following figures, **Fig. 10.10** and **Fig. 10.11**, show the permeability and porosity in the reservoir simulation model. The figures give a visualization of the storage capacity at a depth of 1588 m, representing layer 57 in the bottom of the Fensfjord formation. Multiple studies in the thesis have been completed at this depth, making it interesting to study the permeability and porosity in this layer.

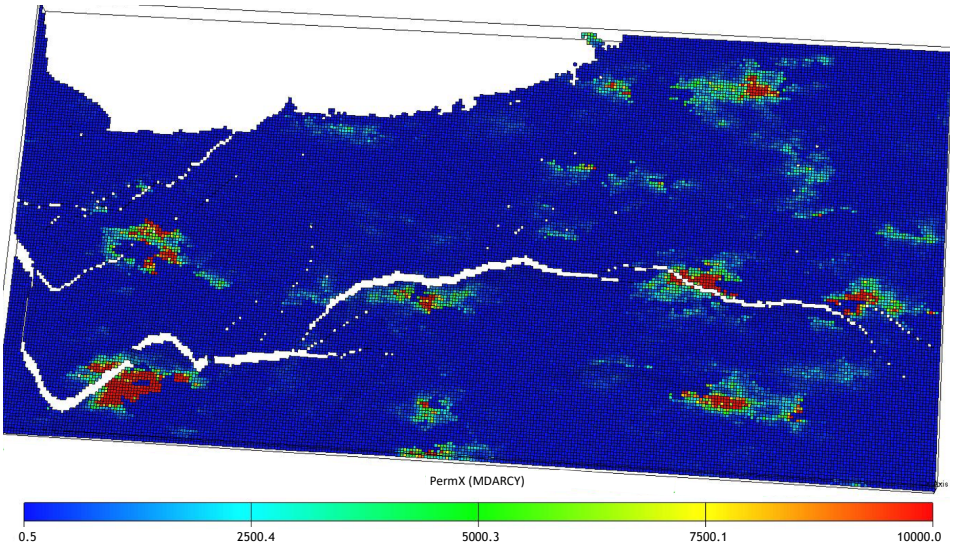

Fig. 10.10: Permeability in the simulation model at a depth of 1588 m.

As can be seen from Fig. 10.10, the permeability in the x-direction is varying between 0.5 mD and 10 D in this layer. The low-permeable area is represented by the dark blue colour, meaning that this layer in particular is in the lower range when considering permeability. However, it should be mentioned that the permeability is highly varying with depth, meaning that overlying and underlying layers may have different permeability values.

There are some advantages with an injection into a low-permeable layer. If the injectivity is sufficient, the low permeability may result in a higher volume of trapped CO_2 and reduced fingering due to dominant viscosity forces.

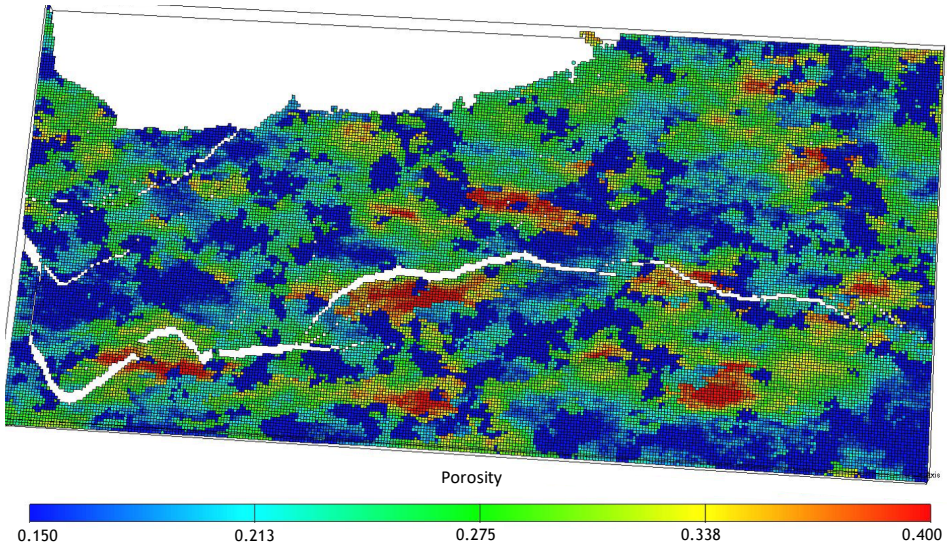

Fig. 10.11: Porosity in the simulation model at a depth of 1588 m.

As can be seen from Fig. 10.11, the porosity at the bottom of the Fensfjord formation is in an interval between 15 and 40 %. On average, the porosity may be noticed to be about 27 to 28 %, represented by the green colour, at this depth. However, the porosity is also highly dependent on the reservoir depth.

From the information given above it can be stated that the Smeaheia storage field, and especially the Alpha structure, is a good option for CO_2 storage. The field has the possibility to store large amounts of CO_2 due to high permeability, porosity and saturation values. However, although the reservoir is proved to be a good alternative for storage, the optimal well design resulting in safe and efficient storage remains to be found. The next chapter will focus on optimizing the well design, including well location, perforation depth and the use of outflow control devices.

10.4 The Smeaheia simulation model

A compositional reservoir model has been developed by Equinor to study CO_2 storage in the Smeaheia field. The model makes it possible to do research related to CO_2 movement and trapping in the reservoir, which is the main focus in this thesis. Schlumberger's Eclipse 300 is used to run the simulations in this report, while ResInsight and Eclipse Office are used for analysis.

The simulation model consists of 3556800 gridblocks distributed on a grid dimension equal to 150 x 312 x 76. The gridblocks are 250 m in x and y-directions, while the length in z direction varies within a few meters depending on the layers. The large amount of gridblocks results in a time-consuming simulation, which takes several days to run.

The model is used to study how the injected CO_2 moves in the reservoir over time. The CO_2 injection starts in 2022 and stops in 2047. The model makes it possible to determine injection rate values, time of injection and other factors affecting the storage. After the injection, the simulation is run until 2300 to clearly illustrate the long-term CO_2 distribution in the field.

Further, the following 6 components are defined in the simulation model. These are based on the captured CO_2 mixture expected from the previously described land plants. Table 10.7 gives information about each component's critical pressure and temperature, molecular weight and boiling point. It should be mentioned that although these components are defined in the model, the only fluid injected into the Smeaheia field is carbon dioxide.

- H_2
- N_2
- Ar
- O_2
- CO_2
- C_1

Table 10.7: Component information.

Component name	Tc [K]	Pc [bars]	MW [g/mol]	Tboil [K]
H2	33.20	12.97	2.02	20.40
N2	126.20	33.94	28.01	77.40
Ar	150.80	48.74	39.95	87.30
O2	154.60	50.46	32	90.20
CO2	304.20	73.76	44.01	194.65
C1	190.60	46.00	16.04	111.60

The critical temperature and pressure will be important factors when considering the stored carbon dioxide volume. At approximately 73 bars and 304 K, which equals 31 °C, the CO_2 will have its critical point. At pressures and temperatures above this point the carbon dioxide will be in a supercritical phase. The Smeaheia field temperature is given in the simulation model and is estimated to be 37 °C, while the reservoir pressure will change with time. Thus, the field temperature will ensure CO_2 in a supercritical phase at all times, while the field pressure development has to be studied to ensure such a storage. Research on the pressure development and other simulations completed in this thesis are described in the next chapter.

10.4.1 Simulation with outflow control device

The nozzle type outflow control device is simulated in this report. Because this modelling is an important part of the thesis, a short description of such a simulation is given below.

Nozzle OCDs are simulated in Eclipse by the keyword WSEGVALV (Schlumberger, 2016). This keyword makes it possible to select certain well segments and make them represent valves in a multisegment well. For an injection well, this may result in a balanced outflow throughout the horizontal wellbore.

The following equations describe how the additional pressure drop is calculated for this type of OCD. Equation 10.3 represents the pressure drop across the injection wellbore and consist of δP_{cons} and δP_{fric}, where δP_{cons} represents the constriction effects and δP_{fric} the additional friction pressure. Equation 10.4 shows the definitions of δP_{cons} and δP_{fric}. (Schlumberger, 2016).

$$\delta P = \delta P_{cons} + \delta P_{fric} \tag{10.3}$$

$$\begin{aligned} \delta P_{cons} &= C_u' \frac{p q_m(q_m)}{2 C_v^2 A_C^2} \\ \delta P_{fric} &= 2 C_u f \frac{L}{D} \rho v_p^2 \end{aligned} \tag{10.4}$$

In the equations above, C_u' is a modified conversion constant, p is pressure, q_m is the volumetric flow rate through the segment, C_v is the valve's dimensionless flow coefficient and A_C is the cross-sectional area of the valve. Further, C_u is a conversion constant, f is the Fanning friction factor, L is additional length of pipe in a segment, D is the pipe diameter, ρ the fluid density and v_p is flow velocity through pipe. (Schlumberger, 2016).

The strength of a nozzle OCD is determined by its cross-sectional area. A larger cross-sectional area will result in a larger valve opening, making it possible for

more fluid to flow through. A smaller Ac will force a higher amount of the fluid to flow through other well segments. In other words, to balance the CO_2 outflow through the well segments and into the reservoir, the strength of OCDs in the well segment may vary as the formation permeability and the injection rate changes. A study of OCDs is completed in the next chapter.

10.4.2 Simulation with FIPNUM

A simulation with FIPNUM is run in this thesis. FIPNUM stands for fluid-in-place region numbers and specifies the amount and type of fluid flow in a specific region (Schlumberger, 2016). Four regions are defined in this thesis, where three of them are of special interest. A study is completed to see how the injected CO_2 moves between these three regions. Further, it should be stated that the reason why the rest of the model will not be discussed when using FIPNUM is that the Alpha and Beta structures are the only interesting areas when considering CO_2 storage.

Fig. 10.12 roughly illustrates the three interesting regions in the model; the upper and the lower parts of the Alpha structure, as well as the Beta structure. The orange area represents the upper Alpha, the underlying yellow region represents lower Alpha and the blue part the Beta structure. The region boundaries are set by fractures on each side and the spill point. A study of the CO_2 flow between these regions are completed in section 11.6.

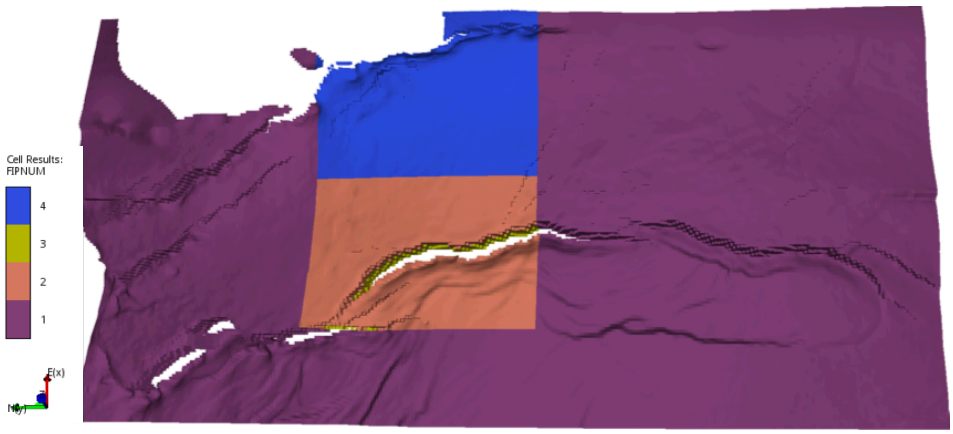

Fig. 10.12: Fluid-in-place region numbers in the simulation model.

Chapter 11

Simulations of well design at Smeaheia

The maximum storage capacity at Smeaheia highly depends on the injection well design. Factors such as the well location, perforation depth and the use of outflow control devices will have a great impact on the stored amount of CO_2. To find the optimal well design resulting in maximized storage volume in the Smeaheia field, these factors have to be studied and discussed. The following sections will analyse and compare different scenarios where these factors are considered.

Some parameters are held constant in mainly all of the completed studies in this thesis. The injection period is set to 25 years with start up in 2022 and ending in 2047. Further, the simulations are run until year 2300 to give a clear indication of the CO_2 distribution in the formation, and thus an indication of the storage safety and efficiency. It will be stated if this period is exceeded or shortened.

The preferable and available injection rate interval for almost all of the completed simulations is 1.5 to 4 Mt of CO_2 per year. This interval is set by the previously discussed industrial land plants and represents the realistic annual CO_2 volume prepared for injection and storage. However, as will be shown in the following sections, some of the well locations may be able to handle higher or lower injection rates compared to this interval. Thus, the focus in this thesis is to find the maximum injection rate preventing CO_2 movement in Beta direction at each well location.

As mentioned, the following sections will focus on finding the optimal well design at the Smeaheia storage area. The first two sections will briefly describe basic concepts regarding the CO_2 storage. Section 11.1 will give a short explanation of how the CO_2 may distribute in the Smeaheia area over time, while section 11.2 will illustrate the impacts on well bottom hole pressure, reservoir pressure and CO_2 storage as the injection rate differs.

Section 11.3 studies six different well locations, four within the Alpha area and two outside the structure. This section will explain why the specific locations are studied, as well as showing the CO_2 distribution at each location and multiple injection rates.

Section 11.4 illustrates the effect of different perforation depths. Six perforation layers have been studied, where three injection depths are located in the Fensfjord formation and the other three in the Krossfjord formation. This section will describe why these depths are considered for injection and illustrate the CO_2 movement in each scenario.

The effect of having outflow control devices installed in the wellbore is studied in section 11.5. This section will focus on one of the most commonly used outflow control devices in the industry, the nozzle type. An explanation of where to place OCDs will be given, as well as illustrations showing the effect of outflow control devices in the wellbore.

At last, section 11.6 illustrates how the CO_2 moves within the three defined regions over time. Three time steps are selected when simulating with the keyword FIPNUM; before and after injection, as well as at the end of simulation. The results give an indication of the carbon dioxide migration as time goes by.

Although the results found in the following sections are described continuously throughout this chapter, they will be further discussed in chapter 12.

11.1 CO2 distribution as a function of time

When CO_2 is being injected into the Alpha structure it will flow through pores and into the formation. As the amount of carbon dioxide in the formation increases, the CO_2 will accumulate and form a plume, which may move further into the formation as time goes by. When considering a CO_2 storage it is important to find the injected amount of CO_2 causing the plume to be stable in the storage site. To be able to find this optimal volume, it is necessary to understand how the CO_2 may migrate in the Smeaheia storage area.

Fig. 11.1 illustrates CO_2 migration through the Smeaheia storage site when CO_2 is being injected into the northern part of the Alpha structure. The injection well location is represented by the red circle. The figure shows a scenario where the injection rate is 3.6 Mt of CO_2 per year and the perforations are made in the lower part of the Fensfjord formation at a depth of 1588 m. The distribution is given at respectively 40, 70, 130 and 278 years after the start of injection.

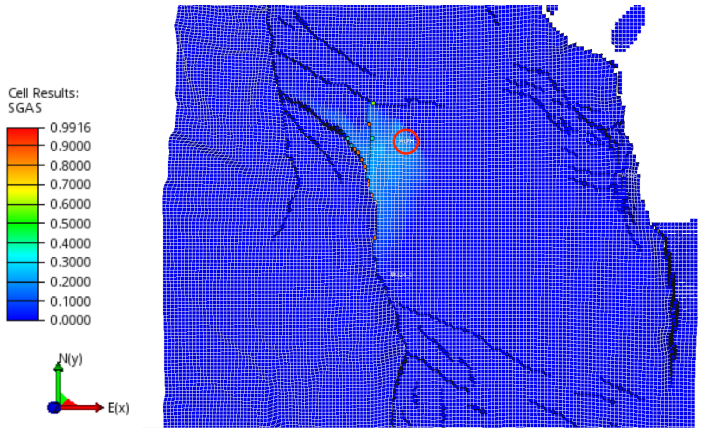

(a) Distribution 40 yrs after start of injection, yr 2062.

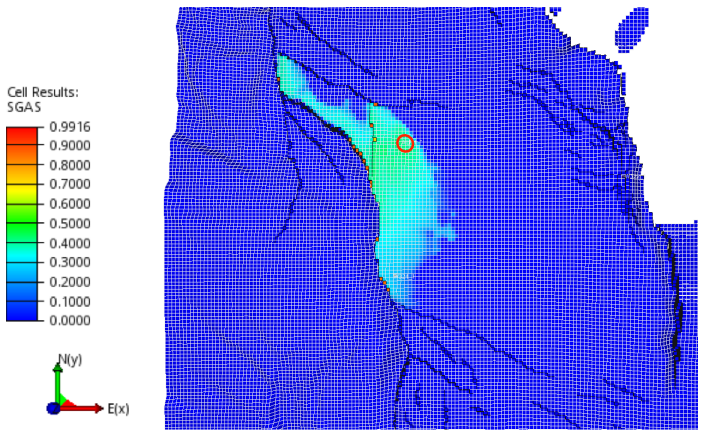

(b) Distribution 70 yrs after start of injection, yr 2092.

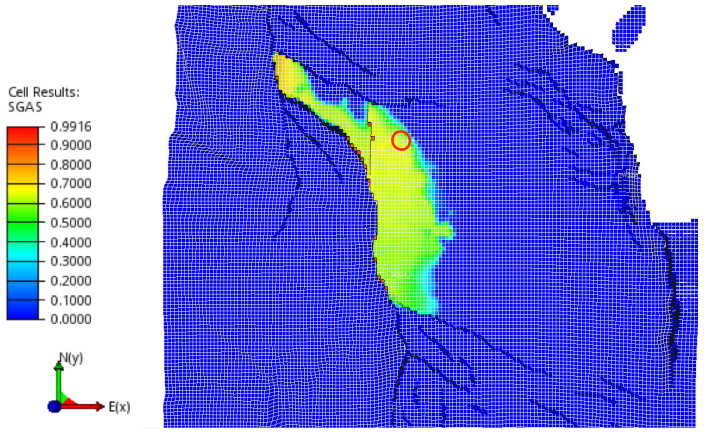

(c) Distribution 130 yrs after start of injection, yr 2152.

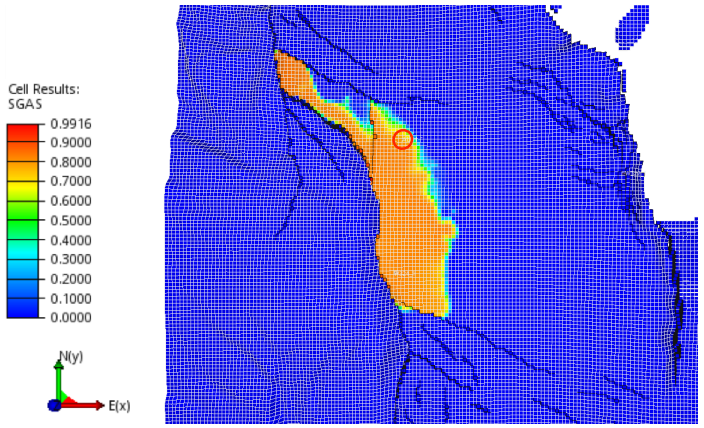

(d) Distribution 278 yrs after start of injection, yr 2300.

Fig. 11.1: CO_2 distribution as a function of time with an injection rate of 3.6 Mt of CO_2 per yr.

As can be observed from Fig. 11.1, the CO_2 will accumulate and form a continuous plume in the Alpha structure after the injection. The plume will grow as time goes by and the amount of injected CO_2 increases, before it stabilizes at the end of simulation. The plume expansion is shown by the change in colour, where light blue represents a CO_2 saturation of 30 %, yellow represents 70 % and orange 80 %.

Further, it can be noticed that the CO_2 will not migrate into the eastern Beta structure at this given rate and well location. The plume will move towards the western Vette fault and remain in the Alpha area. However, the development of the CO_2 plume is highly depending on the injection rate, well location and perforation depth. The following section illustrates the effect of different rates, showing that CO_2 migration into the Beta structure is possible.

11.2 The effect of injection rate

When CO_2 migrates through the Smeaheia field its flow path and velocity are highly dependent on the injection rate. Both the injection period and the rate itself will determine how the CO_2 moves from the injection well and within the formation. In general, the longer the injection period, the more CO_2 may be stored in the reservoir. Further, an increase in the injection rate will result in a higher fluid velocity, which may force the CO_2 to move further into the formation and expand the CO_2 plume. On the other hand, a lower injection rate could result in a lower velocity and thus a smaller CO_2 plume.

The CO_2 injection rate will also affect the well bottom hole pressure and the Smeaheia field pressure. As the amount of CO_2 increases in the formation, the field pressure is supposed to rise if there are no pressure connections in the storage area. Further, the well bottom hole pressure puts a limit on the injection rate. To ensure safe injection, preventing well damage and ensuring storage of supercritical CO_2, it is important to study the pressure development in the well and in Smeaheia at different injection rates.

The following sections give an understanding of how the downhole pressures, both the reservoir and the bottom hole pressures, differ with varying rates, as well as how the CO_2 distribution varies with different injection rates. It should be stated that the injection well location is constant for the following cases, which is equal to the location illustrated in the previous section.

11.2.1 Pressure variation as a function of injection rate

To ensure a safe and efficient injection operation it is necessary to study the bottom hole pressure and the reservoir pressure depletion at multiple injection rates. It is important that the bottom hole pressure does not exceed any well related limits during the injection, as it in worst case may cause well damage. Further, the injection rate will affect the Smeaheia field pressure, which again will have great impacts on the CO_2 density and the storage.

Well bottom hole pressure

It is specified in the reservoir simulation model used in this thesis that the injection well is controlled by surface flow rate as long as the bottom hole pressure is below 1000 bars. In other words, the injection rate is controlling the well as long as the well bottom hole pressure, WBHP, does not exceed 1000 bars, or 14 504 psi. Although it is not realistic to approach this pressure limit in the following simulations, it is important to study different scenarios to observe the bottom hole pressure, BHP.

Fig. 11.2 illustrates the WBHP in ALPHA_F when CO_2 is being injected with different rates. The following four injection rates have been used in this study;

3.6, 5.4, 6.5 and 8.7 Mt of CO_2 per year. It should be noticed that these values represent rates both within the available injection rate interval as well as higher rates.

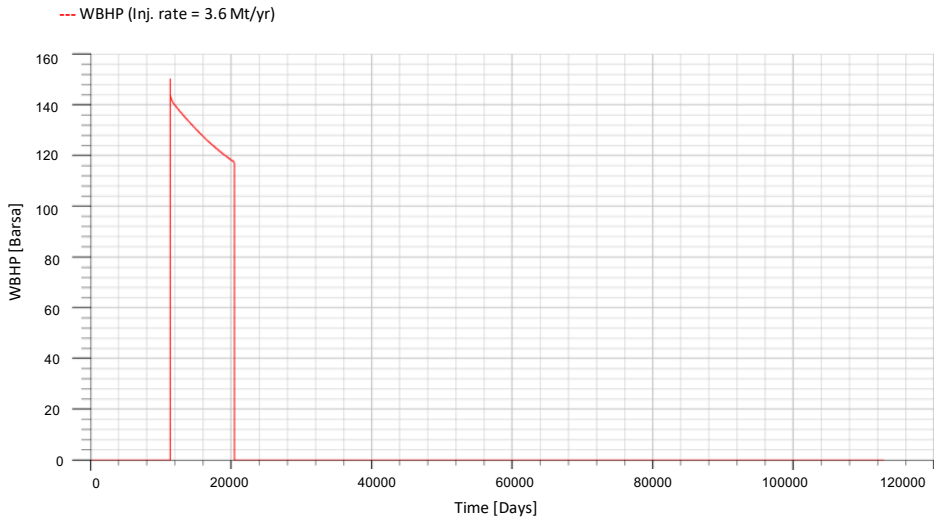

(a) Injection rate: 3.6 Mt of CO_2 per yr.

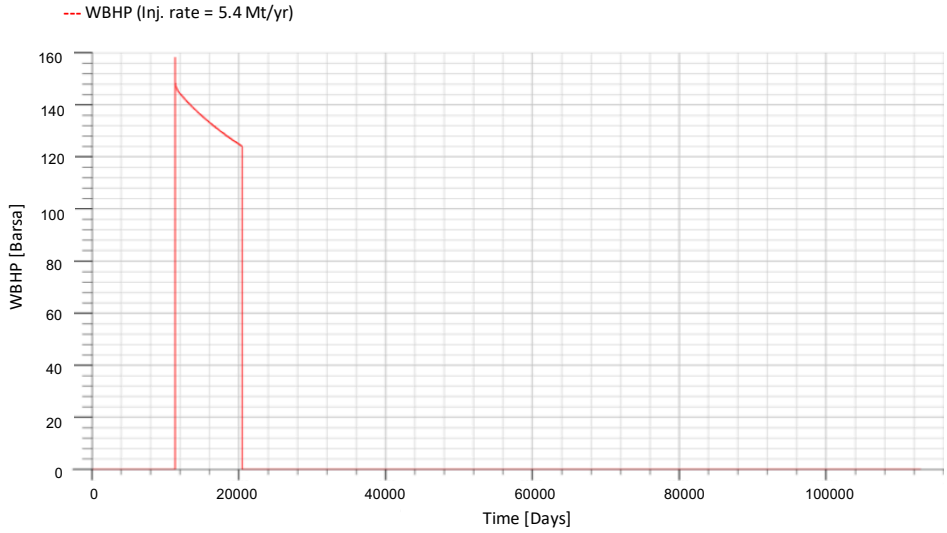

(b) Injection rate: 5.4 Mt of CO_2 per yr.

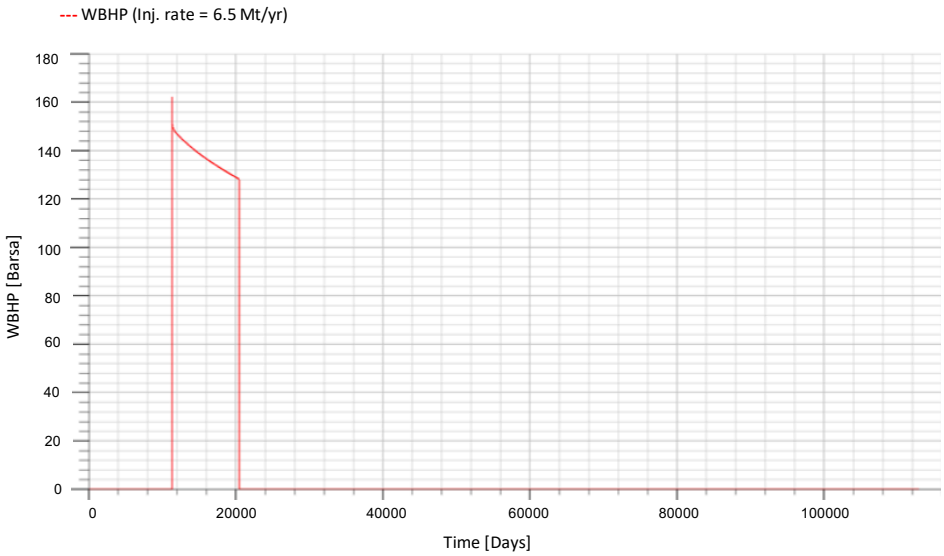

(c) Injection rate: 6.5 Mt of CO_2 per yr.

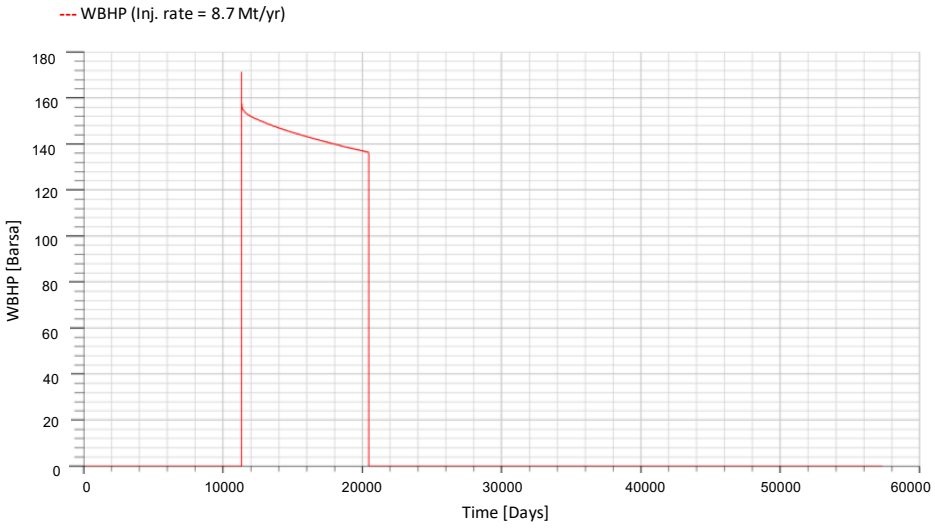

(d) Injection rate: 8.7 Mt of CO_2 per yr.

Fig. 11.2: Well bottom hole pressure at different injection rates.

The peaks in Fig. 11.2 represent the bottom hole pressure during the injection into Alpha. As can be noticed, the WBHP is equal to zero barsa before the injection starts up. During injection the BHP increases to about 150 barsa for all the studied rates before it decreases as the injection period ends. After the CO_2 injection, the bottom hole pressure returns to zero.

Smeaheia field pressure

The Smeaheia field pressure is highly affected by the injection rate and the producing Troll field. Two production wells with relatively high rates are located in the western part of the model, representing the production from the Troll reservoir. In fact, the gas production rate at Troll in March 2018 was measured to be approximately 3.5 billion sm^3 (Norwegian petroleum directorate, 2018). This production will affect the field pressure and the CO_2 storage in Smeaheia, making it an important topic to study.

Due to bridging faults and other geological connections, there will be a pressure connection between the Smeaheia field and the Troll reservoir. This connection will highly impact the Smeaheia pressure development as the production rates in Troll exceed the injection rate at Smeaheia. The pressure variation in the simulation model can be seen in **Fig. 11.3**. The injection well located in the Alpha structure is represented by the blue circle, while the production wells in the Troll field are represented by the two red circles.

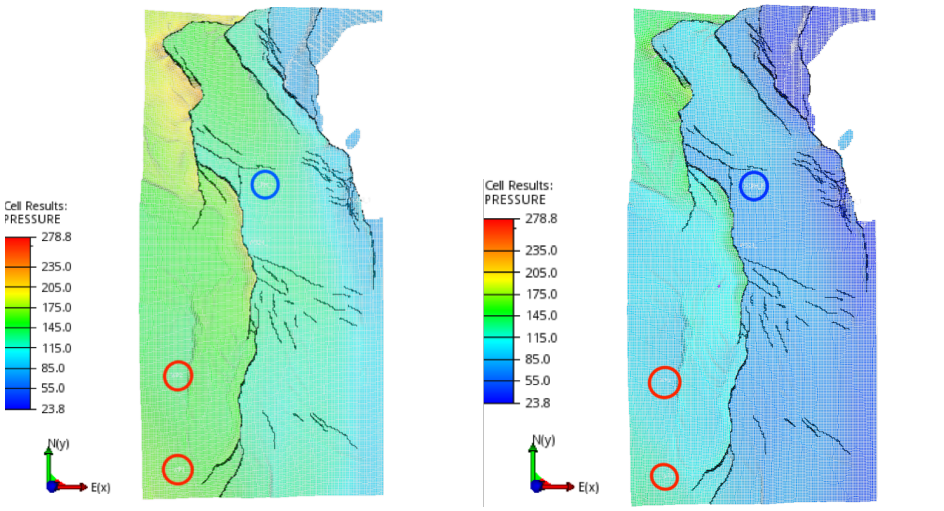

(a) Initial field pressure.

(b) Field pressure at the end of simulation.

Fig. 11.3: Field pressure variation in the Smeaheia model.

As can be noticed from Fig. 11.3, the green colour symbolizes the initial field pressure, which is measured to be approximately 155 bars. The pressure at the end of simulation is represented by the blue colour and is about 80 bars. In other words, a decrease in field pressure can be observed.

This pressure reduction can also be seen in **Fig. 11.4**. The figure illustrates the pressure development in Smeaheia at different injection rates. The red curve represents a rate of 7.2 Mt of CO_2 per year, the dark blue 6.5 Mt per year, the light blue 5.4 Mt per year and the green 3.6 Mt per year.

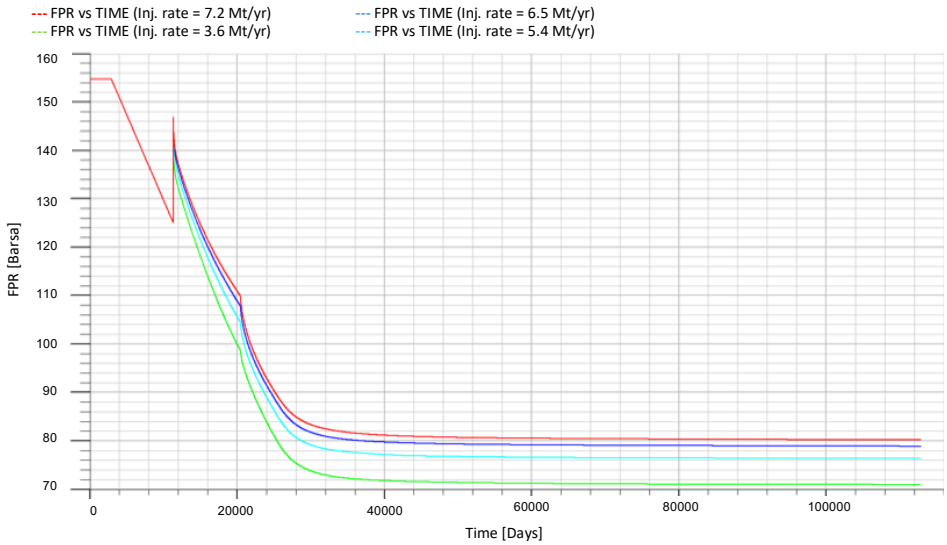

Fig. 11.4: Field pressure in the Smeaheia site at different injection rates.

From the figure above it can be observed that the field pressure will decrease rapidly before the injection of CO_2 starts. At the beginning of 2022, as the injection starts up, the field pressure will increase before it again reduces and stabilizes around 80 barsa for almost all of the rates. Only the lowest injection rate, 3.6 Mt of CO_2 per year, will cause the field pressure to reduce and stabilize at approximately 71 barsa.

Extreme scenario

An extreme case has been completed in this thesis to study the effect of a very high injection rate in the Alpha structure. **Fig. 11.5** illustrates the pressure development in Smeaheia when CO_2 is being injected at a rate of 43.3 Mt per year. This case is not realistic and will, as shown in **Fig. 11.6**, cause the carbon dioxide to move into the Beta structure. However, injection at this rate will result in a high, stable reservoir pressure at the end of simulation.

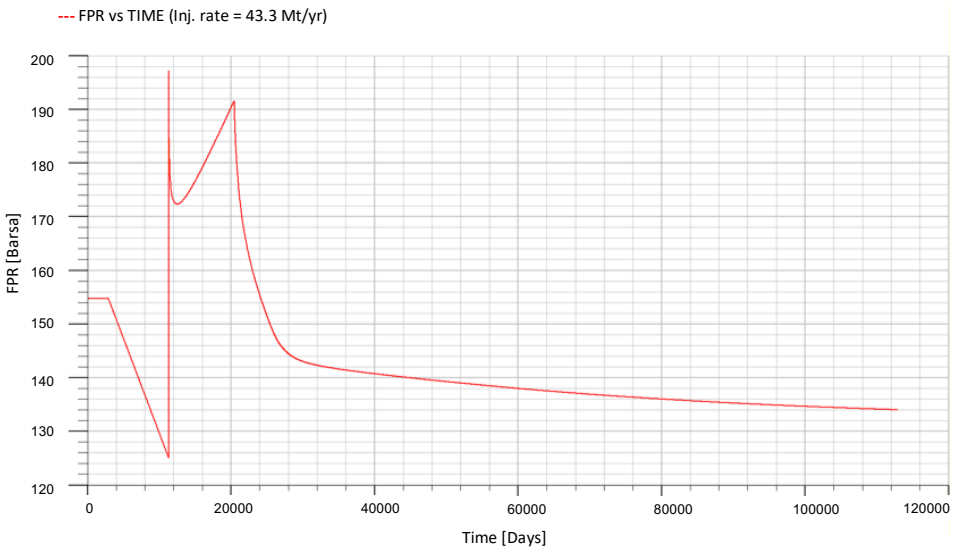

Fig. 11.5: Field pressure in the Smeaheia storage site at injection rate equal to 43.3 Mt of CO_2 per yr.

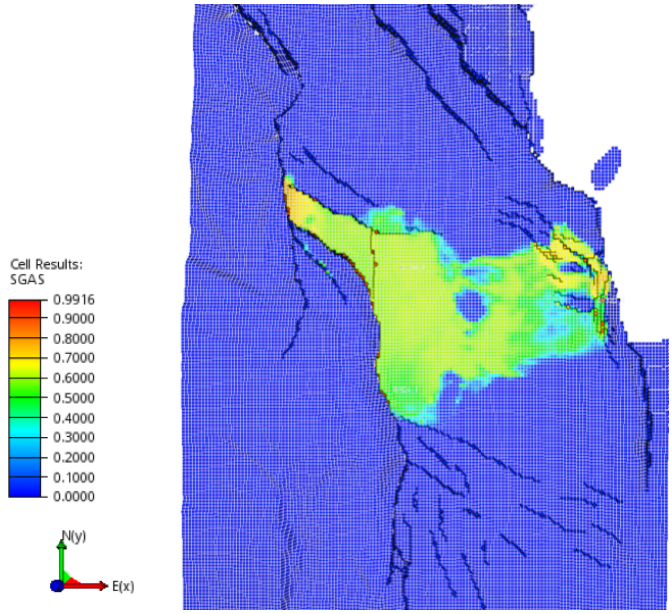

Fig. 11.6: CO_2 distribution in the Smeaheia storage site at injection rate equal to 43.3 Mt of CO_2 per yr.

Fig. 11.5 shows that the field pressure will have the same development, only more extreme, as the previously scenarios with lower injection rates. The pressure will stabilize at approximately 134 barsa at the end of simulation, which is close to the initial reservoir pressure of 155 barsa. However, as can be seen in Fig. 11.6, such a high injection rate will cause the CO_2 to accumulate in the Beta structure and probably migrate up to the surface.

Although the extreme scenario results in a high field pressure, this is not a realistic case. The study where the Troll production highly impacts the Smeaheia field pressure represents the actual reality and the following studies are based on this scenario. In other words, the rest of the studies are simulated with high-rate production wells, causing the field pressure to reduce and stabilize around 80 barsa.

11.2.2 CO2 distribution as a function of injection rate and period

The injection rate into the Smeaheia area is an important factor determining the CO_2 migration through the formation. As the injection rate increases, a higher amount of CO_2 is being pumped into the reservoir causing the carbon dioxide to expand its flow path. When considering a storage operation, it is important to inject a volume that will ensure a safe and efficient storage, meaning maximizing the storage volume and preventing any risk of leakage.

Fig. 11.7 shows the CO_2 distribution at different injection rates at the end of simulation. The figure clearly illustrates that a higher injection rate increases the risk of CO_2 migration into the Beta structure and leakage to the surface. As can be noticed, the CO_2 plume starts to migrate towards the Beta structure at an injection rate of approximately 5.8 Mt of CO_2 per year when the well is located in the northern part of Alpha. As the injection rate increases and the time goes by, a larger amount of CO_2 migrates towards the Beta area and a CO_2 plume may be formed in the Beta structure.

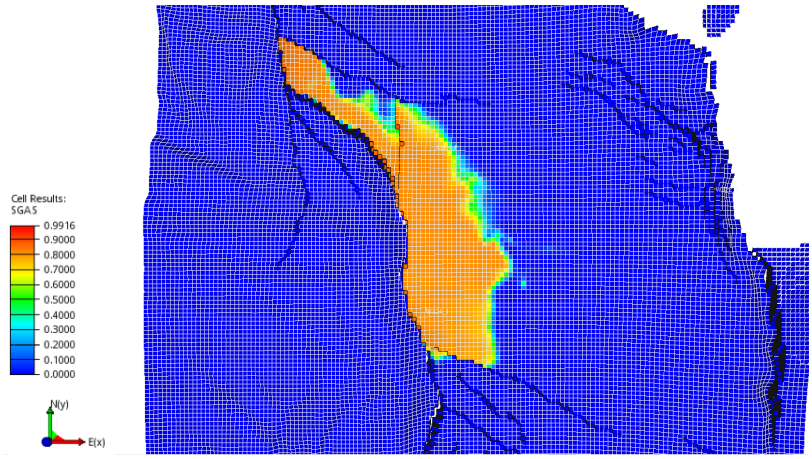

(a) Injection rate: 5.1 Mt of CO_2 per yr.

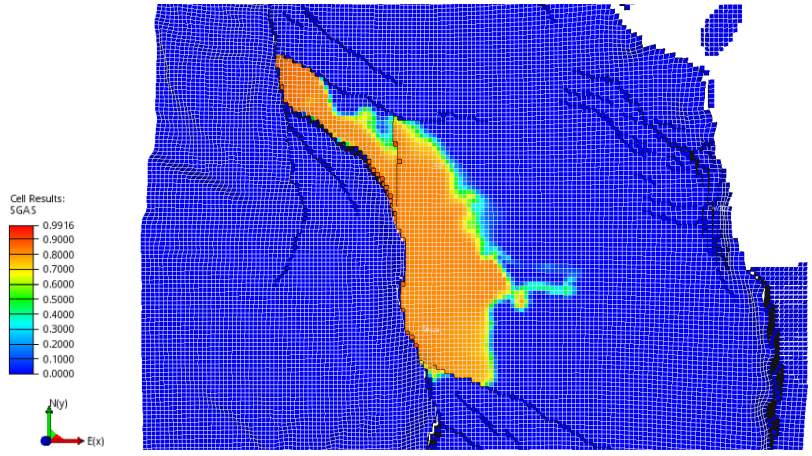

(b) Injection rate: 5.8 Mt of CO_2 per yr.

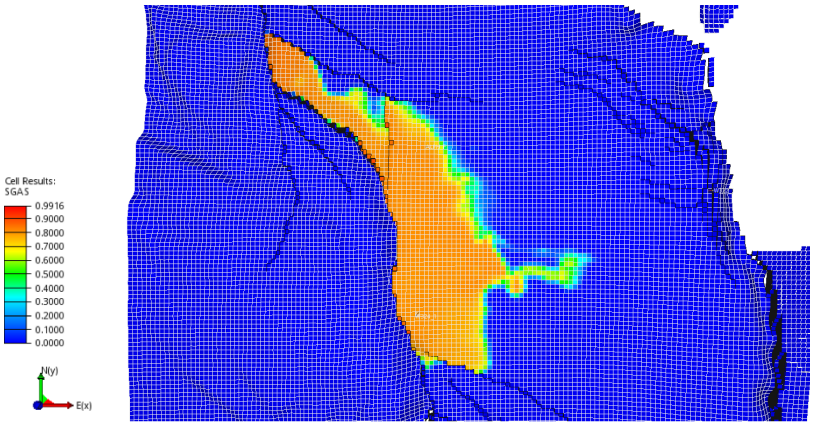

(c) Injection rate: 6.5 Mt of CO_2 per yr.

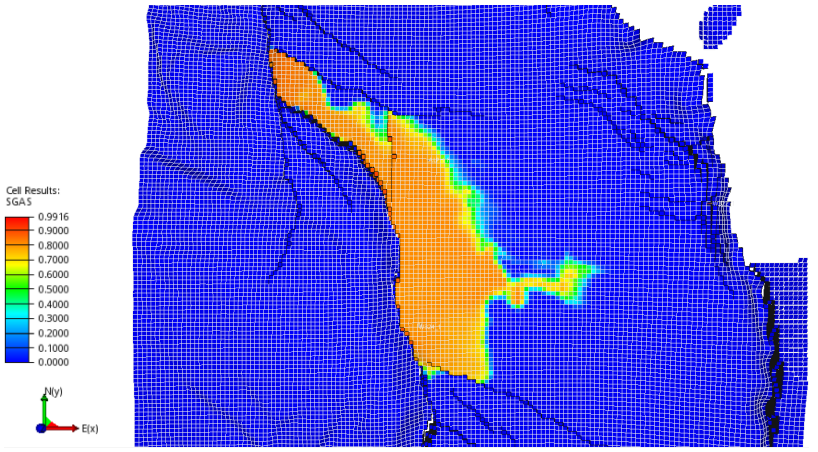

(d) Injection rate: 7.2 Mt of CO_2 per yr.

Fig. 11.7: CO_2 distribution in Smeaheia with varying injection rates.

Further, the injection period and rate may impact the CO_2 distribution when assuming a constant total injected volume. **Fig. 11.8** illustrates the CO_2 distribution when the amount of injected CO_2 is constant, but the rate and period are varying. The top figure shows a scenario when 4.3 Mt of CO_2 are being injected each year for 25 years, making up a total injected volume of 108 Mt. The bottom figure shows a situation where 8.6 Mt are injected for 12.5 years, also making up a total injected volume of 108 Mt of CO_2.

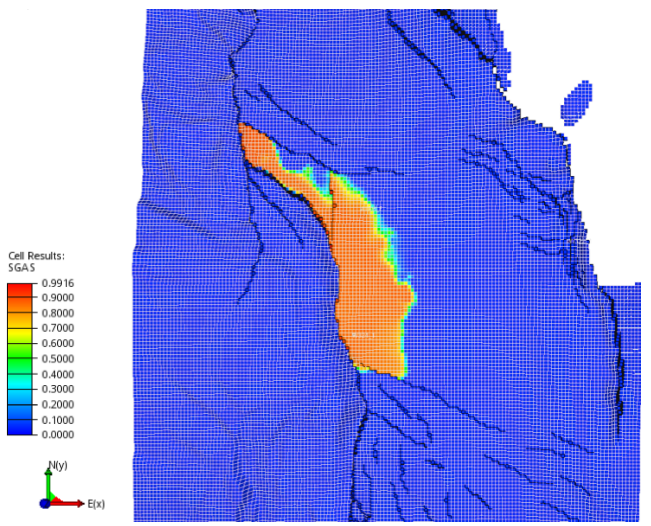

(a) Injection rate: 4.3 Mt of CO_2 in 25 yrs.

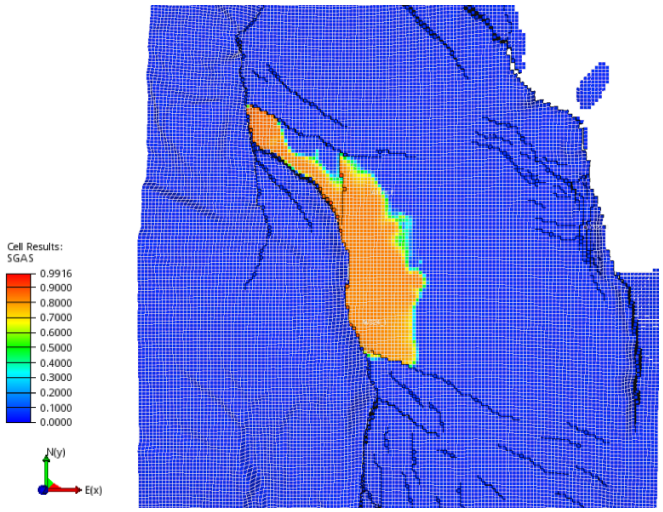

(b) Injection rate: 8.6 Mt of CO_2 in 12.5 yrs.

Fig. 11.8: CO_2 distribution with varying injection rate and period.

From the illustration above, it may be noticed that when carbon dioxide is being injected with a rate of 8.6 Mt in 12.5 years, the CO_2 plume will expand a bit more compared to the bottom scenario. Although the difference is almost not visible from Fig. 11.8, **Fig. 11.9** shows a slightly increase in CO_2 saturation at the injection well location when the injection lasts for 12.5 years. However, the injection period will be the same for all the following simulations as the effect of different periods with constant total injected volume is minimal.

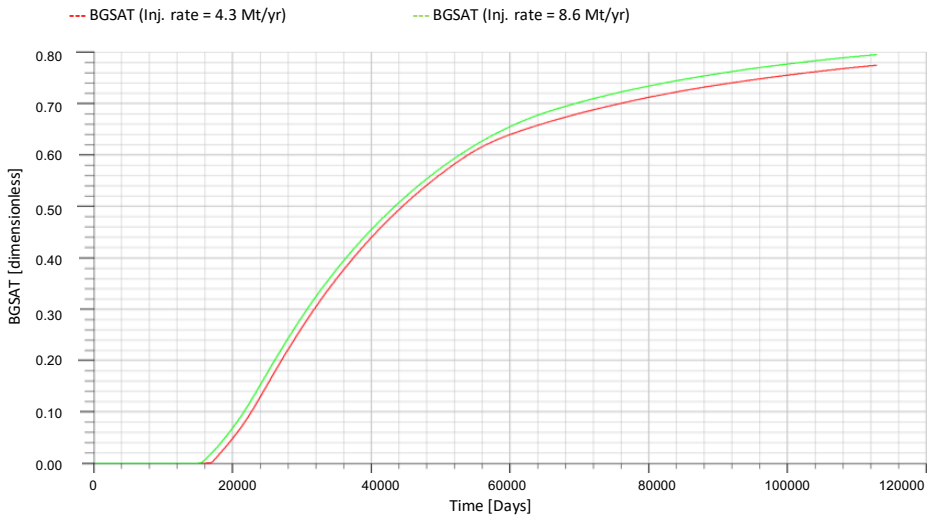

Fig. 11.9: CO_2 saturation at different injection rates and periods.

11.3 The effect of different well locations

The location of the injection well will highly influence the CO_2 distribution in the Smeaheia area. From previous chapters it is clear that the Alpha structure makes up a good option for well placement, but whether the well is placed north, south or in the middle of Alpha will affect the migration of the injected CO_2 and the total storage volume. In addition, locations outside the Alpha structure may also be efficient and safe alternatives when considering CO_2 storage.

As mentioned earlier in this thesis, migration to the Beta structure is unwanted due to the high risk of leakage to the surface. The multiple location studies completed in the following sections will illustrate the importance of injecting the optimal amount of CO_2. Some of the scenarios will cause migration and plume accumulation in the Beta structure, while others will ensure safe storage either in the Alpha area or far away from Beta. It should also be stated that CO_2 movement way up north in the model is unwanted because it may limit the capacity and the area is not under control. (Equinor, 2016).

Six different injection well locations have been studied in this thesis. Four locations within the Alpha structure; well placement in the northern part, north-west part, southern part and in the middle of the structure. In addition, a study where two injection wells are located in the very south of the model is described in section 11.3.5, whereas a case where a well is located in the northern part of the model is described in section 11.3.6. At each location the maximum injection rate preventing CO_2 migration into the Beta structure is tried to be found. A location's optimal injection rate may exceed the available rate interval of 1.5 to 4 Mt of CO_2 per year. However, this only emphasizes the low possibility of leakage during an actual injection.

Further, it should be stated that all wells studied in the following sections are perforated at the same depth. The CO_2 is injected into the lower part of the Fensfjord formation at approximately 1588 m. This perforation layer is selected due to its good reservoir quality and suitable depth. It should also be mentioned that it is the horizontal part of the wellbore that is located in this layer. A study of different perforations depths will be described in section 11.4.

The following sections give a short description of the well placements and the reasons why they are selected, in addition to compare several injection rates at each location. Multiple rates have been simulated and a selection of these are illustrated in this thesis. To be able to understand where the different wells are located, an overview of the model can be helpful. **Fig. 11.10** gives an overview of the described well locations used for simulations in the following sections.

At last, an overview of the different well locations, their optimal injection rate and storage volume is given in section 11.3.7. These are the results that will be further discussed in chapter 12.

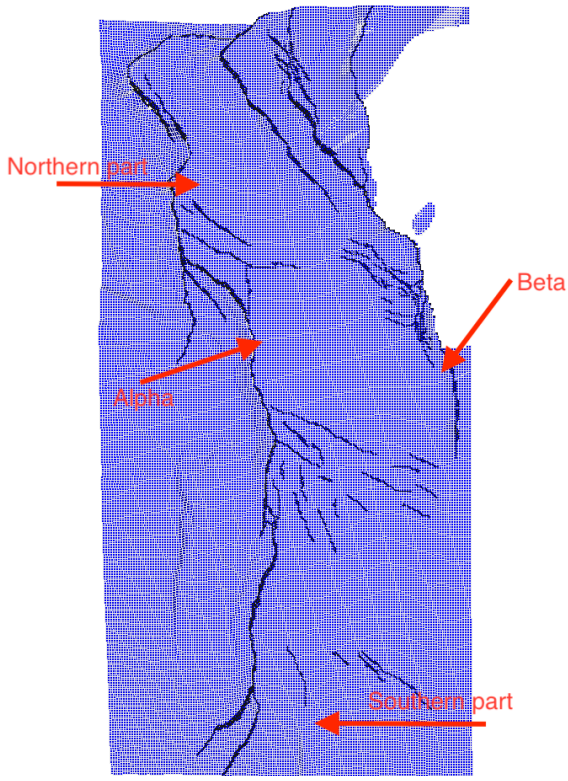

Fig. 11.10: The different well locations in the Smeaheia storage site model.

11.3.1 Well location 1 - Northern part of Alpha

The first study was completed with one injection well located in the northern part of the Alpha structure, as illustrated by the red circle in **Fig. 11.11**. This location is selected based on the long distance between the well placement and the Beta structure, in addition to the fact that the western Vette fault creates a safe structural trap. As mentioned earlier, the horizontal wellbore is placed at approximately 1588 m depth.

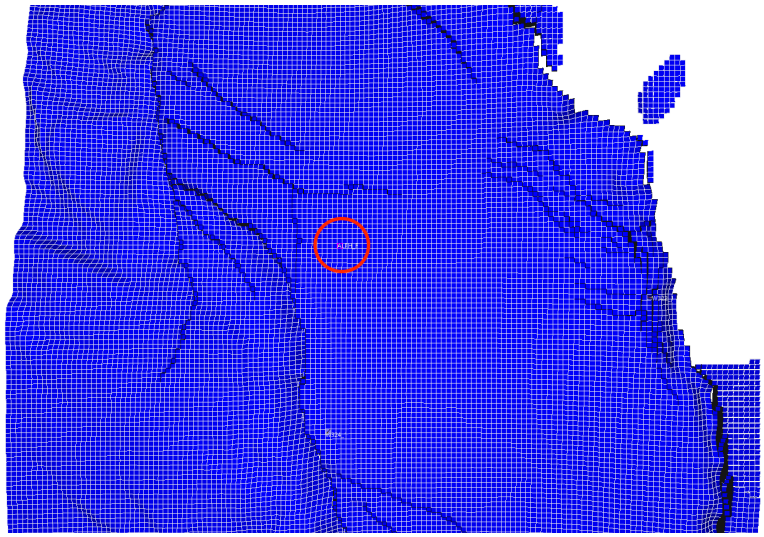

Fig. 11.11: Well location in the northern part of Alpha.

Fig. 11.12 illustrates how the CO_2 distributes through the storage site when it is injected with different rates. All the simulations are run until year 2300. The figure shows a collection of the studies completed in this report where the following rates are represented; 2.9, 5.4, 5.8 and 6.5 Mt of CO_2 per year. It should be observed that three of the injection rates in the following illustrations are higher than the available rate interval, 1.5 to 4 Mt of CO_2 per year, given from the industrial plants.

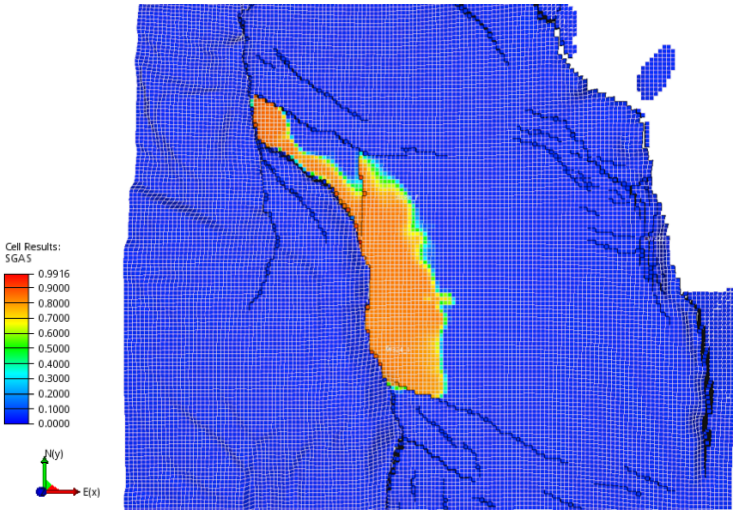

(a) Injection rate of 2.9 Mt of CO_2 per yr.

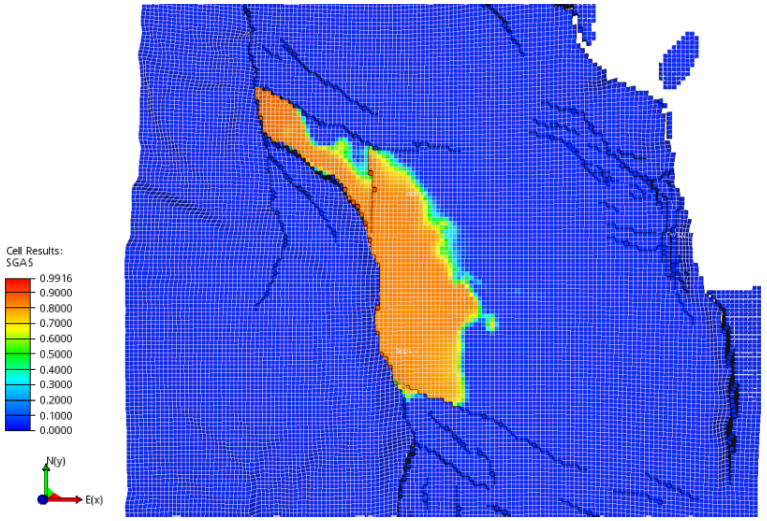

(b) Injection rate of 5.4 Mt of CO_2 per yr.

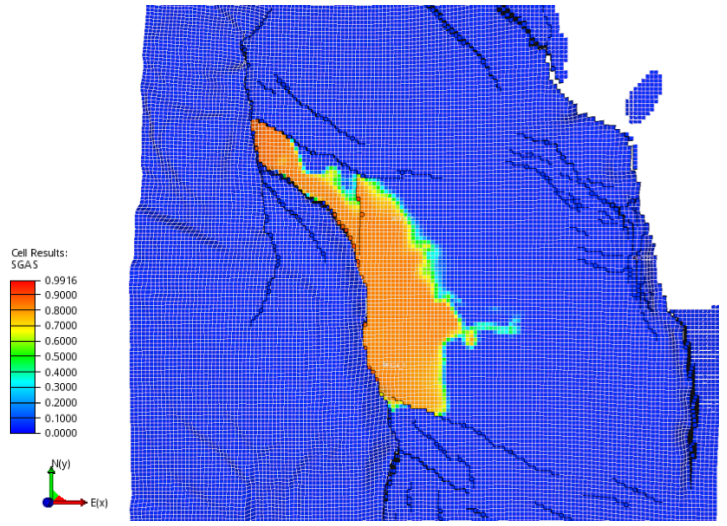

(c) Injection rate of 5.8 Mt of CO_2 per yr.

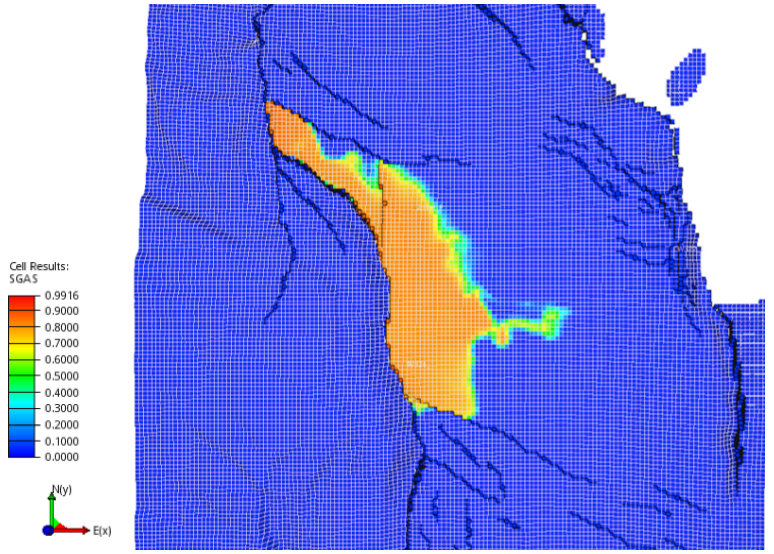

(d) Injection rate of 6.5 Mt of CO_2 per yr.

Fig. 11.12: CO_2 distribution at well location 1 with varying injection rates given in year 2300.

As can be seen from Fig. 11.12, the CO_2 accumulates and form a plume in all of the scenarios. The plume is growing a bit differently in the selected cases, but similar to all of them is the movement close to the western Vette fault. Further, it can be seen that the CO_2 starts to migrate towards the Beta structure just below a rate of 5.8 Mt per year. The last scenario shows that the amount of CO_2 flowing towards the Beta structure will increase as the injection rate gets higher.

11.3.2 Well location 2 - Middle part of Alpha

The second study was done with the injection well located in the middle of the Alpha structure. The main reasons to put the well at this location were to find the optimal injection rate when the well is located closer to the Beta structure, as well as study whether the CO_2 would migrate along the western Vette fault or directly start moving in Beta direction.

The red circle in **Fig. 11.13** shows the second well location. As previously stated, the CO_2 is injected in the lower part of the Fensfjord formation.

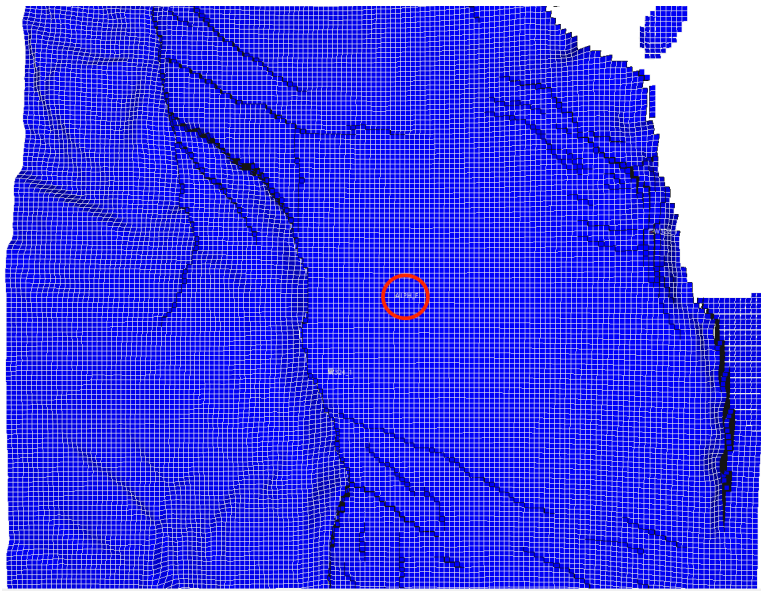

Fig. 11.13: Well location in the middle of Alpha.

Fig. 11.14 compares the CO_2 movement in the storage site at different injection rates. Multiple rates have been tested and studied, and the following rates are presented in this report; 0.7, 1.4, 3.6 and 5.1 Mt of CO_2 per year. It should be noticed that both higher and lower rates compared to the available injection interval are tested, as well as rates within the interval.

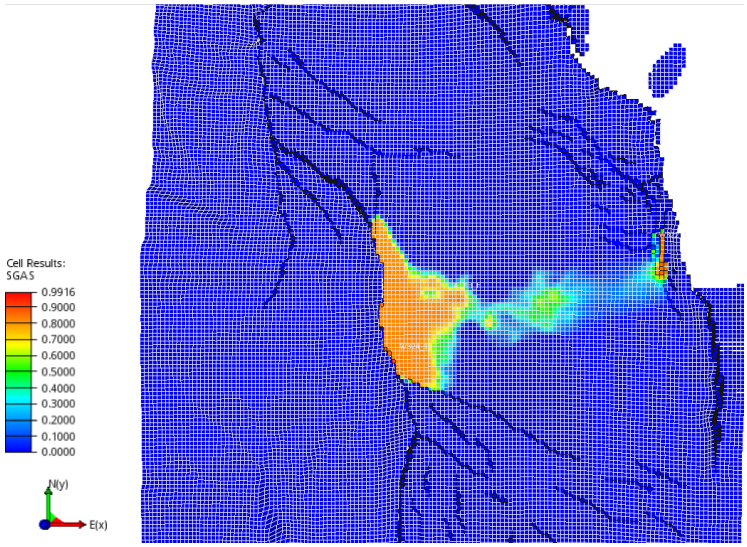

(a) Injection rqate of 0.7 Mt of CO_2 per yr.

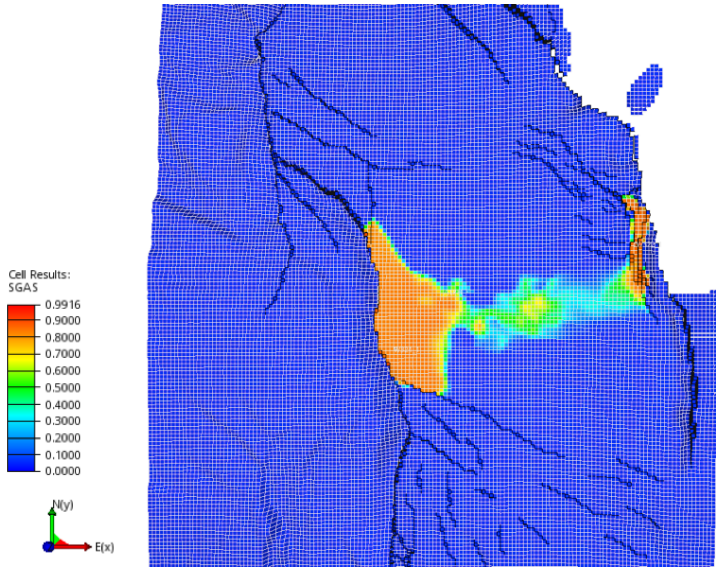

(b) Injection rate of 1.4 Mt of CO_2 per yr.

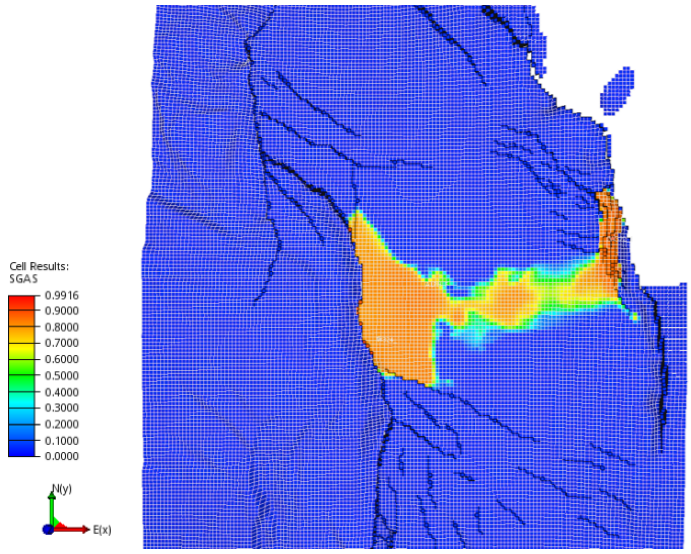

(c) Injection rate of 3.6 Mt of CO_2 per yr.

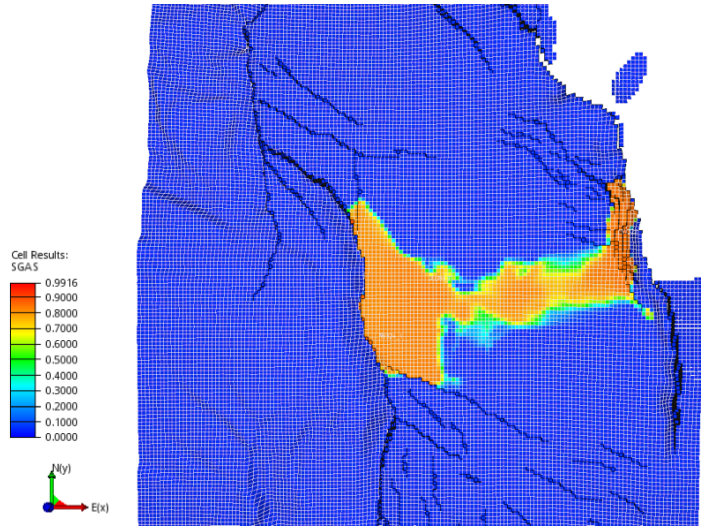

(d) Injection rate of 5.1 Mt of CO_2 per yr.

Fig. 11.14: CO_2 distribution at well location 2 with varying injection rates given in year 2300.

From Fig. 11.14 it can be seen that injection at this well location will result in CO_2 migration into the Beta structure even at low injection rates. It can be noticed that the CO_2 plume in the Alpha structure is relatively small when the CO_2 starts to move into the Beta area. As the rate increases, the amount of carbon dioxide moving towards the Beta structure gets higher.

11.3.3 Well location 3 - North-West part of Alpha

The third study was completed with the injection well placed in the north-west part of the Alpha structure, as shown in **Fig. 11.15**. Studies of well location 3 is conducted to see the effect of a well location closer to the western Vette fault. As should be noticed, this location is not far away from well location 1 in the northern part of Alpha, making it interesting to see if there are any effects of CO_2 injection closer to the fault.

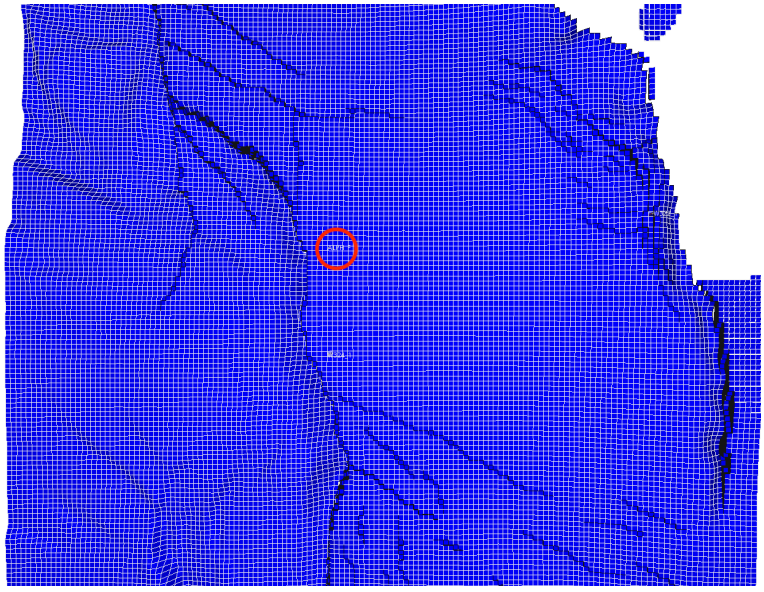

Fig. 11.15: Well location in the north-west part of Alpha.

Fig. 11.16 shows the CO_2 movement at the following injection rates; 2.5, 2.9, 3.6 and 5.4 Mt of CO_2 per year. In other words, most of the rate simulations run in this study are within the annual available injection rate interval given from the land plants.

It should be stated that the last figure, showing a rate of 5.4 Mt CO_2 each year, is simulated to year 2250, while the rest is simulated to 2300. The difference in simulation time, which is 50 years, will not have any great impacts on the results as the following figure gives a clear indication of the long-term CO_2 distribution.

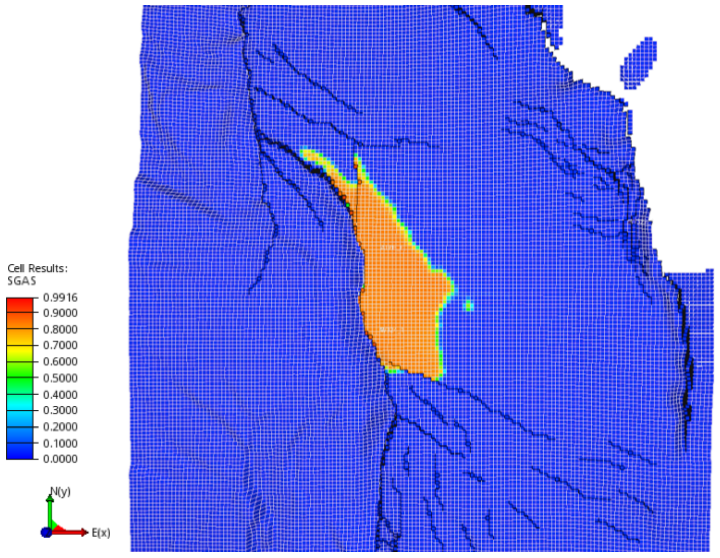

(a) Injection rate of 2.5 Mt of CO_2 per yr.

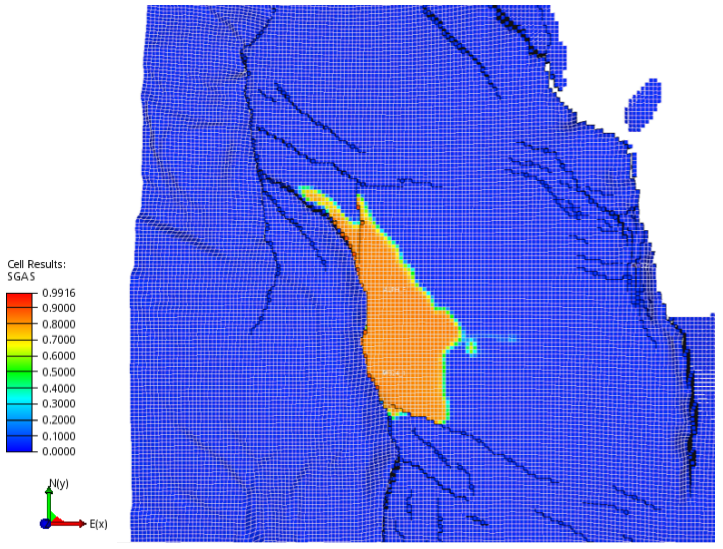

(b) Injection rate of 2.9 Mt of CO_2 per yr.

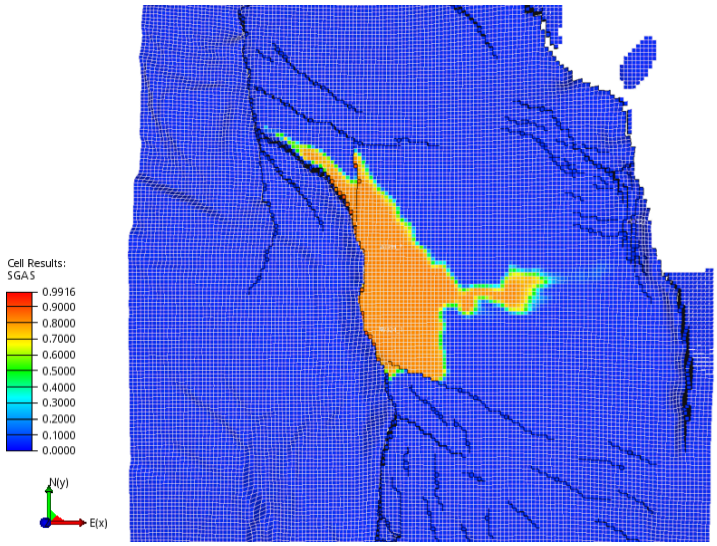

(c) Injection rate of 3.6 Mt of CO_2 per yr.

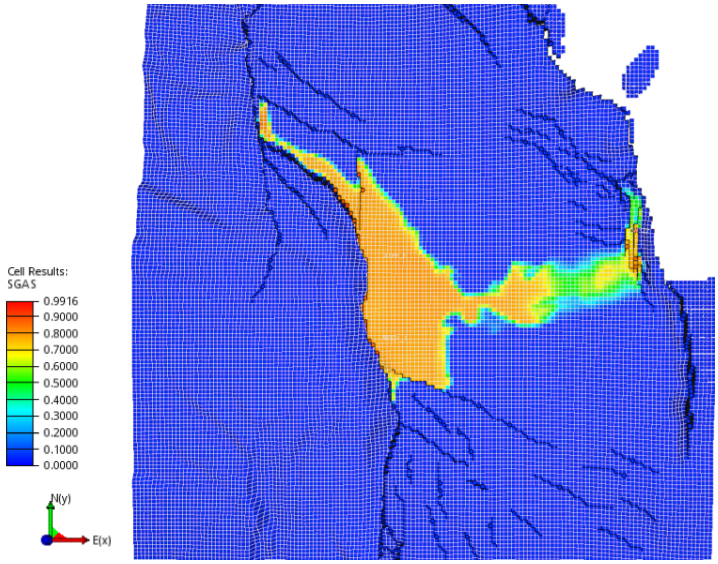

(d) Injection rate of 5.4 Mt of CO_2 per yr.

Fig. 11.16: CO_2 distribution at well location 3 with varying injection rates given in year 2300 and 2250.

As can be noticed from the figure above, the CO_2 will move along parts of the Vette fault. Further, carbon dioxide will start to migrate towards the Beta structure just above a rate of 2.9 Mt of CO_2 per year. Higher rates will cause a larger CO_2 flow migrating in the Beta direction.

11.3.4 Well location 4 - Southern part of Alpha

The last study completed with the injection well located within the Alpha structure was done with the well placed in the southern part. The location is based on the curiosity whether the CO_2 will move directly to the Beta area or if the Alpha structure will be filled to its spill point before the CO_2 migrates in the Beta direction.

The injection well depth is still 1588 m, with the perforations made in the lower part of the Fensfjord formation. The red circle shown in **Fig. 11.17** illustrates the southern well location.

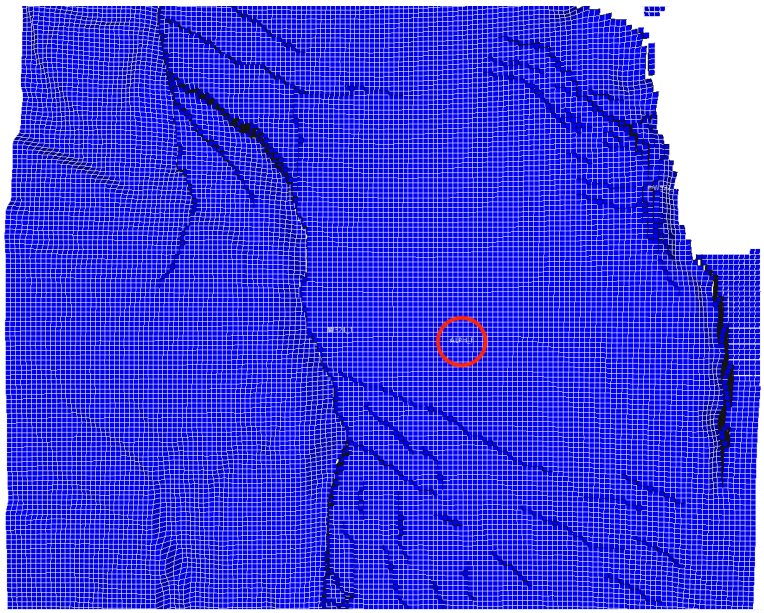

Fig. 11.17: Well location in the southern part of Alpha.

Fig. 11.18 compares the CO_2 movement within the storage site with injection rates equal to 1.4, 1.8, 2.2 and 2.9 Mt of CO_2 each year. Due to the short distance between well location 4 and the Beta structure, the injection rates tested at this location are in the lower range of the available injection rate interval given from the industrial land plants.

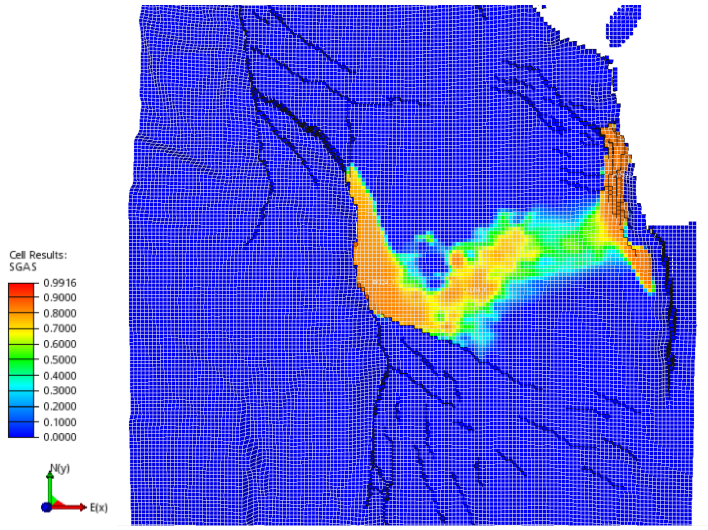

(a) Injection rate of 1.4 Mt of CO_2 per yr.

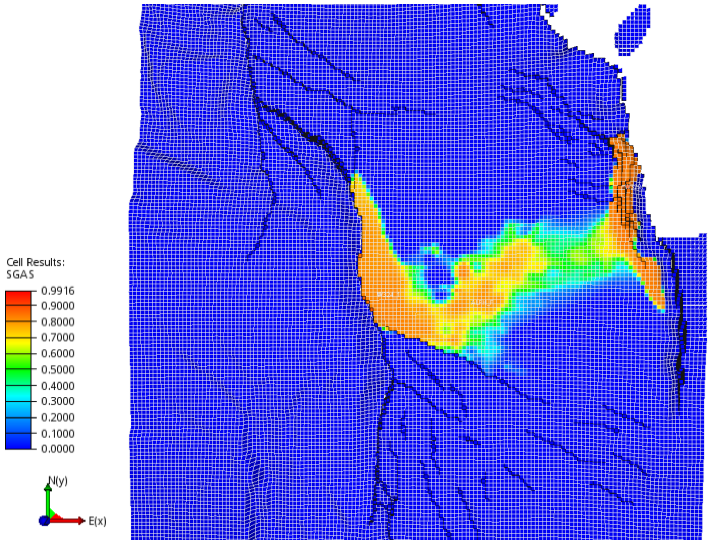

(b) Injection rate of 1.8 Mt of CO_2 per yr.

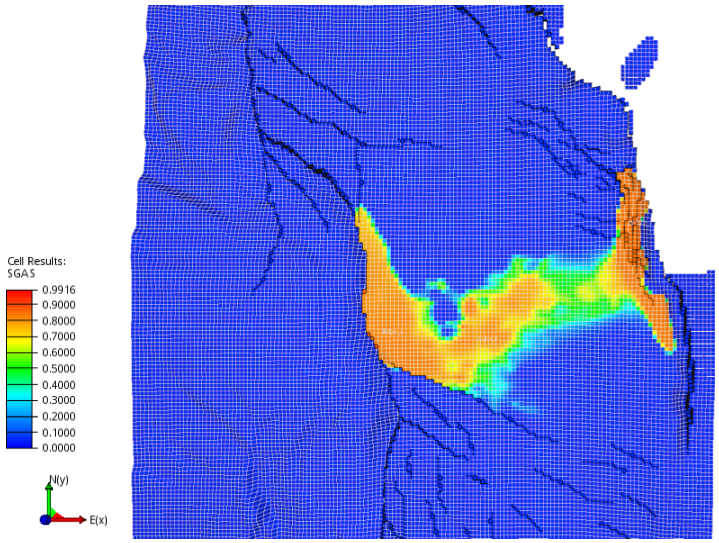

(c) Injection rate of 2.2 Mt of CO_2 per yr.

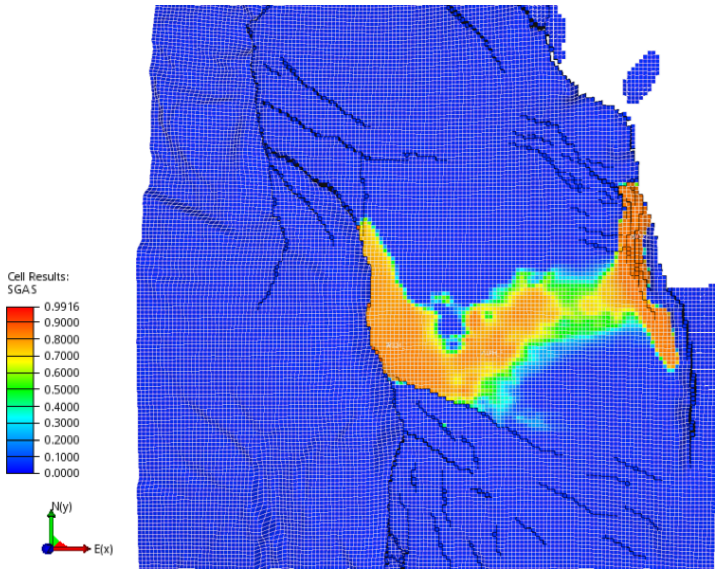

(d) Injection rate of 2.9 Mt of CO_2 per yr.

Fig. 11.18: CO_2 distribution at well location 4 with varying injection rates given in year 2300.

Fig. 11.18 shows that all of the studied injection rates will cause the CO_2 to move into the Beta structure. It can be noticed that the Alpha structure is not being filled up to its spill point before the CO_2 starts to move in the Beta direction. As can be seen by the change in CO_2 saturation, higher injection rates will cause a larger amount of carbon dioxide to migrate into Beta.

11.3.5 Well location 5 - Southern part of the model

Another study was completed with two injection wells located in the southern part of the model. The injection wells are illustrated by the two red circles in **Fig. 11.19**. These placements are based on two reasons. First, the injection wells are located far away from the Beta structure, meaning that a larger amount of CO_2 can be injected and stored without risking movement into the Beta area. Second, there is a fault acting as a bridge connecting the Alpha area and the southern part of the model. This fault makes it possible for the injected CO_2 to migrate into the Alpha structure and thus increase the storage volume. The fault is indicated by the green circle in Fig. 11.19.

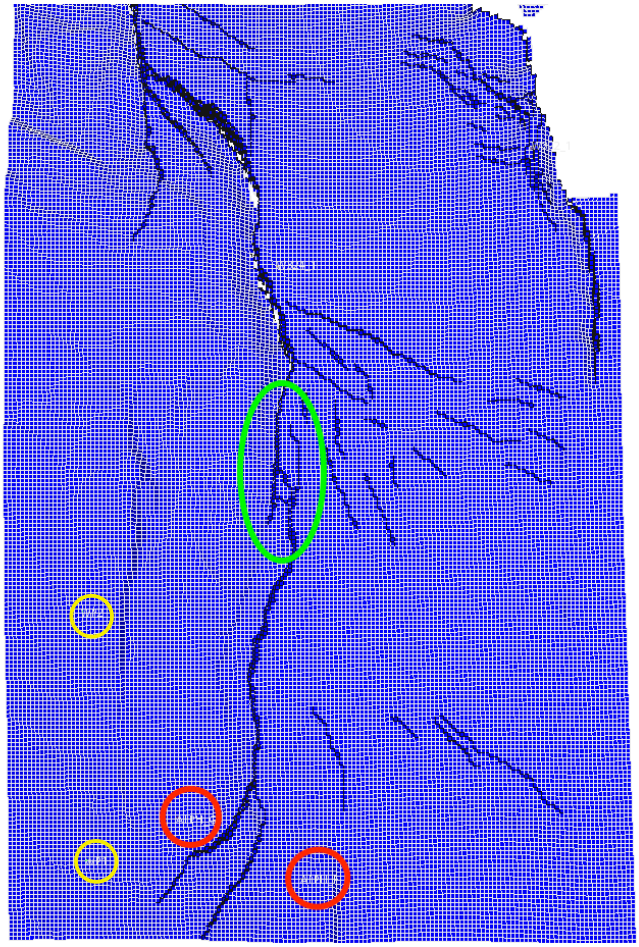

Fig. 11.19: Well locations in the southern part of the model.

Further, two wells highlighted by the yellow circles can be observed in the south-west part of the model. These wells represent production of oil and gas from the Troll field and will cause a pressure depletion in the reservoir model. However, it should be mentioned that these wells may not be placed correctly compared to the actual locations in the Troll reservoir, as they are only simulated to get a realistic scenario with pressure reduction in the field.

Multiple injection rates have been studied to observe the CO_2 distribution in the southern part of the model and **Fig. 11.20** illustrates the distribution at several rates. Higher injection rates have been researched at this location and the figure shows a selection with rates equal to 40, 60, 80 and 100 Mt of CO_2 per year. The injection rates are determined by the reasons mentioned above, which make it possible to inject higher amounts of CO_2 compared to the previous locations.

It should be stated that the injection wells cannot handle such rates in reality. A possible maximum rate for an injection well is about 10 Mt each year. However, although this study may be unreasonable, the high rates emphasize the possibility of storing a large CO_2 volume in the southern part of the model.

Another observation should be made when considering the figure below. The simulations completed at this well location are modelled for a longer time compared to the previous studies, and the results below are given in year 2500. The additional simulation time is applied to get better results.

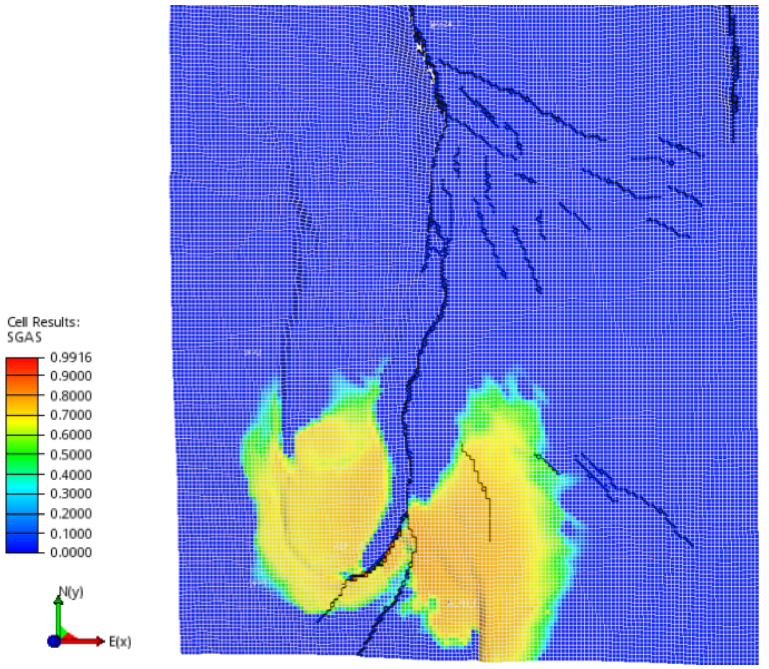

(a) Injection rate: 40 Mt of CO_2 per yr.

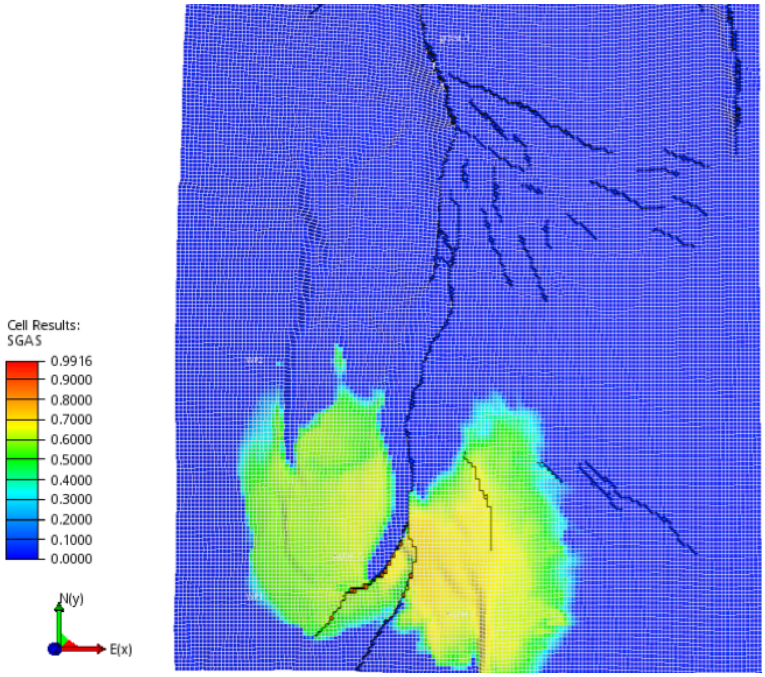

(b) Injection rate: 60 Mt of CO_2 per yr.

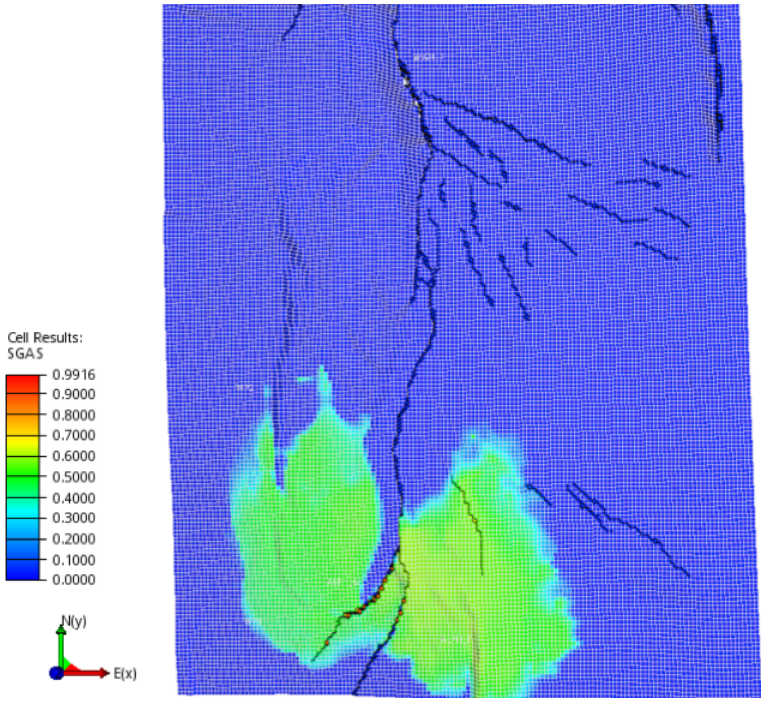

(c) Injection rate: 80 Mt of CO_2 per yr.

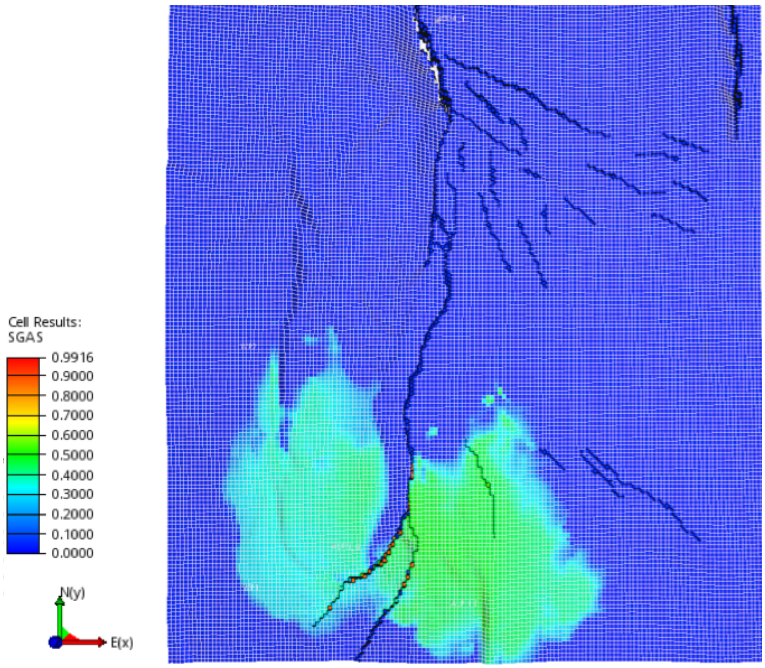

(d) Injection rate: 100 Mt of CO_2 per yr.

Fig. 11.20: CO_2 distribution in the southern part of the model with varying injection rates at year 2500.

As can be seen from the figure above, the CO_2 will form a large plume in the southern part of the model. The plume will be continuous for all the studied injection rates although the wells are located on each side of a fault. Further, the CO_2 may move upwards towards the Alpha structure and the bridging fault as time goes by.

It should also be noticed that some of the carbon dioxide will move towards the production wells in the Troll reservoir regardless of the injection rate. As can be seen, some of the CO_2 from the western injection well will migrate close to the producing Troll field, while some of the carbon dioxide will move towards the bridging fault and the Alpha structure. These results are further discussed in chapter 12.

11.3.6 Well location 6 - Northern part of the model

The sixth study looked at a well placement in the northern part of the model. The objective of studying this well location, illustrated by the red circle in **Fig. 11.21**, is to see if the CO_2 will migrate directly into the Alpha structure, and possibly Beta, or if it will accumulate and form a plume in the northern part.

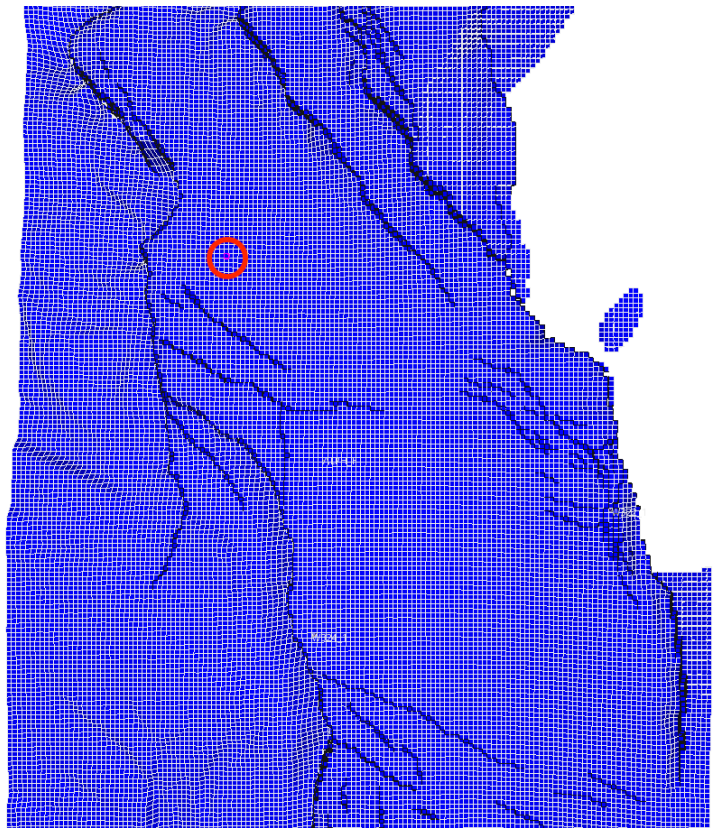

Fig. 11.21: Well location in the northern part of the model.

Since the injection well is located far from the Beta structure, which reduces the risk of leakage to the surface, the injection rate may be higher compared to injection rates in the Alpha structure. Several rates have been tested in this thesis and **Fig. 11.22** shows the result from respectively 8.7, 11.0, 21.6 and 28.9 Mt of injected CO_2 per year for 25 years. It should be stated that two of the injection rates, 8.7 and 11.0 Mt of CO_2 per year, are realistic rates for an injection well. The other two are not realistic but give a clear indication of the storage capacity in the northern area.

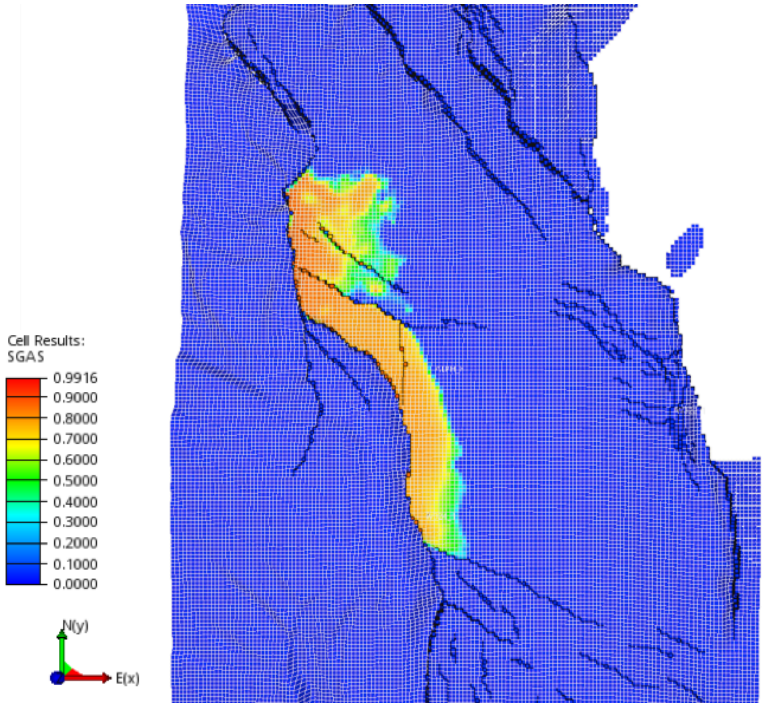

(a) Injection rate: 8.7 Mt of CO_2 per yr.

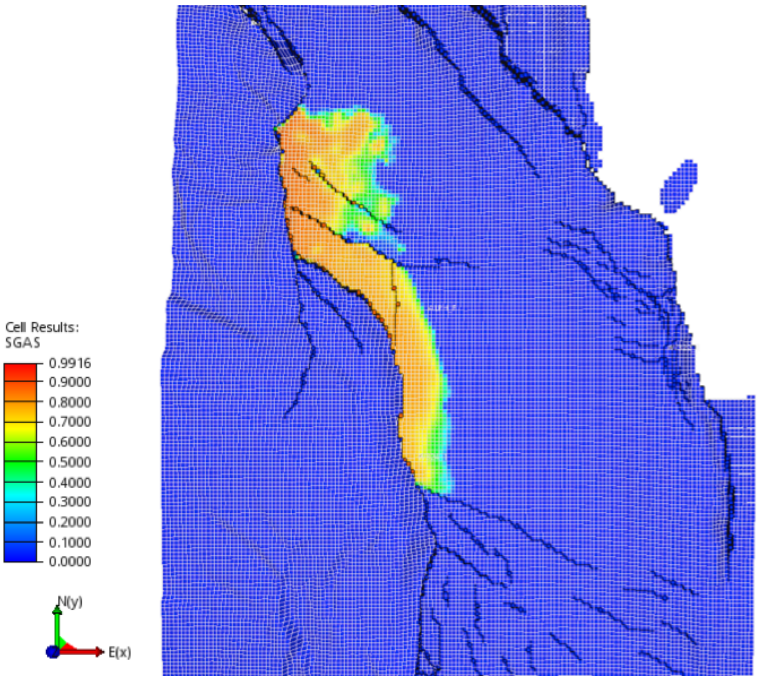

(b) Injection rate: 11.0 Mt of CO_2 per yr.

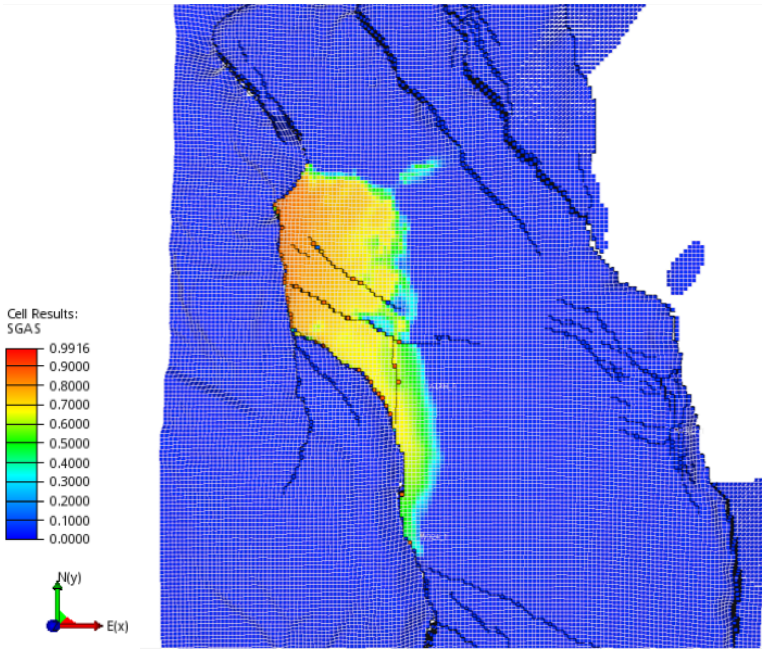

(c) Injection rate: 21.6 Mt of CO_2 per yr.

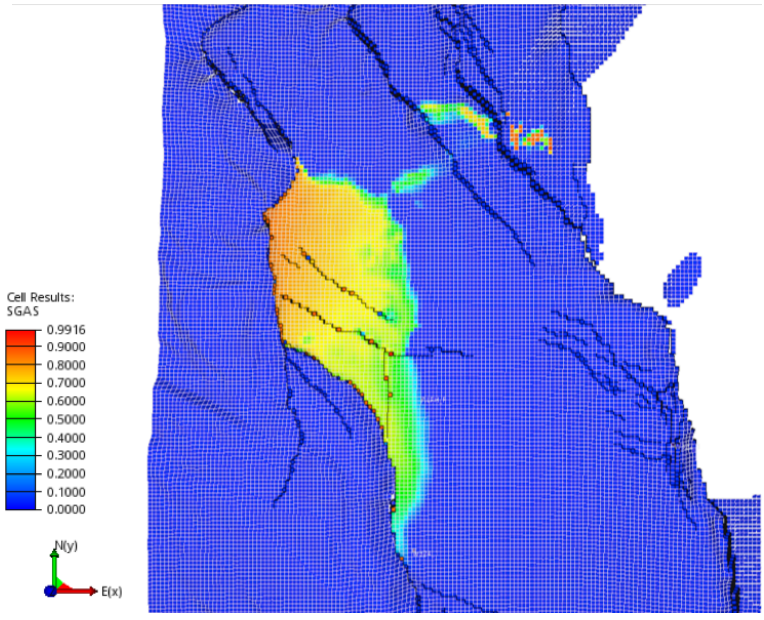

(d) Injection rate: 28.9 Mt of CO_2 per yr.

Fig. 11.22: CO_2 distribution in the northern part of the model with varying injection rates at year 2300.

As can be seen from the figure above, the CO_2 will migrate south along the western Vette fault and into the Alpha structure. As the injection rate increases the CO_2 plume will expand, which results in a movement further north in the model. At a rate of 28.9 Mt of CO_2 per year the carbon dioxide has migrated into the northern part of the model.

It should be noticed that the CO_2 is not moving into the Beta direction although the injection rate is high. But, as can be observed from the figure, a lower injection rate will cause a larger CO_2 accumulation in the Alpha structure, making it possible that the higher rates may cause larger plumes in the Alpha area as time goes by.

11.3.7 Well location overview

Six different well locations and multiple injection rates are studied in this thesis, making it hard to remember all the details. The following tables give an overview of the best results found in this section, which will be further discussed in chapter 12.

Table 11.1 gives the highest possible injection rate ensuring no migration into the Beta structure for each of the locations studied above. Table 11.2 gives the total injected volume of carbon dioxide at each well location when the optimal amount of CO_2 is being injected. Where no results are given, the studied injection rates caused a CO_2 movement into Beta and thus a high risk of leakage to the surface. It should also be noticed that for location 5 the results are given for one injection well multiplied by two.

Table 11.1: Optimal injection rate at each well location.

Well location	Optimal injection rate [Mt of CO_2 per year]
Location 1 - Northern part of Alpha	5.4
Location 2 - Middle part of Alpha	-
Location 3 - North-West part of Alpha	2.9
Location 4 - Southern part of Alpha	-
Location 5 - Southern part of the model	$100 \cdot 2$
Location 6 - Northern part of the model	21.6

Table 11.2: Total CO_2 volume injected after 25 years.

Well location	Total injected volume of CO_2 after 25 years [Mt]
Location 1 - Northern part of Alpha	135
Location 2 - Middle part of Alpha	-
Location 3 - North-West part of Alpha	72
Location 4 - Southern part of Alpha	-
Location 5 - Southern part of the model	$2500 \cdot 2$
Location 6 - Northern part of the model	540

11.4 The effect of perforation depths

As described previously in this report, the Sognefjord delta aquifer consists of three formations; Sognefjord, Fensfjord and Krossfjord. The Fensfjord and Sognefjord formations have significant reservoir characteristics such as high porosity and permeability, making them good options for injection. The pores and the connection between them, make it possible to store large amounts of CO_2 in these layers.

Although the Krossfjord formation has lower permeability, it is located at a deeper depth making it possible for the injected CO_2 to rise upwards through the Krossfjord layer and into the Fensfjord and Sognefjord formations. In addition, due to its reservoir characteristics, the Krossfjord formation may make it possible for some of the CO_2 to be trapped in this layer, which will increase the total amount of stored carbon dioxide. It is therefore important to study how the different injection depths impact the total storage amount of CO_2.

Section 11.4.1 illustrates the effect of injecting CO_2 into three different depths within the Fensfjord formation. Perforations made in the upper, lower and middle part of Fensfjord are studied. Section 11.4.2 describes the effect of CO_2 injection in the Krossfjord formation. Three perforation depths within this formation are considered. At last, an overview of the results are given in section 11.4.3.

It should be stated that perforations in the Sognefjord formation will not be studied in this report. Injection into this layer will result in a non-effective storage since the underlying Fensfjord and Krossfjord formations will be undisturbed by CO_2 movement because the carbon dioxide rises through the subsurface.

11.4.1 Perforations in the Fensfjord formation

As mentioned earlier in this thesis, the Fensfjord formation makes up a good alternative for CO_2 injection. The reservoir quality of the Fensfjord layers are good, but as stated in chapter 10, the permeability and porosity values are varying with depth. It may therefore be valuable to study different injection depths within this formation.

Three different perforation depths within the Fensfjord formation are studied in this report. To better study possible CO_2 movement differences in the formation, the carbon dioxide has been injected at the top, bottom and in the middle of Fensfjord. The horizontal injection well is placed in layer 50, 54 and 57, which represent depths equal to 1553, 1572 and 1588 m. **Fig. A.1** in the appendix shows the simulation model as a function of depth in layer 57.

When the CO_2 is injected into the Fensfjord formation, the carbon dioxide will migrate upwards in the reservoir and be trapped in the Fensfjord and the Sognefjord formations. It will not be stored in the underlying Krossfjord formation as

the CO_2 will not move downwards. Thus, some of the potential storage area will therefore not be used. Further, it should be mentioned that the injection rate is constant and equal to 5.4 Mt of CO_2 per year in all the following cases.

Fig. 11.23 shows the CO_2 distribution when it is being injected into different layers in the Fensfjord formation. The simulations are run to year 2300 to clearly see the long-term effect of different perforation depths.

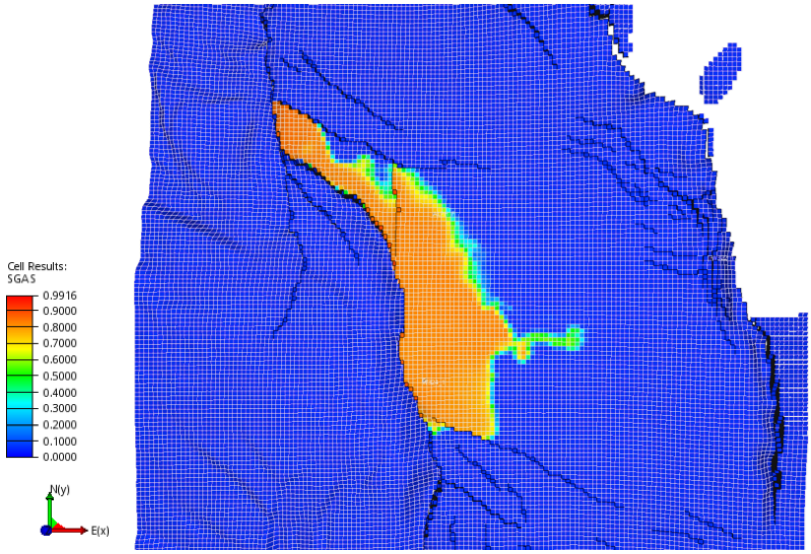

(a) Perforations in the upper part of the Fensfjord formation.

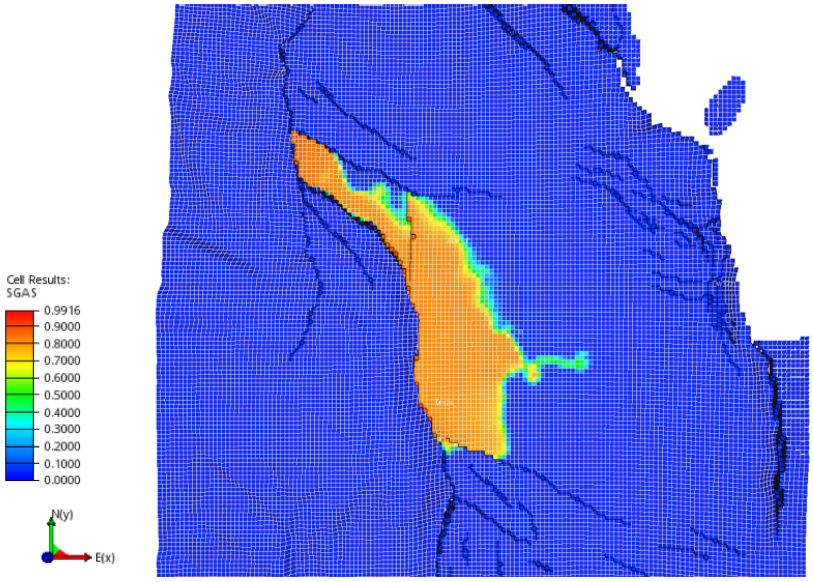

(b) Perforations in the middle part of the Fensfjord formation.

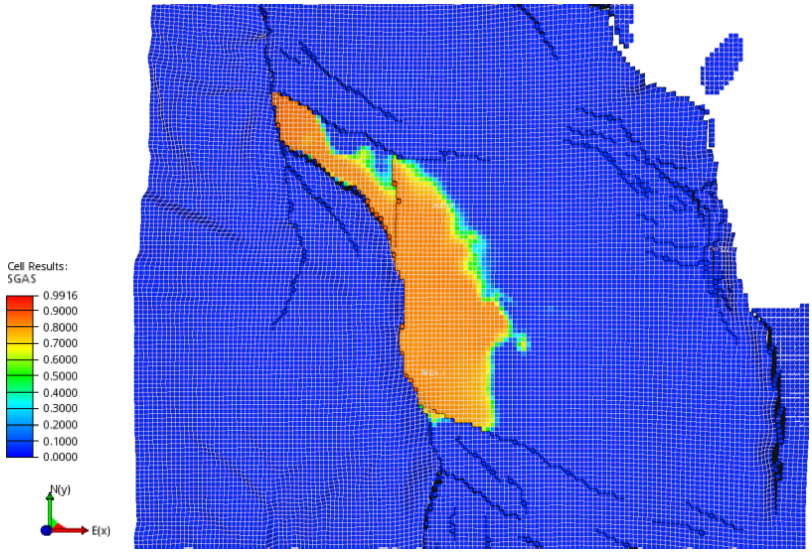

(c) Perforations in the lower part of the Fensfjord formation.

Fig. 11.23: Different perforation depths in the Fensfjord formation.

From the illustration above, it can be noticed that the perforation depth is impacting the CO_2 movement in the Alpha structure. When CO_2 is being injected into the upper and middle part of the Fensfjord formation, the CO_2 will start to migrate towards the Beta structure at the given rate and location. It should be noticed that the CO_2 movement in the Beta direction is approximately equal for the two shallowest layers.

When the CO_2 is being injected into the lower part of Fensfjord, the carbon dioxide will accumulate and stabilize in the Alpha structure. No migration in the Beta direction is seen when the CO_2 is injected in the northern part of Alpha with this rate. The results shown in the figure above are further discussed in the next chapter.

11.4.2 Perforations in the Krossfjord formation

Although the Krossfjord formation has poorer reservoir quality, its depth may cause it to be a good alternative for CO_2 injection. As previously stated, the migrating CO_2 can be trapped in the Krossfjord formation due to the lower permeability values. The amount of CO_2 that will continue moving through the Krossfjord formation will be stored in the overlying Fensfjord and Sognefjord formations. Thus, the following studies may lead to an increase in the storage efficiency in the Smeaheia area, making it important to investigate the Krossfjord layers.

Three perforation depths are studied within the Krossfjord formation; layer 60, 65 and 70, representing depths of 1604, 1631 and 1658 m. These layers are found at the top, bottom and in the middle of the formation, and will give an indication of possible storage differences within the Krossfjord area. The injection rate is still set to 5.4 Mt of CO_2 each year, which is the same as the rate used in the Fensfjord studies. The equal injection rate makes it possible to directly compare the results related to different injection points.

Fig. 11.24 shows how the CO_2 distributes when it is being injected into different layers in the Krossfjord formation. All the simulations are run until year 2300, making it easier to compare the results and see the long-term effect of different perforation depths.

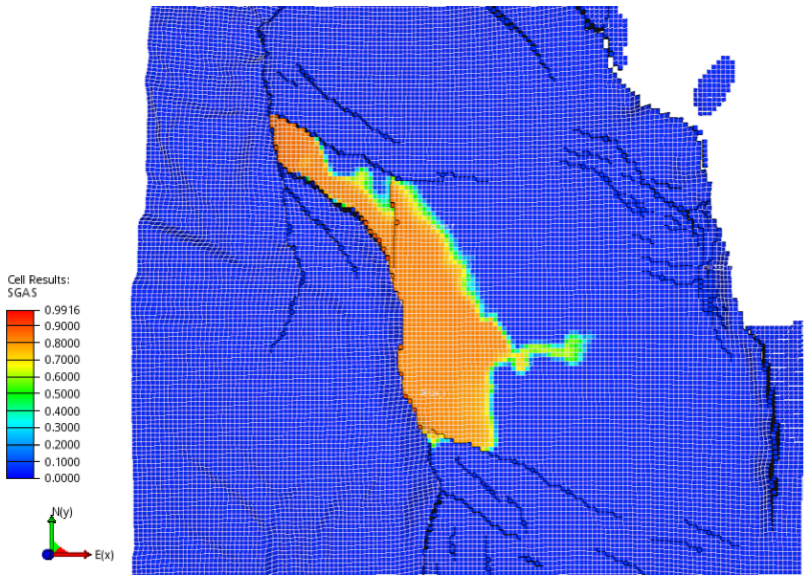

(a) Perforations in the upper part of the Krossfjord formation.

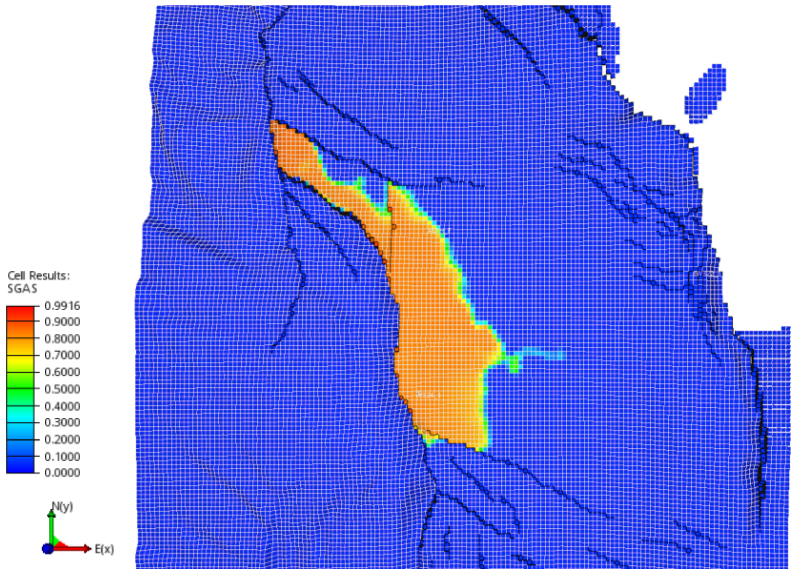

(b) Perforations in the middle part of the Krossfjord formation.

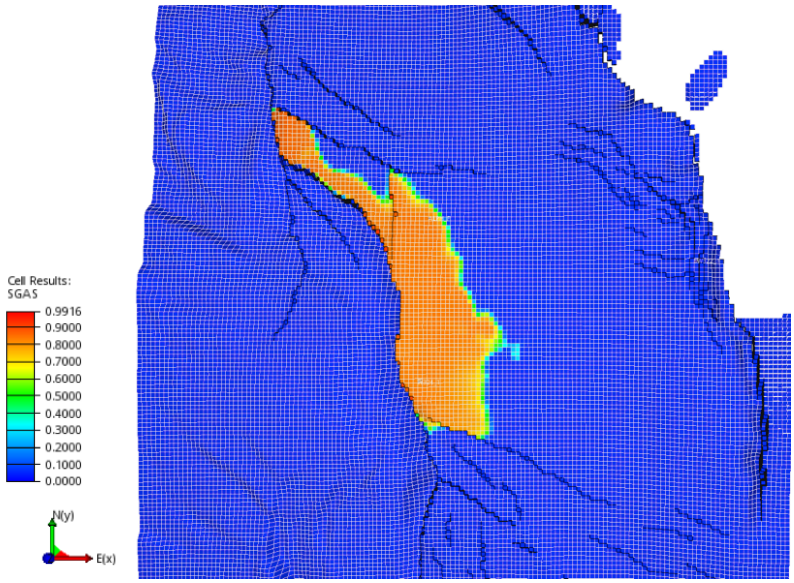

(c) Perforations in the lower part of the Krossfjord formation.

Fig. 11.24: Different perforation depths in the Krossfjord formation.

As can be noticed from the figure above, the injection depth impacts the CO_2 migration. Injection into layer 60 will cause a clear migration in the Beta direction, while injection into layer 65 only shows a slightly CO_2 movement towards Beta. When CO_2 is being injected into the lower part of the Krossfjord formation, the CO_2 will form a stable plume in the Alpha structure.

11.4.3 Perforation depth overview

An overview of the perforation depth results is given in this section. This thesis has mainly focused on CO_2 injection into the middle and lower part of the Smeaheia storage area, respectively in the Fensfjord and Krossfjord formations. Three studies have been completed for both formations, and the table below, Table 11.3, gives the results from this study.

The column representing the total storage volume is based on the constant injection rate equal to 5.4 Mt of CO_2 per yr. Thus, the total storage volume after 25 years will be 135 Mt. Perforation depths causing the CO_2 to migrate in the Beta direction is represented by <135 Mt in the following table. Further, the column presenting CO_2 saturation gives the saturation values in the injection well point in the Alpha structure at year 2300. These results will be further discussed in the next chapter.

Table 11.3: Perforation depth results.

Perforation point	Storage volume [Mt]	CO2 saturation at injection well [%]
Fensfjord form. - layer 50	<135	77
Fensfjord form. - layer 54	<135	77
Fensfjord form. - layer 57	135	78
Krossfjord form. - layer 60	<135	67
Krossfjord form. - layer 65	<135	78
Krossfjord form. - layer 70	135	80

11.5 The effect of outflow control device

All of the studies described above are completed without outflow control devices. The next sections will focus on the effect of OCDs in the horizontal part of the wellbore when the well is located in the northern part of the Alpha structure. It is known that an OCD will balance the pressure drop throughout a wellbore, which again will affect the CO_2 distribution in a reservoir. Thus, the effect of using OCDs is an important topic to study due to the impact on the total CO_2 storage.

As mentioned, well location 1 is used in all the cases below. Further, an injection rate of 5.4 Mt of CO_2 per year is held constant to better compare the possible variations in CO_2 distribution due to OCDs. However, it should be mentioned that different injection depths are being considered to study the effect of OCDs in layers with different reservoir characteristics. Layer 57 and 56, representing depths of 1588 and 1582 m, are studied due to the difference in permeability.

Further, section 11.5.1 explains how to determine OCD placement in a well. Section 11.5.2 illustrates the use of nozzle OCDs in layer 56 and 57, showing the effect of control devices in formation layers with respectively high and low permeability. The results found in this section are further discussed in chapter 12.

11.5.1 Placement of outflow control devices

The functionality of outflow control devices is described previously in this thesis. Thus, it is known that the purpose of installing such control devices is to balance the fluid flow throughout the well. However, to ensure the balancing effect due to OCDs, the placement has to be carefully thought through. The following paragraphs will describe how these locations can be determined.

One way to decide the placement of outflow control devices is to look at the distribution of injection rate along the wellbore before OCDs are installed. A varying rate throughout the well characterizes an unbalanced flow, which may cause an OCD installation to be necessary for balancing the rate distribution. Further, a balanced flow where the injection rate is approximately the same along the wellbore may not need control devices for optimization.

There are several factors that will influence the rate distribution throughout a well, and thus determine if the flow will be balanced or not. The formation permeability is such a factor, and this thesis will focus on this reservoir parameter.

OCD placement in layer 57

Fig. 11.25 shows the injection rate distribution without installed OCDs. Each of the five gridblocks constituting the horizontal well are represented, and the figure gives the outflow rate from the well heel to the well toe. The well is located in layer 57, in the lower part of the Fensfjord formation. As shown in Fig. 10.10, the permeability in this layer is relatively low. Further, **Fig. A.3** in the appendix combines the rates below, making it easier to observe the rate differences in the gridblocks.

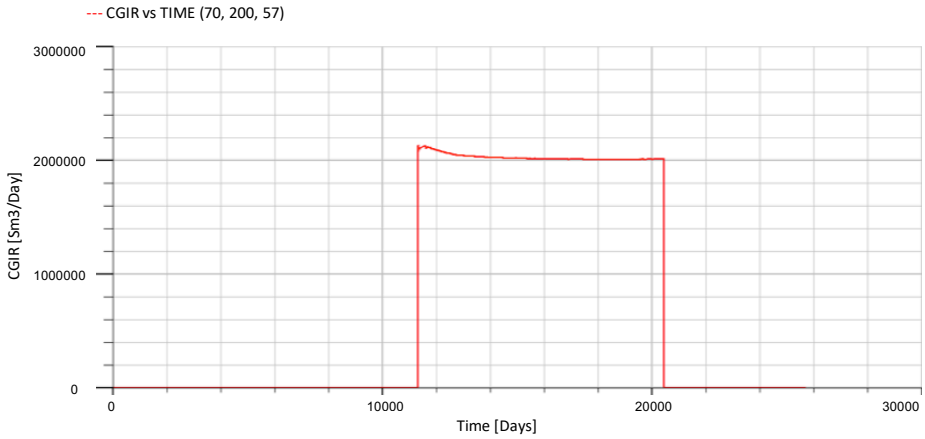

(a) Injection rate at well heel.

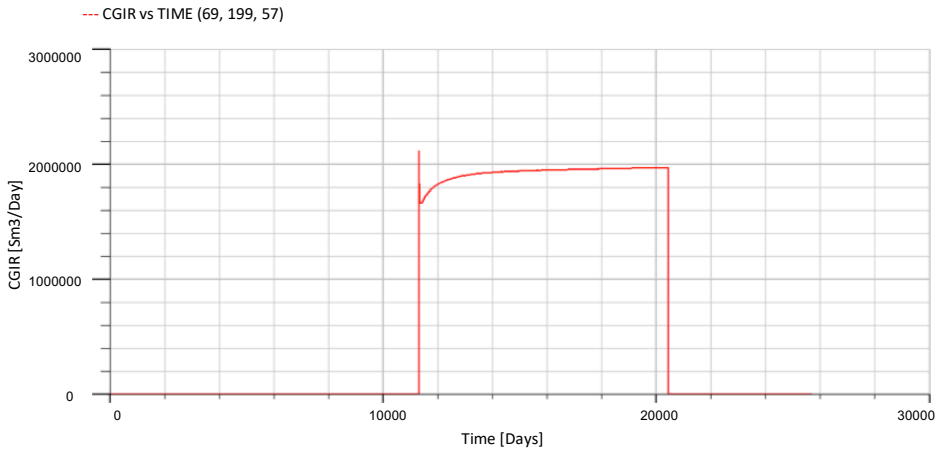

(b) Injection rate in the middle of the well.

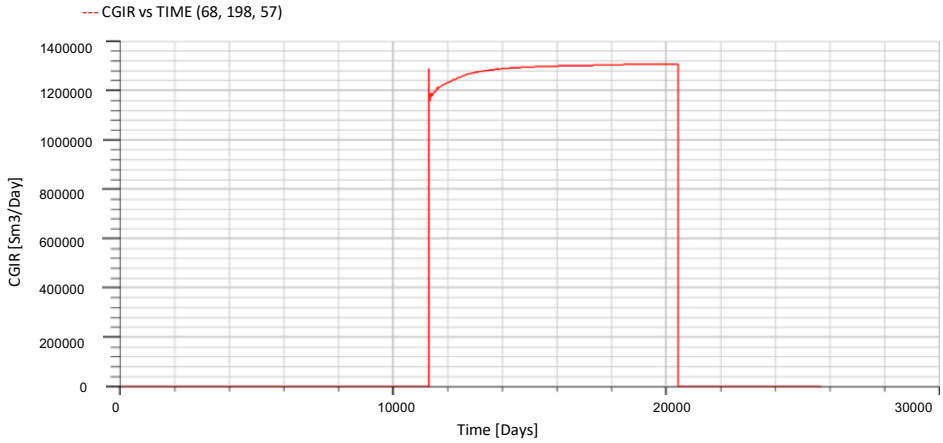

(c) Injection rate in the middle of the well.

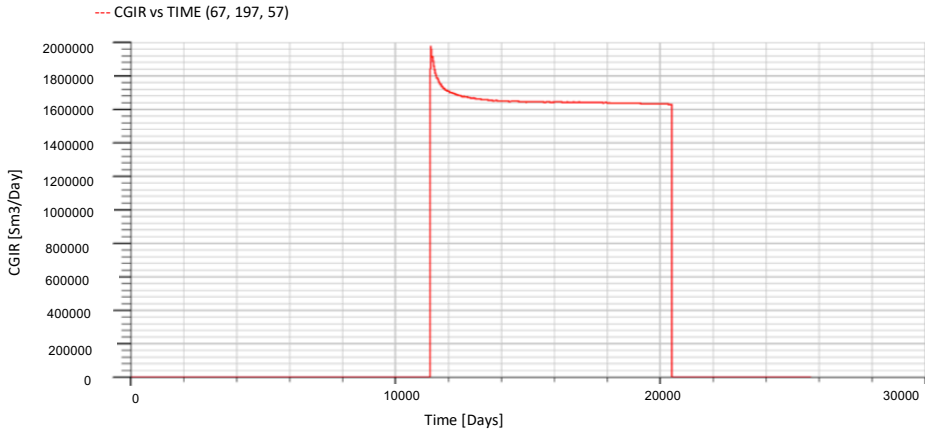

(d) Injection rate in the middle of the well.

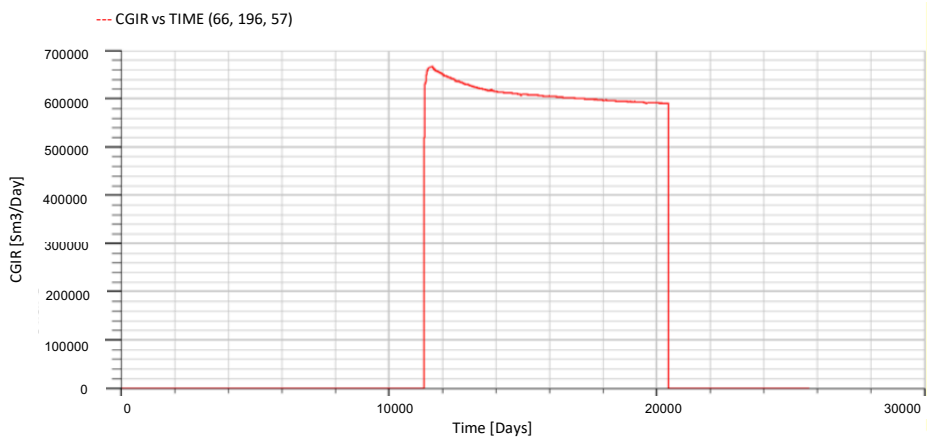

(e) Injection rate at well toe.

Fig. 11.25: CO_2 injection rate in layer 57 without OCDs.

As can be noticed from Fig. 11.25, the injection rate is slightly varying and decreasing throughout the wellbore. It can be observed that the rate in almost all of the gridblocks is in an interval between 1000000 and 2000000 sm^3/day. In other words, the rate distribution is relatively stable. It should be stated that such an injection rate profile through the well, where most of the fluid flows out at the well heel, is common. However, the flow may become even more stable if OCDs are being installed into the well.

To create a possible flow balance, the control devices should be installed in the gridblocks with the highest injection rate. In this case in gridblock 70, 69 and 67. This decision is due to the fact that the OCDs can distribute the CO_2 flow, such that the injection rate increases in the low-rate zones and decreases in the high-rate zones. The strength of an OCD, which decides the possible flow rate in each gridblock, is determined by the nozzles' cross-sectional area.

OCD placement in layer 56

Layer 56 is studied due to its higher permeability values. **Fig. A.2** in the appendix shows the permeability at a depth of 1582 m. It can be seen that although the Alpha structure consists of low-permeable regions within this layer, the total permeability at this depth is higher compared to layer 57.

Fig. 11.26 illustrates the CO_2 injection rate distribution without installation of outflow control devices in layer 56. As can be observed, the rate distribution throughout the wellbore is varying. The injection rate at the well heel is lower compared to the well toe, meaning that more CO_2 is flowing from the well and

into the reservoir at the end of the wellbore. **Fig. A.4** in the appendix combines the rates below and shows the same scenario.

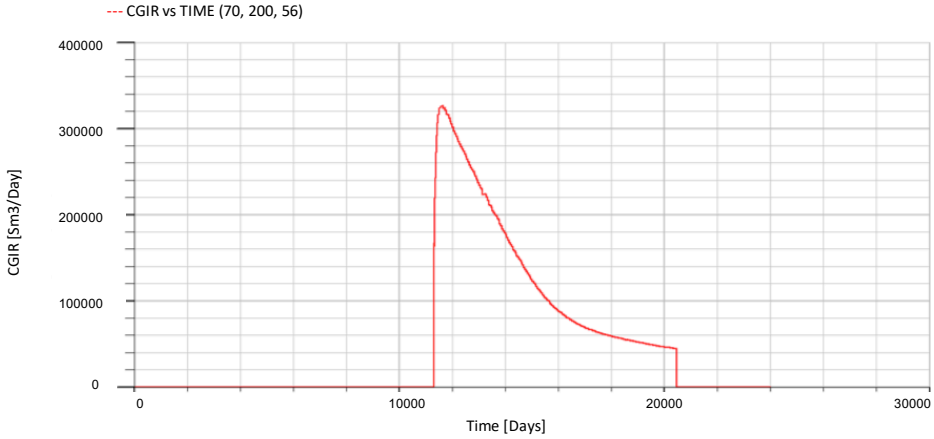

(a) Injection rate at well heel.

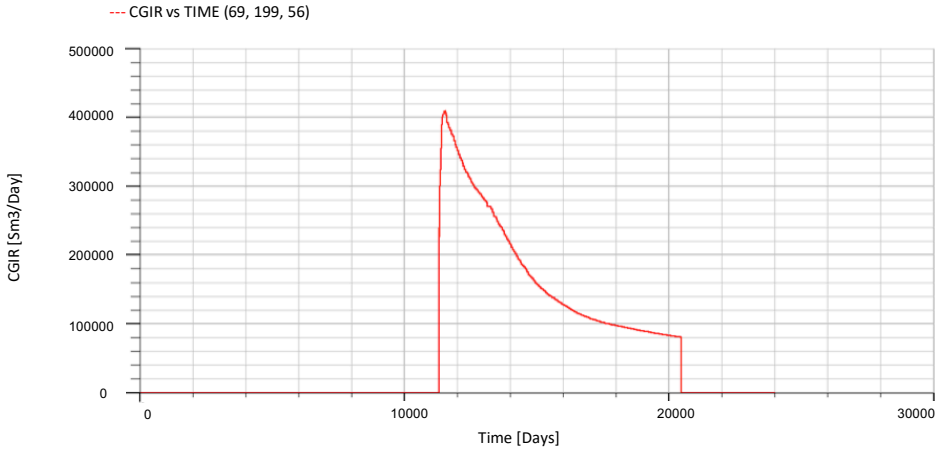

(b) Injection rate in the middle of the well.

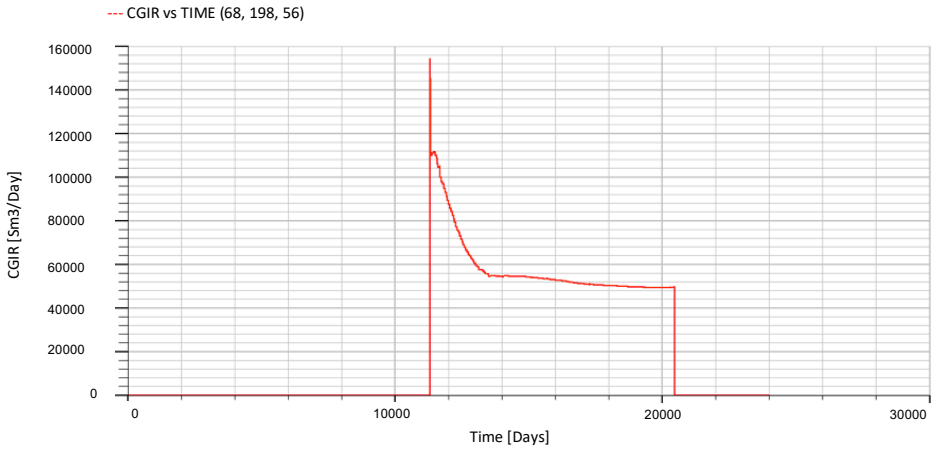

(c) Injection rate in the middle of the well.

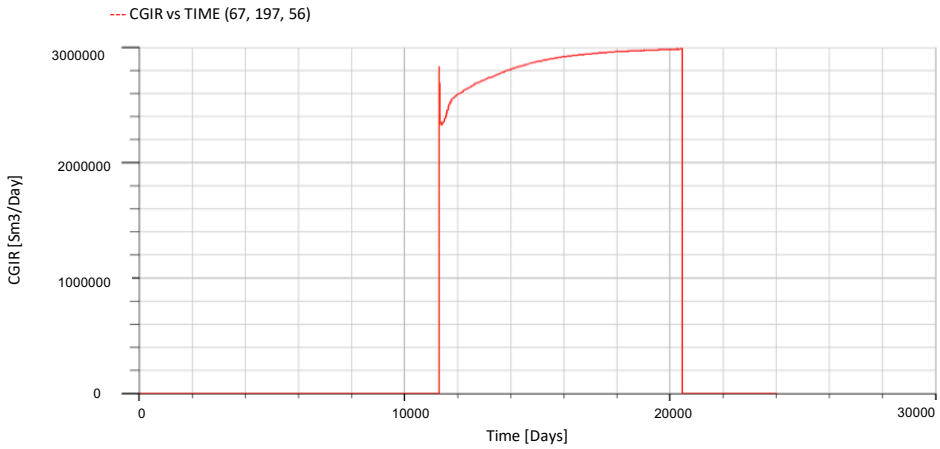

(d) Injection rate in the middle of the well.

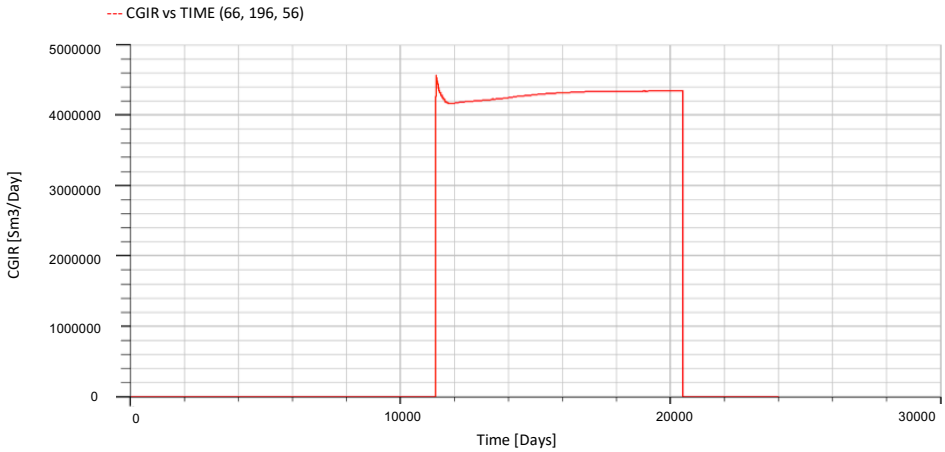

(e) Injection rate at well toe.

Fig. 11.26: CO_2 injection rate in layer 56 without OCDs.

Fig. 11.26 shows that the injection rate distribution in layer 56 is highly varying between the different gridblocks. It can be observed that the rate is varying between 200000 and 4200000 sm^3/day throughout the wellbore. The CO_2 flow in the cells closer to the well heel, gridblock 70, 69 and 68, are relatively low compared to the rate at the well toe. In other words, more CO_2 is flowing from the well and into the reservoir at the end of the well.

To balance the carbon dioxide outflow seen in Fig. 11.26, outflow control devices are installed in the wellbore. The principle of OCD placement is the same as stated for layer 57; OCDs have to be located where the rate is high to decrease the CO_2 flow in these areas and to increase the CO_2 in the low-flow regions. In other words, OCDs should placed in the well toe, more specifically in gridblock 66 and 67, when considering layer 56.

11.5.2 The effect of nozzle outflow control devices

The effect of using nozzle outflow control devices in the wellbore is discussed in this section. Nozzle OCDs are installed in the horizontal part of the injection well in layer 56 and 57, in the specified gridcells discussed in the previous section. The effect of OCD installation will be further discussed in chapter 12.

Nozzle OCDs in layer 57

As stated previously in this section, the outflow control devices have to be placed in the regions where the flow of CO_2 is highest. When considering layer 57, these areas are found in three of the gridblocks; number 70, 69 and 67. Although the

flow throughout the wellbore in this layer is said to be quite stable, it is valuable to study any possible effect of an OCD installation.

As discussed in section 10.4, the strength of a nozzle OCD is determined by the size of its cross-sectional area, A_C. A larger cross-sectional area, meaning a larger valve opening, will increase the amount of CO_2 flowing through the device. A smaller A_C will reduce the CO_2 flow in the specific OCD well segment. Multiple simulations with different cross-sectional areas have been completed in this thesis. However, it is found that the effect of different OCD strengths is minor, which is the reason why this thesis includes one study of nozzle OCDs with equal cross-sectional areas.

Fig. 11.27 illustrates the scenario where OCDs are placed in three of the five wellbore gridblocks. The red curve represents the CO_2 flow with the use of OCDs, while the green curve illustrates the carbon dioxide injection without any OCDs installed in the wellbore. A simulation where the cross-sectional areas are small have been completed in this thesis, and the figure shows the results of using nozzle OCDs with cross-sectional areas equal to 7.5E-5 m^2.

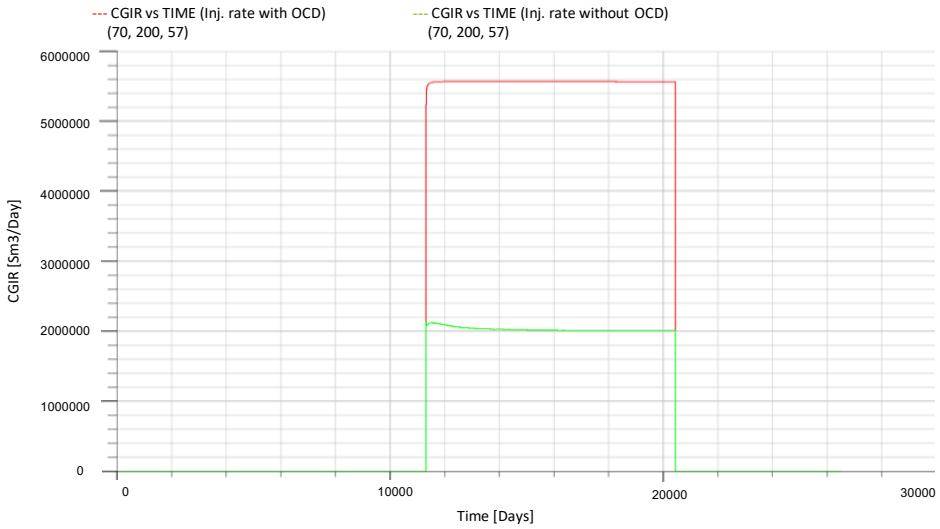

(a) Injection rate at well heel.

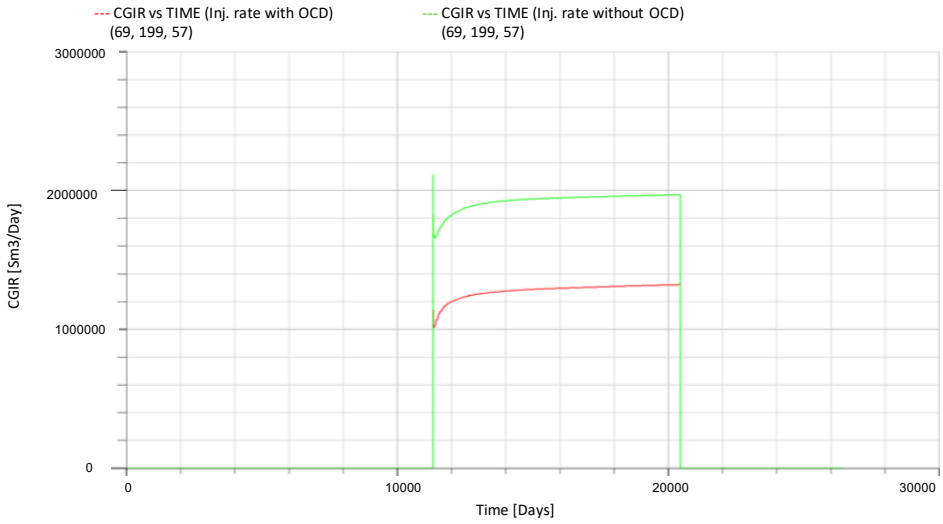

(b) Injection rate in the middle of the well.

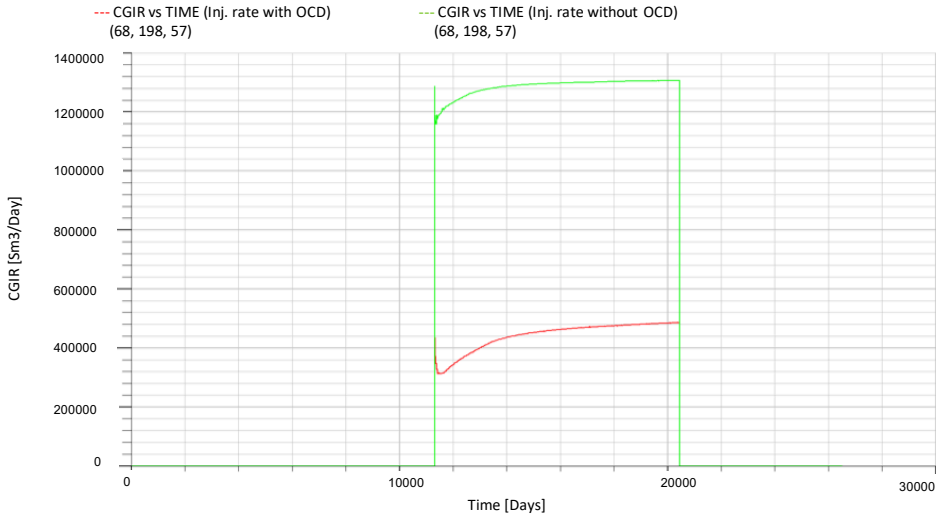

(c) Injection rate in the middle of the well.

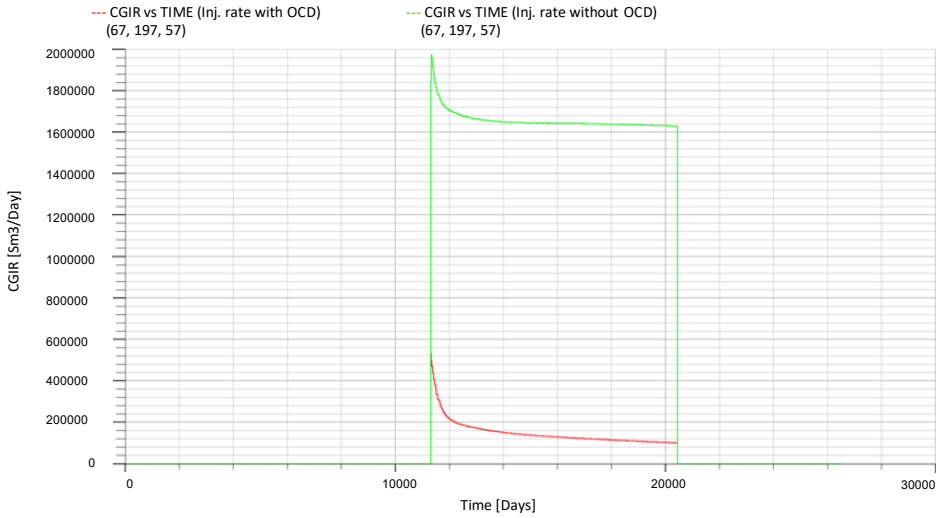

(d) Injection rate in the middle of the well.

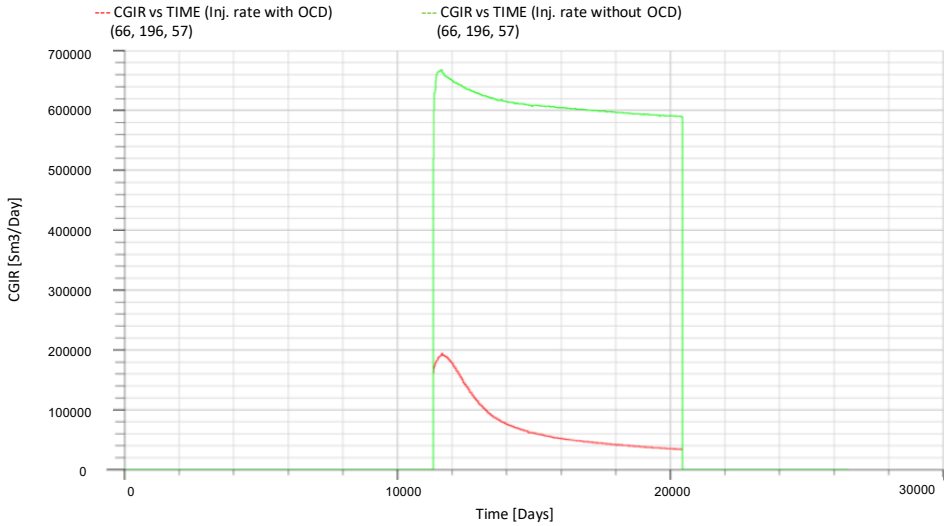

(e) Injection rate at well toe.

Fig. 11.27: CO_2 injection with and without OCDs in layer 57.

From Fig. 11.27 it can be seen that the injection rate throughout the well is highly varying when OCDs are installed in the wellbore. The figure clearly illustrates a difference in injection rate in each gridblock between the two scenarios, showing that the case where OCDs are being installed varies the most.

A simplified overview of the injection rates studied in Fig. 11.27 is illustrated in **Fig. 11.28**. The figure shows the injection rate in each gridblock side by side,

giving a clear indication of the injection rate profile along the wellbore with and without control devices.

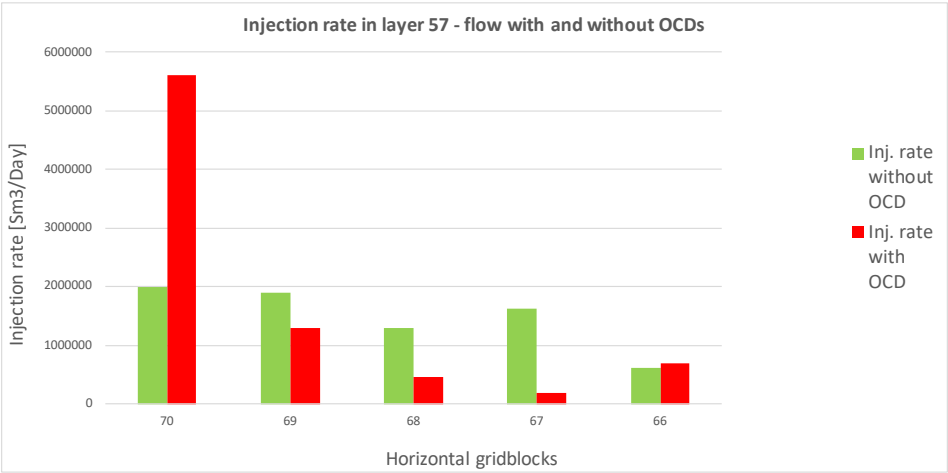

Fig. 11.28: Injection rate overview in layer 57.

As can be seen from Fig. 11.28, the injection rate profile is more stable without the use of OCDs in the wellbore. A stable flow throughout the wellbore indicates that the CO_2 is flowing into the formation with approximately the same rate from each gridcell. It can be observed from the figure above that the injection rate is varying between 600000 and 2000000 sm^3/day when no control devices are installed.

Fig. 11.28 shows that the flow rate throughout the wellbore is highly varying when OCDs are installed in the well. It can be observed that the rate varies between 180000 and 5600000 sm^3/day at this scenario. A large amount of the injected CO_2 flows out near the well heel, whereas the injection rate is decreasing as the flow reaches the well toe. From the figures above, it can be seen that the use of OCDs in layer 57 will not balance the outflow, but rather make the total injection distribution more unstable. These results will be further discussed in chapter 12.

Nozzle OCDs in layer 56

Layer 56 in the Fensfjord formation has a high permeability causing the injected CO_2 to flow easily in the reservoir. However, Fig. 11.26 shows that the CO_2 injection rate highly differs throughout the wellbore. The rate increases towards the well toe, meaning that the CO_2 injection is higher at the well toe compared to the well heel. This variation results in OCD installation at the end of the wellbore, more specific in gridblock 66 and 67.

Nozzle OCDs with a cross-sectional area equal to 7.5E-5 m^2 are used in this layer. The same types of OCDs are installed in layer 57, making it easier to compare the results. The following figure, **Fig. 11.29**, illustrates the effect of installing outflow control devices of this size in layer 56. The green curve represents injection without OCD installation, while the red curve gives the injection distribution with OCDs installed in the wellbore.

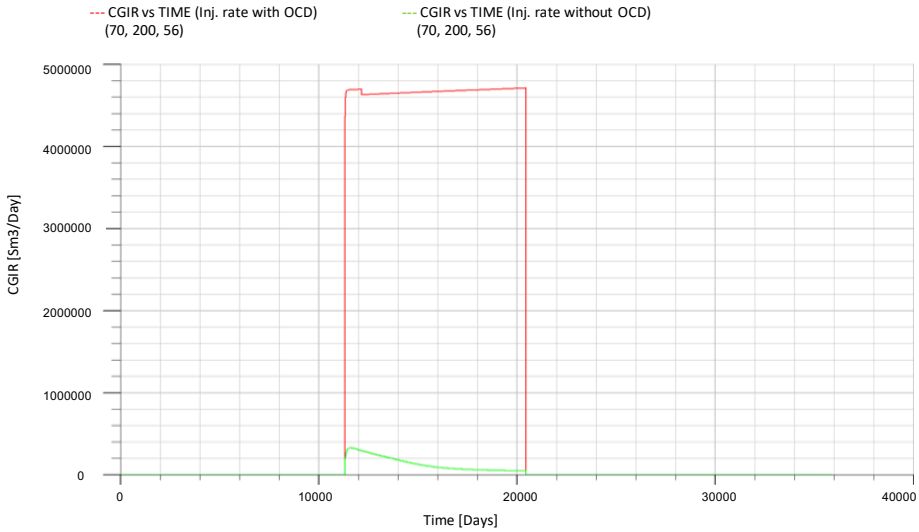

(a) Injection rate at well heel.

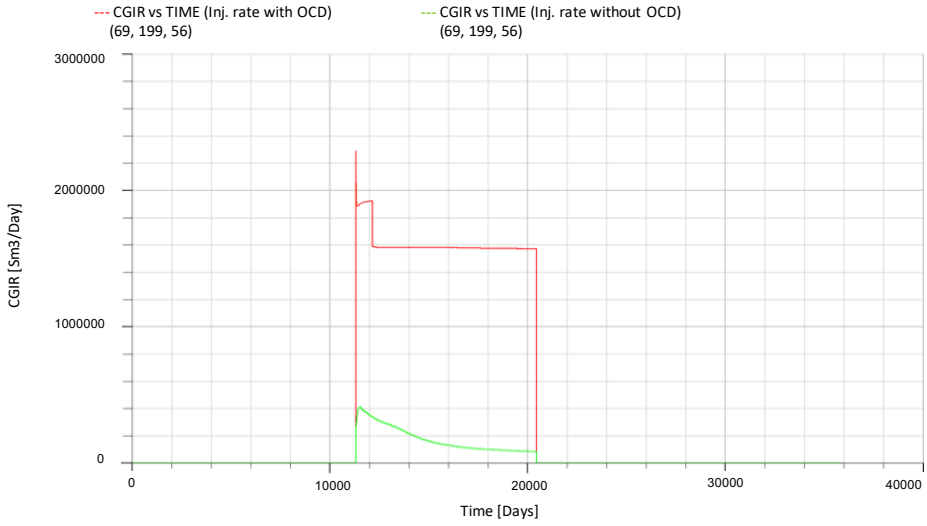

(b) Injection rate in the middle of the well.

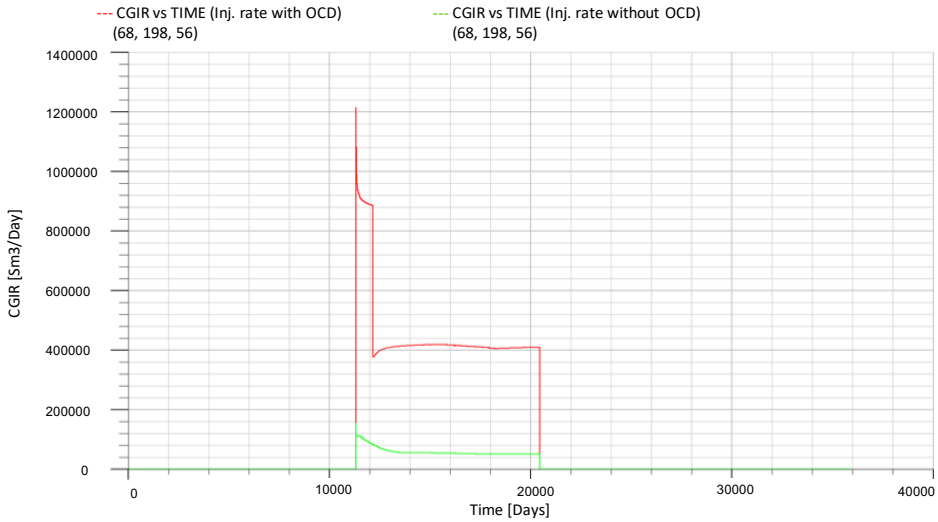

(c) Injection rate in the middle of the well.

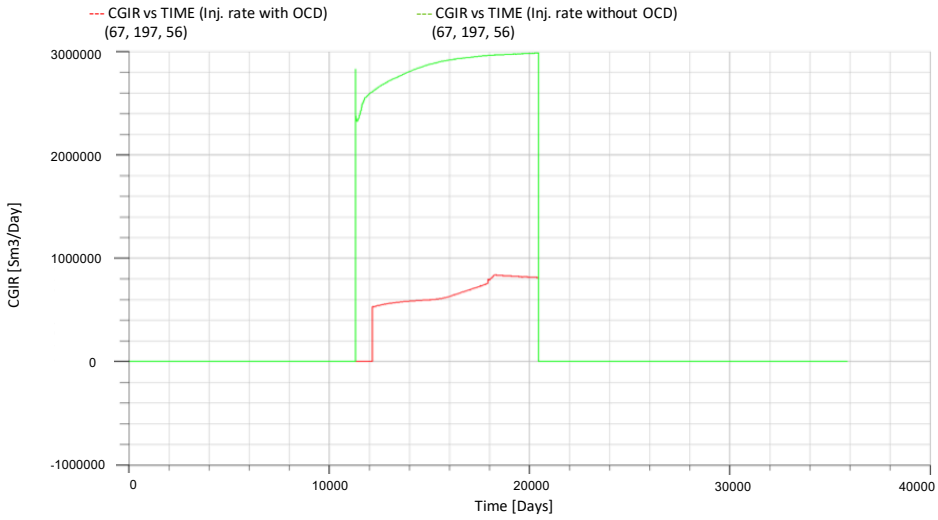

(d) Injection rate in the middle of the well.

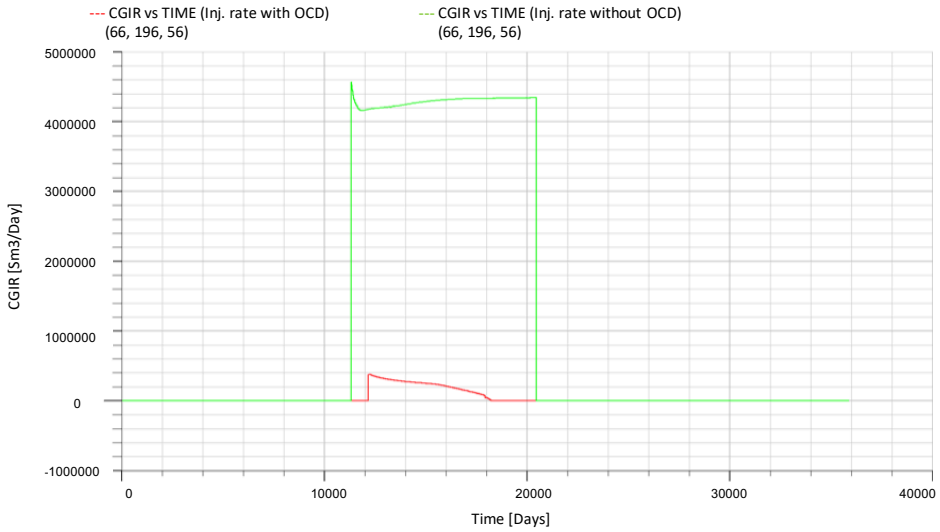

(e) Injection rate at well toe.

Fig. 11.29: CO_2 injection with and without OCDs in layer 56.

Fig. 11.29 clearly shows that the injection rate distribution differs between the two studied scenarios. It can be seen that the injection rate when OCDs are installed in the wellbore is higher for the three gridblocks close to the well heel, whereas the injection without OCDs has the highest rate near the well toe.

A simplification of the results above is given in **Fig. 11.30**. The figure shows the injection rate in each gridblock for the horizontal part of the well. The green curve illustrates the injection without OCDs installed in the wellbore, while the red curve represents injection with OCDs.

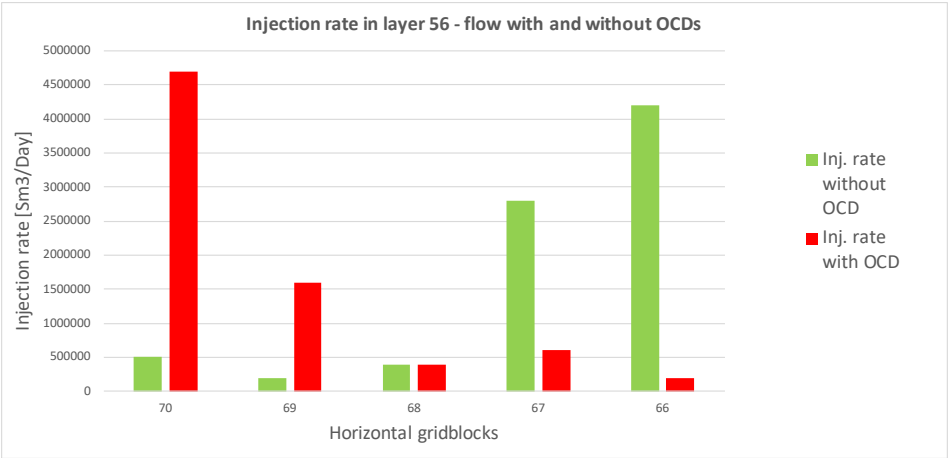

Fig. 11.30: Injection rate overview in layer 56.

As can be seen from Fig. 11.30, the use of OCDs in layer 56 will create an opposite CO_2 injection profile through the well compared to the injection without control devices installed. When CO_2 is being injected in a well without control devices, most of the carbon dioxide flows through the well toe. It can be observed that the injection rate varies between 200000 and 4200000 sm^3/day in this scenario.

When OCDs are installed in the well toe, most of the CO_2 flows through the wellbore heel. The figure above shows that the injection rate varies between 200000 and 4700000 sm^3/day in this case. These results will be further discussed in chapter 12.

11.6 Fluid-in-place region numbers

As mentioned earlier in this thesis, a simulation is run with the keyword FIPNUM to study the fluid flow between defined regions in the storage site. The FIPNUM keyword is tracking the CO_2 movement between specified regions in the model, giving a clear indication of how the CO_2 migrates in the Smeaheia field. As stated, four regions where defined in this thesis, where three of them were of special interest.

Table 11.4 illustrates the CO_2 movement between the different regions at year 2022, start of injection, 2047, end of injection and 2300, end of simulation. As can be seen from the table, flow between region 2 and 3, 2 and 4, and 3 and 4 are tracked in this simulation. From Fig. 10.12 it can be seen that region 2 represents the upper part of Alpha, region 3 the lower part of Alpha, while region 4 represents the Beta structure.

Table 11.4: CO_2 flow between regions.

Year	CO2 flow from region	CO2 flow to region	Moles CO2 [Kg-m/D]
2022	2	3	0
2022	2	4	0
2022	3	4	0
2047	2	3	- 122 274.3
2047	2	4	0
2047	3	4	0
2300	2	3	- 622.4
2300	2	4	272.6
2300	3	4	0

From the table above it can be observed that no CO_2 will flow between the defined regions at the start of injection. No carbon dioxide has been injected into the formation yet, and thus no CO_2 flow can exist. At the end of the injection period, a negative flow will occur from region 2 to region 3, meaning that the CO_2 will move from region 3 to 2.

At the end of the injection, a flow between region 2 and 3, and 2 and 4 will exist. The flow within the Alpha structure is reduced compared to the flow at the end of injection. Furthermore, flow between the upper part of Alpha and the Beta structure will occur at the end of simulation. These results are discussed in more detail in the following chapter.

Chapter 12

Discussion

12.1 CO2 distribution with time

As the results show, the CO_2 will accumulate and form a continuous plume after the end of injection. This plume will expand as the time goes by and the amount of carbon dioxide increases in the formation, causing it to move further into the reservoir. This CO_2 distribution is expected since the injected CO_2 will stick together and form one expanding plume over time.

Further, the results show that when the CO_2 is being injected into the Alpha structure, the plume will grow and stabilize in Alpha at the given injection rate and location. The plume will move along the western Vette fault and be safely stored within the Alpha area. The safe storage may be due to a rate and location causing the Alpha structure not to be filled to its spill point. However, later results show that this may not be the case for all well locations and injection rates.

12.2 Effect of injection rate

It is given in the simulation model that the CO_2 injection is controlled by the surface flow rate and the well limits are not exceeded if the bottom hole pressure is below 1000 bars. Results in this thesis show that the bottom hole pressure will increase to about 150 barsa for a wide range of injection rates during injection, before the pressure decreases. Since a pressure of 150 barsa is far below the model's pressure limit of 1000 bars, the simulations completed in this master thesis are controlled by the injection rate. Further, the bottom hole pressure will not exceed any well limits. The rise in BHP is expected as CO_2 is being injected into the subsurface, which will cause the pressure to increase.

Results show that the Smeaheia field pressure will decrease during the simulation. It is shown that the initial field pressure is about 155 barsa, while the

pressure at the end of simulation is reduced to approximately 80 barsa. Several injection rates show the same trend of a decreasing field pressure, which stabilizes at about 80 barsa for almost all the cases. This outcome is expected and is probably due to the high production rates from the Troll reservoir.

The Troll field is located to the west of the Smeaheia area and the production wells have higher rates compared to the available injection rates in Alpha. As mentioned, results show that the field pressure will decrease and stabilize around 80 barsa. Although the pressure reduction is large, 80 barsa will still cause the CO_2 to be stored in its supercritical phase as the supercritical pressure is 73.8 bars. In other words, the CO_2 will be stored safely and efficiently in its supercritical phase for all of the studied rates, except from the injection rate of 3.6 Mt of CO_2 per year, which will cause the CO_2 to be in a liquid state.

Further, an extreme scenario is simulated in this thesis, showing that an injection rate of 43.3 Mt of CO_2 per year will cause the field pressure to be at a much higher level at the end of simulation. The reservoir pressure will stabilize at approximately 134 barsa, which definitely will cause the CO_2 to be in a supercritical state as it is close to the initial reservoir pressure and far above 73.8 bars. However, the results show that such a high rate is not necessary for storing the carbon dioxide in a supercritical phase. Although the Troll production will have greater impact on the field pressure at lower injection rates, lower rates will ensure supercritical CO_2 storage. It is also shown that a rate of 43.3 Mt of CO_2 per year will cause movement and CO_2 accumulation in the Beta structure, which highly increases the risk of leakage to the surface.

Results show that the CO_2 distribution is highly affected by the injection rate. Higher rates will cause the CO_2 to move further into the Smeaheia formation, which may cause the carbon dioxide to migrate into the Beta structure. This is expected as a higher injection rate will increase the velocity and probably the amount of CO_2, and thus force the CO_2 to move into pores located further away from the well. As stated previously in this thesis, such movement is unwanted due to the high risk of leakage to the surface.

At last, the effect of different injection rates was described in this thesis. 4.3 Mt of CO_2 were injected for 25 years and 8.6 Mt of CO_2 injected for 12.5 years. The results show that the CO_2 plume is slightly larger when the injection period is shorter and the rate higher. Further, the CO_2 saturation in the reservoir is a bit higher in this scenario. This may be due to the fact that a higher rate at a shorter period forces the CO_2 to be pushed further into the reservoir compared to a longer period where the rate is relatively low. However, the results show a minimal impact in CO_2 plume size and saturation when the rate is multiplied by two and the period is halved.

12.3 Effect of injection well location

The study of injection well locations shows how the CO_2 will be stored at different locations and rates. Six studies are completed in this thesis, which compares locations within the Alpha structure and outside.

The results show that the optimal scenario in well location 1, the northern part of Alpha, will occur when the CO_2 is injected with a rate of 5.4 Mt per year. This rate is higher than the available injection interval given from the industrial land plants and will ensure safe storage within the Alpha structure. Further, injection at this rate will cause the CO_2 to be stored in its supercritical phase. The high injection rate is expected as the injection well is located far from the Beta structure, causing a large amount of CO_2 to be stored in Alpha before any possible leakage. However, the results show that if the injection rate exceeds this value, a CO_2 migration in the Beta direction will occur since the Alpha is filled up to and above its spill point.

Well location 2 in the middle of Alpha will result in CO_2 movement and accumulation in the Beta structure even at low rates. This outcome is expected as the well is located close to the Beta area. The results show that carbon dioxide will form a plume in the middle and lower part of Alpha before it migrates towards Beta, meaning that the Alpha structure is not filled to its spill point before the CO_2 moves out of the area. Due to the high risk of leakage to the surface when the carbon dioxide reaches the Beta structure, this well location will cause the storage operation to be unsafe and non-efficient. Since the CO_2 migration will occur even at rates below the available injection rate interval, this location will also be uneconomical and cause the CO_2 to be stored in the liquid phase.

The result show that location 3, when the well is located in the north-west part of Alpha, will cause a safe CO_2 storage at rates lower than 2.9 Mt of CO_2 per year. This rate is within the available injection rate interval set by the industrial plants and will not cause the CO_2 to migrate in the Beta direction. This scenario is expected as the well is located relatively far from Beta. It should be stated that for higher rates, this location will cause the carbon dioxide to move into the Beta structure. This is illustrated in the study where 5.4 Mt of CO_2 is injected per year, which is the optimal amount found in well location 1. This rate will result in an unsafe storage operation when the well is placed in the north-west part of Alpha, as this location is closer to the Beta structure compared to location 1.

Further, when considering well location 3 and the optimal injection rate of 2.9 Mt of CO_2 per year, it should be noticed that this rate will cause the CO_2 to be stored as a liquid. As described earlier in this thesis, injection rates below 3.6 Mt of CO_2 per year will cause the field pressure to be lower than 73.8 bars, which is the critical pressure for CO_2. In other words, this rate and location will ensure safe storage in terms of no migration towards the Beta structure, but the CO_2 will not be stored in its supercritical phase.

When the injection well is located in the southern part of Alpha, injection rates within the available rate interval will cause CO_2 migration into the Beta structure. No simulations have been completed with rates below this interval, as the storage operation at this location will be unsafe, uneconomical and non-efficient. The scenarios are expected as the well is located close to the Beta area, making it close to the leakage point.

The results show that when two injection wells are located in the southern part of the model, the injection rate may be significantly higher compared to the previous locations. Rates of 40, 60, 80 and 100 Mt of CO_2 per year have been studied. The long distance between the well locations and the Beta structure makes this an expected outcome. Although this study illustrates the possibility of storing large amounts of carbon dioxide in a supercritical phase, it should be mentioned that such high rates are not realistic for injection wells. In other words, multiple wells should be used for injection to generate rates at this level.

Further, the results show that there will be some CO_2 migration towards the producing Troll field. Especially the western injection well will cause some CO_2 movement in the Troll direction. This result is expected and the scenario is not critical as the production wells are placed randomly in the simulation model and only used to simulate a realistic case with pressure depletion in the reservoir. The production well locations can change, which will affect the pressure reduction in the model, causing a possible prevention of CO_2 migration in this direction. In other words, there may be a risk of CO_2 migration in Troll direction when the injection wells are located in the southern part of the model, especially considering the western well. However, this may be prevented by changing the location of the production wells.

The last well location shows a location in the northern part of the model. One injection well is placed further north compared to the Alpha structure, causing a longer distance to Beta and therefore higher injection rates. The results show that a rate of approximately 21.6 Mt of CO_2 per year will ensure a safe storage where the CO_2 is in its supercritical phase, which is expected due to the distance to Beta. Higher rates will cause the CO_2 to migrate further north, causing a reduction of the capacity, whereas lower rates will not be effective since this CO_2 volume will not maximize the storage capacity.

12.4 Perforation depth

Results from the perforation depth study show that several layers within the Fensfjord and Krossfjord formations may be efficient as injection depths. The optimal perforation depth within the Fensfjord formation is layer 57. A storage volume of 135 Mt may be stored when the CO_2 is injected into this layer, and the CO_2 saturation at the injection well will be 78 %. Shallower layers within this formation will result in a lower total storage volume and lower CO_2 saturation. The outcome of this study is expected. An injection into the deepest layer

in Fensfjord will make it possible for more CO_2 to be stored, increasing both the storage volume and the saturation.

The result show that the optimal injection layer in the low-permeable Krossfjord formation is layer 70. A storage volume of at least 135 Mt of CO_2 can be stored when it is injected at this depth, and the results show that the saturation near the injection well will be 80 % at the end of simulation. This is an expected outcome as the layer is located deeper compared to the other layers studied in this thesis, and the low permeability may force some of the CO_2 to be trapped in this formation as the carbon dioxide migrates upwards.

Further, layer 65, located at a depth of 1631 m, will results in a saturation of 78 % in the Alpha structure. Although the storage volume will be a bit lower than 135 Mt, this layer may work as an efficient injection depth as well. Layer 60 will result in a lower CO_2 storage amount in addition to a lower saturation, and will thus not be optimal as an injection depth. A possible reason why the shallower part of the Krossfjord formation would store less CO_2 may be lower permeability and less storage space compared to the lowest Krossfjord layer.

12.5 Outflow control device

As the results show, the use of outflow control devices will have various impacts on the CO_2 injection flow into the reservoir. When considering layer 57, representing a formation layer with relative low permeability, the results show that the injection flow rate throughout the wellbore is relatively stable when no control devices are installed. This may be due to the natural resistance in the formation, causing a low and stable CO_2 flow throughout the wellbore.

When OCDs are installed in layer 57 the CO_2 flow will vary from 180000 sm3/day to 5600000 sm3/day throughout the wellbore. The highest injection rate is found in the well heel, while the CO_2 flow out in the formation is low from the well toe. This result is expected and may be due to the low formation permeability. When OCDs are installed in layers where there already exists flow resistance, the OCD effect will be low and the flow balance will not be improved. Thus, the OCD will cause a higher flow variation within the wellbore in this layer.

Results from the high-permeable layer, layer 56, show that the flow rate through the wellbore is highly varying when there are no OCDs installed. The injection rate will be low near the well heel, while most of the CO_2 will flow out in the formation from the well toe. This result is not expected as a high permeability should have caused the CO_2 injection rate to be high at the well heel. One possible reason causing this scenario may be that although the permeability in layer 56 is high, some areas may have lower permeability values, causing the CO_2 to flow in the high-permeable areas. Further, it should be stated that due to the high variation in wellbore flow, it should be effective to install OCDs to balance the outflow.

The results show that when OCDs are installed in the well toe, an opposite rate situation will occur. Most of the CO_2 will flow out in the reservoir through the well heel, while the rate will be lower at the well toe. This scenario is not expected but could be due to OCDs with too low cross-sectional areas. When Ac is low, representing a strong outflow control device, the CO_2 will be forced to flow through the other gridblocks. It is therefore possible that OCDs with larger cross-sectional areas would balance the outflow in this high-permeable layer.

12.6 FIPNUM

Results show that the CO_2 flow between defined regions in the Smeaheia field will vary with time. Before injection there will be no CO_2 flowing between the Alpha and Beta structure. This is expected as there is no CO_2 in the formation yet. At the end of injection, in year 2047, there will be some flow from the lower part of Alpha to the upper part. A flow of approximately 122274 Kg-M/D will occur, which is expected since the carbon dioxide is being injected in the lower part of the Alpha structure and will rise and migrate upwards. At the end of simulation, in year 2300, there will be CO_2 movement between lower and upper part of Alpha, as well as migration between the upper part of Alpha and Beta. This is also expected as a higher amount of CO_2 will cause the Alpha structure to be filled to its spill point. If the CO_2 injection is continuing after this point, the CO_2 will leak and migrate to other locations outside the Alpha structure.

Chapter 13

Conclusion and further work

13.1 Conclusion

Parts of the following list are modified from my semester project, CO_2 storage - Review of theory and literature (Brobakken, 2017).

- To prevent further changes on the Earth's systems the level of carbon dioxide in the atmosphere has to be reduced. Carbon capture and storage is a method combining further use of fossil fuel energy and reduction of the CO_2 level. It is thus a good option for lowering the atmospheric level of carbon dioxide.
- CCS makes up the most economical option to reduce large amounts of CO_2 emissions. It can reduce today's emissions with 20% and is necessary for reaching the world's 2 °C goal.
- CO_2 may be captured and separated from a gas stream by three operations; post-combustion, pre-combustion or oxygen-fired combustion process. The post-combustion process is currently the dominated method, using monoethanolamine as the solvent.
- A concentrated CO_2 stream can be transported by ships, pipelines, trucks or railways. Pipelines and ships make up the best transport options for CO_2. Pipelines are commonly used for relative high temperatures and pressures, while ships are used for low pressure and temperature conditions. Transport by road or railway are only used on small scale and when flexibility is very important.
- CO_2 transport by pipelines may face several challenges. The possibility of dry-out zones, corrosion, impurities, accidents, reduced injectivity, dispersion of CO_2 into the atmosphere and blow-outs should be carefully concerned when planning such a transportation.

- The geological storage options include depleted oil and gas reservoirs, deep saline aquifer formations, coalbed formations and storage in association with enhanced oil recovery. Depleted reservoirs are the most appealing storage sites, while saline aquifers have the largest potential making them most profitable. Storage in combination with EOR is cost-effective and are commonly used in the USA, whereas coalbed formations, containing several possible leakage pathways, must be carefully considered.
- Several factors are important when considering secure and long-term CO_2 storage: The storage formation has to consist of a porous basin and an impermeable caprock. Several trapping mechanisms, including physical and geochemical trapping, will work over time and fix long-term storage. Most importantly are the structural and stratigraphic trapping, residual CO_2 trapping, solubility and mineral trapping. Maintenance and monitoring of the storage complex and the wellbore are important during the whole CCS project.
- Several factors such be considered when optimizing the CO_2 injection into the Smeaheia storage field; inclination of the injection well, perforation depths and the use of outflow control devices. It is proven that a horizontal injection well will result in optimal CO_2 injection.
- As time goes by the injected CO_2 will accumulate and form a continuous plume that will move through the formation.
- The Smeaheia field pressure will decrease over time due to the high production rates at the western Troll field. Although this will affect the reservoir pressure in the storage area, the field pressure will be sufficiently high, ensuring that the CO_2 is in its supercritical phase.
- As long as the injected CO_2 volume is constant, different injection rates and injection periods will not have any significant effects on the CO_2 distribution.
- The most efficient well location inside the Alpha structure in the Smeaheia field is in the northern part. This location results in a total CO_2 storage volume of 135 Mt, which exceeds the actual estimated storage capacity. Such a storage volume is achieved when 5.4 Mt of CO_2 is being injected for 25 years.
- The most efficient well location outside the Alpha structure is in the southern part of the model. Two injection wells, where both have an injection rate of 100 Mt of CO_2 per year, will result in a total storage volume of 5000 Mt after 25 years. However, it should be stated that the studied scenarios in this thesis will cause some of the CO_2 to migrate towards the producing Troll reservoir, but this is not critical as the production well locations are randomly selected and can be placed further north in the model.
- The CO_2 should be injected either into the lower part of the Fensfjord formation or in the lower part of the Krossfjord formation to maximize the

storage volume. Layer 57, representing a depth of 1588 m in Fensfjord, will result in a storage volume of 135 Mt and a CO_2 saturation equal to 78 %. Layer 70, representing a depth of 1658 m in Krossfjord, will store minimum 135 Mt of CO_2 and has a saturation of 80 %.

- Outflow control devices will not be effective in low-permeable layers such as layer 57. The CO_2 outflow through the wellbore will be most stable without OCDs installed.
- OCDs with small cross-sectional areas will not improve the CO_2 outflow through the wellbore in the high-permeable layer 56. However, OCDs with large Ac may balance the flow and increase the volume of stored CO_2.
- The injected CO_2 will mainly migrate within the Alpha structure short time after the end of injection. As the time goes by, the CO_2 will move within the Alpha area and towards the Beta structure.

13.2 Suggestion for further work

- Study the effect of using nozzle outflow control devices with larger cross-sectional areas and compare with the results in this thesis.
- Do more research on the use of outflow control devices and study the effect of spiral OCDs. Compare with the use of nozzle OCDs.
- Run simulations with the production wells in the Troll field located further north in the model. Compare results with this thesis regarding CO_2 migration and pressure depletion.
- Study the effect of several injection wells in the northern part of the model and multiple wells, more than two, in the southern part of the model.
- Study the impact on CO_2 storage volume with perforations made in the Sognefjord formation.

Nomenclature

$\mathbf{A}_c$	Cross-sectional area
$\mathbf{C}_u$	Conversion constant
$\mathbf{C'}_u$	Modified conversion constant
$\mathbf{C}_v$	Dimensionless flow coefficient of valve
$\mathbf{D}$	Diameter of pipe
$\mathbf{Dq}_g$	Rate dependent skin
δP	Pressure drop
δP_{cons}	Constriction effect
δP_{fric}	Frictional pressure
$\mathbf{f}$	Fanning friction factor
$\mathbf{h}$	Net thickness
$\mathbf{k}$	Permeability
$\mathbf{L}$	Length of pipe
$\mathbf{Mass}_{sc}$	Structural closure capacity
$\mathbf{MW}$	Molecular weight
μ_g	CO_2 viscosity
$\mathbf{Net}_{res}$	Reservoir net-to-gross range
$\mathbf{p}$	Pressure
$\mathbf{p}_R$	Reservoir pressure
p_{wf}	Bottomhole flowing pressure
$\mathbf{Phi}_{res}$	Reservoir porosity range
$\mathbf{q}_g$	CO_2 flow rate

$\mathbf{q}_m$	Volumetric flow rate
$\mathbf{r}_e$	External boundary radius
$\mathbf{r}_w$	Wellbore radius
$\mathbf{Rho}_{gas}$	CO_2 density
ρ	Fluid density
$\mathbf{s}$	Steady-state skin factor
Sat_{gas}	Saturation range
$\mathbf{T}$	Temperature
v_p	Flow velocity
$\mathbf{Z}$	Compressibility

Abbreviations

Ar	Argon
atm	Atmosphere
barsa	Bars absolute
bbl	Barrel
BGSAT	CO_2 saturation in specific gridcell
BHP	Bottom hole pressure
BRV$_{trap}$	Bulk rock volume
C	Celsius
C1	Methane
C^{13}	Carbon-13 isotope
C^{14}	Carbon-14 isotope
Ca	Calcium
CaCO$_3$	Calcium carbonate
Ca(OH)$_2$	Calcium hydroxide
CCS	Carbon capture and storage
CGIR	Component gas injection rate
CO$_2$	Carbon dioxide
CO$_2$**-ECBM**	Carbon dioxide for enhanced coalbed methane recovery
CO$_2$**-EOR**	Carbon dioxide for enhanced oil recovery
CO$_3^{2-}$	Carbonate
Cp	Centipoise
D	Darcy

D	Depth
Dm	Darcy meter
ECBM	Enhanced coalbed methane recovery
EOR	Enhanced oil recovery
F	Fahrenheit
Fe	Iron
FIPNUM	Fluid-in-place region numbers
Form.	Formation
FPR	Field pressure
FSI	Floating storage and injection ship
FVF	Formation volume factor
g/mol	gram/mole
H_2, H^+	Hydrogen
H_2O	Water
HCO_3^-	Hydrogen carbonate
ICD	Inflow control device
IRGA	Infrared gas analyzer
K	Kelvin
kg	Kilo gram
Kg-M/D	Kilogram mole per day
kh	Permeability thickness
km	Kilo meter
LDL	Leak detection log
LIDAR	Light detection and range finding
LNG	Liquid natural gas
LPG	Liquefied petroleum gas
m	Meter
m^2	Square meters
m^3	Cubic meters

mD	MilliDarcy
Mg	Magnesium
mol%	Mole percentage
MPa	Megapascal
Mscf	Million standard cubic feet
Msm^3	Million standard cubic meters
Mt	Million tonnes
N_2	Nitrogen
nD	NanoDarcy
N/G	Net-gross ratio
NOx	Nitrogen oxides
O_2	Oxygen
OCD	Outflow control device
P_c	Critical pressure
ppm	Parts per million
Psia	Pounds per square inch absolute
RB	Reservoir barrels
scf	Standard cubic feet
sm^3	Standard cubic meters
STB	Stock tank barsrel
STL	Submerged turret loading
t	Tonnes
T_{boil}	Boiling temperature
T_c	Critical temperature
T_g	Glass-to-rubber transition temperature
TD	Total depth
t/hr/bars	Tonnes per hour per bars
US$	US dollar
VF	Vette fault

WBHP	Well bottom hole pressure
yr	Year
yrs	Years
ØGF	Øygarden fault

References

Amjad, M. (2014). Imaging reservoir geology of the troll west field in the north sea by 3d seismic interpretation. .

Aspelund, A., Mølnvik, M. J., and d. Koeijer, G. (2006). Ship transport of co_2. technical solutions and analysis of costs, energy utilization, exergy efficiency and co_2 emissions. *Chemical Engineering Research and Design*, 84(9):847–855. https://doi.org/10.1205/cherd.5147.

Bachu, S. (2015). Review of co_2 storage efficiency in deep saline aquifers. *International Journal of Greenhouse Gas Control*, 40:188–202. https://doi.org/10.1016/j.ijggc.2015.01.007.

Birchenko, V., Muradov, K., and Davies, D. (2010). Reduction of the horizontal well's heel–toe effect with inflow control devices. *Journal of Petroleum Science and Engineering*, 75:244–250. https://doi.org/10.1016/j.petrol.2010.11.013.

Birkholzer, J. T., Oldenburg, C. M., and Zhou, Q. (2015). Co_2 migration and pressure evolution in deep saline aquifers. *International Journal of Greenhouse Gas Control*, 40:203–220. https://doi.org/10.1016/j.ijggc.2015.03.022.

Brobakken, I. (2017). Project report - co2 storage – review of theory and literature. *TPG4560 Petroleum Engineering, Specialization Project*. .

CO2-Earth (2018). Earth's co2 home page. https://www.co2.earth, (Accessed: 2 June 2018).

Cooper, C. (2009). *A technical basis for carbon dioxide storage*. UK: CPL Press.

Coronado, M. P., Garcia, L. A., and et al., R. D. R. (2009). New inflow control device reduces fluid viscosity sensitivity and maintains erosion resistance. https://doi.org/10.4043/19811-MS.

d. Koeijer, G., Drescher, M., and Ringrose, P. (2017). Co_2 storage: operation and integrity of engineered co_2 storage. 4. thermodynamics and transport. Presentation given at NTNU in the course TPG4255, Fall 2017. Equinor/NTNU.

Directorate, N. P. (2018). 4.1 - geology of the north sear (last modified: 13 november 2014). http://www.npd.no/en/Publications/Reports/Compiled-CO2-atlas/4-The-Norwegian-North-Sea/41-Geology-of-the-North-Sea/, (Accessed: 6 April 2018).

Ellis, T., Erkal, A., and et al., G. G. (2009). Inflow control devices - raising profiles. *Oilfield Review*, 21(4):30–37. https://www.slb.com/~/media/Files/resources/oilfield_review/ors09/win09/03_inflow_control_devices.pdf.

Equinor (2016). Selected extracts from equinor internal report on subsurface evaluation of smeaheia as part of 2016 feasibility study on co_2 storage in the norwegian continental shelf. *OED*.

Evensen, J., Skaug, M., and Goodyear, P. (1993). Production geological challenges of characterizing the thin oil rims in the troll field. *Offshore Technology Conference*. https://www.onepetro.org/download/conference-paper/OTC-7172-MS?id=conference-paper%2FOTC-7172-MS.

Fernandes, P., Li, A., and Zhu, D. (2009). Understanding the roles of inflow-control devices in optimizing horizontal-well performance. *Society of Petroleum Engineers*. https://doi.org/10.2118/124677-MS.

Feron, P. H. M. and Hendriks, C. A. (2005). Co_2 capture process principles and costs. *Oil gas science and technology*, 60(3):451–459. https://doi.org/10.2516/ogst:2005027.

Furre, A. K., Bussat, S., and et al., P. S. R. (2017). Optimizing monitoring strategies for contrasting offshore co_2 storage sites. *EAGE/SEG Research Workshop 2017*. 10.3997/2214-4609.201701950.

Gaurina-Međimurec, N. and Pašić, B. (2011). Design and mechanical integrity of co_2 injection wells. *Rudarsko-geološko-naftni zbornik*, 23(1):1–8.

Gibbins, J. and Chalmers, H. (2008). Carbon capture and storage. *Energy policy*, 36(12):4317–4322. https://doi.org/10.1016/j.enpol.2008.09.058.

Halland, E. K., Johansen, W. T., and Riis, F. (2011). *CO_2 storage atlas North Sea*. Stavanger: Norwegian Petroleum Directorate.

Heidug, W., Lipponen, J., and et al., S. M. (2015). Storing co_2 through enhanced oil recovery - combining eor with co_2 storage (eor+) for profit. *OECD/IEA*. https://www.iea.org/publications/insights/insightpublications/Storing_CO2_through_Enhanced_Oil_Recovery.pdf.

Herzog, H. (2009). Carbon dioxide capture and storage. *na*, 12(8).

Li, Z., Dong, M., and et al., S. L. (2005). Co_2 sequestration in depleted oil and gas reservoirs - caprock characterization and storage capacity. *Energy Conversion and Management*, 47(11):1372–1382. https://doi.org/10.1016/j.enconman.2005.08.023.

Loizzo, M., Lecampion, B., and et al., T. B. (2010). Reusing og-depleted reservoirs for co_2 storage: pros and cons. *SPE Projects, Facilities Construction*, 5(03):166–172. https://doi.org/10.2118/124317-PA.

Nasa Earth observatory, N.-E. (2018). Global warming. https://earthobservatory.nasa.gov/Features/GlobalWarming/page2.php, (Accessed: 2 June 2018).

Norwegian petroleum directorate, N. (2018). Field - factpages. http://factpages.npd.no/factpages/default.aspx?culture=en&nav1=field&nav2=PageView|All&nav3=46437, (Accessed: 8 June 2018).

Nygaard, R. (2010). Well design and well integrity - wabamun area co_2 sequestration project (wasp). *Energy environmental systems, EES*.

Olje-og energidepartementet, O. (2017). Mulighetsstudier av fullskala co2-håndtering i norge. https://www.regjeringen.no/globalassets/departementene/oed/pdf/mulighetsstudien.pdf.

Oljedirektoratet (2018). The sognefjord delta aquifer (last modified: 13 november 2014). http://www.npd.no/no/Publikasjoner/Rapporter/CO2-samleatlas/4-The-Norwegian-North-Sea/42-Storage-options-in-the-North-Sea/421-Saline-aquifers/The-Sognefjord-Delta-aquifer/, (Accessed: 5 April 2018).

Petroblogweb (2018). Advantages, limitations, and classification of horizontal wells. https://petroblogweb.wordpress.com/2016/08/14/advantages-limitations-and-classification-of-horizontal-wells/, (Accessed: 2 May 2018).

Petrowiki (2017). Phase behavior of pure fluids (last modified: 4 june 2015). http://petrowiki.org/Phase_behavior_of_pure_fluids, (Accessed: 16 October 2017).

Petrowiki (2018). Horizontal wells. http://petrowiki.org/Horizontal_wells, (Accessed: 26 April 2018).

Ringrose, P. (2016). Assessing options for offshore transport and storage and onshore capture in norway. Presentation given at International Workshop on Offshore Geologic CO2 Storage - Austin TX, USA, Spring 2016. Equinor/NTNU.

Ringrose, P. (2017a). Co_2 storage: operation and integrity of engineered co_2 storage. Presentation given at NTNU in the course TPG4255, Fall 2017. Equinor/NTNU.

Ringrose, P. (2017b). Co_2 storage: operation and integrity of engineered co_2 storage. 2. geological storage: trapping processes capacity. Presentation given at NTNU in the course TPG4255, Fall 2017. Equinor/NTNU.

Ringrose, P. (2017c). Co_2 storage: operation and integrity of engineered co_2 storage. 3. injection wells, pressure and geomechanics. Presentation given at NTNU in the course TPG4255, Fall 2017. Equinor/NTNU.

Ringrose, P. (2017d). Co_2 storage: operation and integrity of engineered co_2 storage. 6. integrated monitoring portfolio for co_2 storage: Down-hole and geochemical monitoring. Presentation given at NTNU in the course TPG4255, Fall 2017. Equinor/NTNU.

Ringrose, P. (2017e). Co_2 storage: operation and integrity of engineered co_2 storage. 7. storage integrity. Presentation given at NTNU in the course TPG4255, Fall 2017. Equinor/NTNU.

Ringrose, P. (2017f). Co_2 storage: operation and integrity of engineered co_2 storage. 8. ccs economics and co2 eor. Presentation given at NTNU in the course TPG4255, Fall 2017. Equinor/NTNU.

Ringrose, P., Thorsen, R., and et al., P. Z. (2017). Ranking and risking alternative co_2 storage sites offshore norway. Presentation made by Equinor, Fall 2017. Equinor RT.

Rutqvist, J. (2012). The geomechanics of co_2 storage in deep sedimentary formations. *Geotech Geol Eng*, 30(3):525–551. https://doi.org/10.1007/s10706-011-9491-0.

Schlumberger (2014). Resinject, injection icd. https://www.slb.com/-/media/Files/sand_control/product_sheets/resinject.pdf?la=en&hash=3C29CC3C3AEA9AC9A37D4E9FA491429BBF40D489, (Accessed: 22 April 2018).

Schlumberger (2016). Eclipse reference manual. .

Schlumberger (2018). Permeability thickness. http://www.glossary.oilfield.slb.com/Terms/p/permeability_thickness.aspx, (Accessed: 2 May 2018).

Shi, J. Q. and Durucan, S. (2005). Co_2 storage in deep unminable coal seams. *Oil gas science and technology - Rev. IFP*, 60(3):547–558. https://doi.org/10.2516/ogst:2005037.

Skovholt, O. (1993). Co_2 transportation systems. *Energy Conversion and Management*, 34(9-11):1095–1103. https://doi.org/10.1016/0196-8904(93)90058-I.

Suekane, T., Nobuso, T., and et al., S. H. (2007). Geological storage of carbon dioxide by residual gas and solubility trapping. *International journal of greenhouse gas control*, 2(1):58–64. 10.1016/S1750-5836(07)00096-5.

White, C. M., Strazisar, B. R., and et al., E. J. G. (2003). Separation and capture of co_2 from large stationary sources and sequestration in geological formations - coalbeds and deep saline aquifers. *Journal of the air waste management association*, 53(6):645–715. 10.1080/10473289.2003.10466206.

Whitson, C. H. and Brulé, M. R. (2000). *Phase behavior*. Richardson, TX: Henry L. Doherty Memorial Fund of AIME, Society of Petroleum Engineers.

Wildbolz, C. (2007). Life cycle assessment of selected technologies for co2 transport and sequestration. *Diplom Thesis. Zurich: Swiss Federal Institute of Technology*.

Chapter A

Additional figures

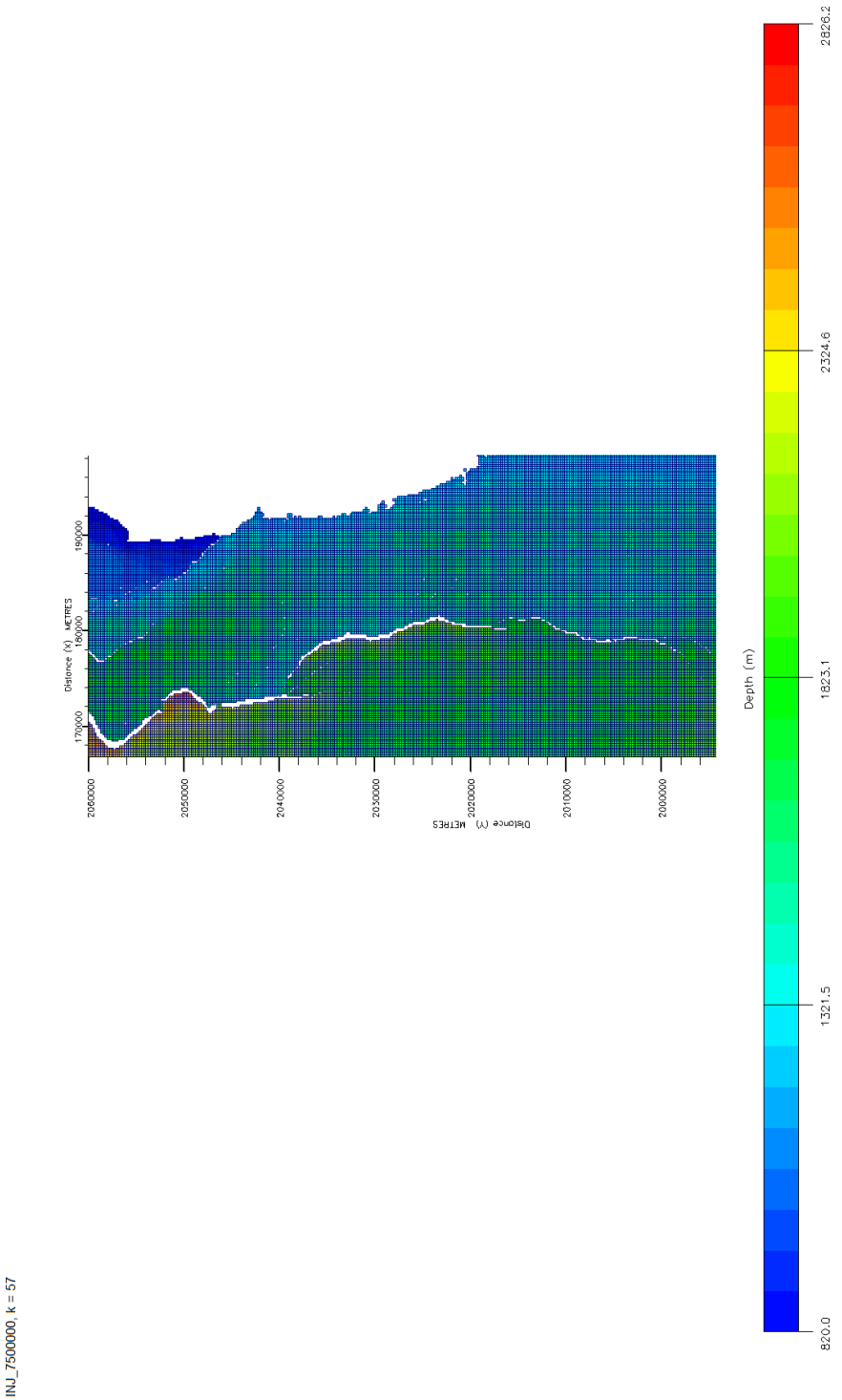

Fig. A.1: The depth at layer 57 in the Smeaheia storage area.

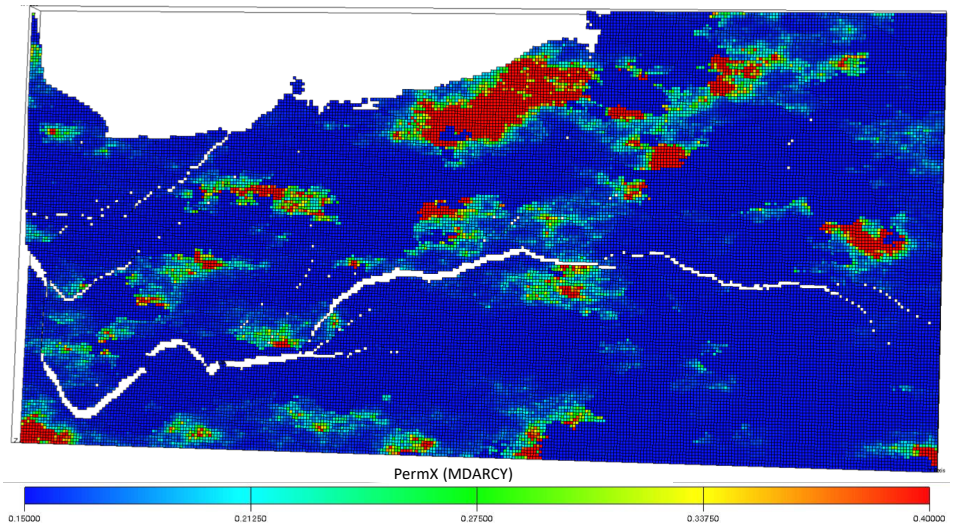

Fig. A.2: The permeability in layer 56 in the Smeaheia storage area.

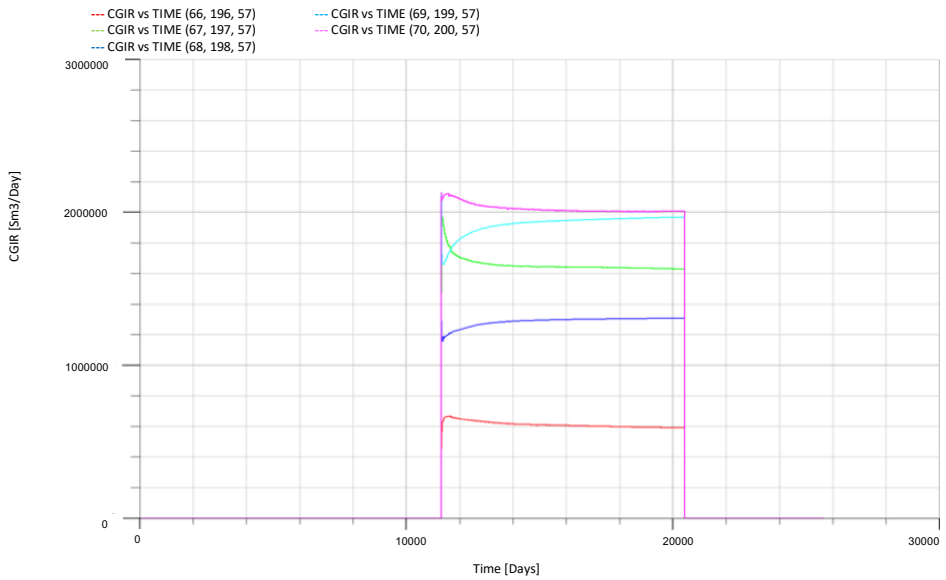

Fig. A.3: Injection rates into horizontal gridblocks in layer 57 without OCD.

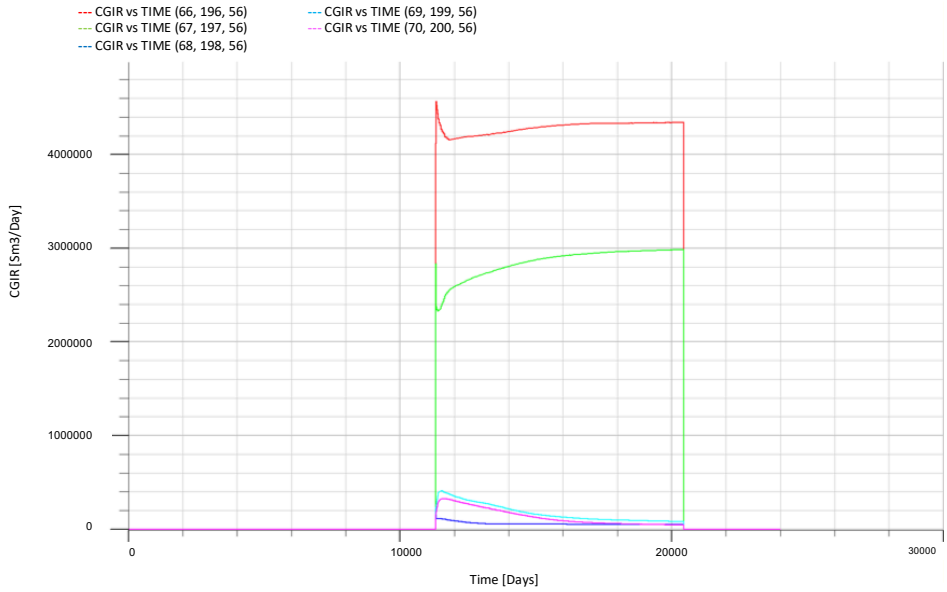

Fig. A.4: Injection rates into horizontal gridblocks in layer 56 without OCD.